39TH ANNUAL MEETING OF THE SOCIETY FOR THERMAL MEDICINE

DELIVERING CLINICAL SOLUTIONS

MAY 13-15, 2024 • HOUSTON, TEXAS

Abstracts from STM 2024
DO NOT REDISTRIBUTE

39TH ANNUAL MEETING OF THE SOCIETY FOR THERMAL MEDICINE

DELIVERING CLINICAL SOLUTIONS

MAY 13-15, 2024 • HOUSTON, TEXAS

WE THANK OUR SPONSORS!

SILVER LEVEL

Pyrexar® MEDICAL

heckel

hyperthermia

39TH ANNUAL MEETING OF THE SOCIETY FOR THERMAL MEDICINE

DELIVERING CLINICAL SOLUTIONS

MAY 13-15, 2024 • HOUSTON, TEXAS

WE THANK OUR SPONSORS!

FRIENDS LEVEL

MedTech International group

OSENSA INNOVATIONS

MSI AUTOMATION

SUPPORTING

Focused Ultrasound Foundation

1

EXPLORING THE IDEAL SYNERGY OF FRACTIONATED STEREOTACTIC BODY RADIOTHERAPY (SBRT) AND HYPERTHERMIA IN TUMORS BEARING MICE

Mr Folefac C. Asonganyi, Master of Sciences[1], Mr. Priyanshu M. Sinha, Master of Sciences[1], Prof Niels Bassler, Ph.D[2], Prof. Michael R. Horsman, Ph.D[1]
[1]Experimental Clinical Oncology-Dept. Oncology, Aarhus University Hospital, Aarhus, Denmark. [2]Danish Center for Particle Therapy, Aarhus University Hospital, Aarhus, Denmark

Mr Folefac C. Asonganyi,
Position (at Institution/Hospital/Company)
Ph.D Researcher

Mr. Priyanshu M. Sinha,
Position (at Institution/Hospital/Company)
Ph.D Researcher

Prof Niels Bassler,
Position (at Institution/Hospital/Company)
Primary Researcher

Prof. Michael R. Horsman,
Position (at Institution/Hospital/Company)
Primary Researcher

Abstract

INTRODUCTION: SBRT which kill more cancer cells than conventional radiotherapy also damages their blood vessels, making them radiation-resistant via hypoxia induction, but hyperthermia-sensitive. Combining SBRT and heat offers therapeutic benefits. Our unpublished data in preliminary studies applying both modalities indicated positive results in terms of tumor delayed growth or tumor control with specific fractionated SBRT doses and heat (41.5°C for 1 hour, 30-minute interval), preserving normal tissues. The focus of this study is to further examine 3 fractions of 15Gy SBRT doses with hyperthermia at different temperatures and time intervals on tumor growth.

METHODS: C3H mammary carcinomas implanted in the rear leg of CDF1 mice were irradiated over one week period with 3 fractions of 15 Gy irradiation beams using photons or protons when tumor reach around 200mm^3. Additionally, animals received the same irradiation doses with a single hyperthermia treatment at temperatures 40.5°C, 41.5°C, or 42.5°C for 1-hour, administered 30, 90, or 180 minutes following the last irradiation fraction. The experiment ended when the animal's tumors reached three times the starting treatment volume (TGT3) or tumor control at 90 days posttreatment. Using Student's t test, the radiation groups alone are compared with radiation plus heat groups.

RESULTS: Preliminary results of mean TGT3 values and corresponding P-values of various treatment groups are summarized in **table 1** below with various standard deviations plus or minus the mean.

CONCLUSION: Combining fractionated SBRT doses with a single heat treatment shows a synergetic effect in treating a C3H mammary carcinoma in vivo. This synergy is most pronounced at higher temperatures and shorter time intervals, benefiting tumor studies

and sparing healthy tissues.

Table 1. Tumor growth time results

Treatment Groups and time intervals	Radiation Results of TGT3 (Days) results of animals	
Temperature 40.5°C	**Photon** [c]	**Proton** [d]
3X15Gy alone	54±6 (n=12)	48±5 (n=8)
3X15Gy + heat (30-minute interval)	78±7 (n=3)	63±2* (n=4)
3X15Gy + heat (90-minute interval)	88±2* (n=4)	52±7 (n=4)
3X15Gy + heat (180-minute interval)	67±2 (n=4)	47±5.2 (n=4)
Temperature 41.5°C		
3X15Gy alone	54±6 (n=12)	48±5 (n=8)
3X15Gy+ heat (30-minute interval)	74±7* (n=10)	63±4* (n=11)
3X15Gy+ heat (90-minute interval)	73±9 (n=4)	51±4 (n=4)
3X15Gy+ heat (180-minute interval)	56±8 (n=3)	51±4 (n=4)
Temperature 42.5°C		
3X15Gy alone	54±5 (n=12)	48±5 (n=8)
3X15Gy + heat (30-minute interval)	83±7*(n=5)	78±7* (n=5)
3X15Gy + heat (90-minute interval)	80±7(n=5)	69±7 (n=4)
3X15Gy + heat (180-minute interval)	90**(n=5)	57±4 (n=4)

[c,d] Results show mean TGT3 values with various standard deviations of the mean at 95% CI. Significant difference between radiation and radiation plus heat at P<0.05=* or P<0.001=**. n= number of animals per group.

1.

2

“Obesity, Cancer and Inflammation--can Thermal Therapy Play a Therapeutic Role?”

Dr. JOAN M. Bull M.D.
The University of Texas McGovern Medical School, Houston, TX, USA

Dr. JOAN M. Bull
Position (at Institution/Hospital/Company)
Professor of Medicine

Abstract

Obesity is an enormous health problem in the United States. Obesity affects more than 40% of the population and is increasing.

Obesity is associated with a significantly increased incidence of many types of cancer, most notably breast and colon cancer. Also, obesity is associated with a worse outcome in the therapy of cancer. Data suggests that 14% of deaths from cancer in men, and 20% of the deaths from cancer in women are associated with obesity.

Chronic inflammation appears to be a major cause of the association of obesity and cancer. NFkB and JNK have been traced as molecular inciters of inflammation in obesity. The low grade inflammatory response linking obesity and cancer is associated to immune cells infiltrating the white adipose tissue in obesity, particularly macrophages, and are a major source of inflammatory cytokines in obese white adipose tissue. Obesity also affects immune cells from the adoptive and innate immune cells.

Semiglutinides, such as Ozempic, have proven effective in reducing obesity, but semiglutinides are expensive and appear also to require continuous treatment for years.

Alternative methods to reduce inflammation and thus to reduce cancer caused by obesity, both heat and cold thermal therapies can reduce inflammation.

3

Pseudodifferential approximations of ultrasound waves for biomedical applications

Dr. Sebastian Acosta PhD
Baylor College of Medicine, Houston, TX, USA. Texas Children's Hospital, Houston, TX, USA

Dr. Sebastian Acosta
Position (at Institution/Hospital/Company)
Assistant Professor

Abstract

Computational simulations are playing an increasingly important role to improve therapeutics and diagnostics using ultrasound waves. To unleash the full potential of computer simulations, the computational method must strike the right balance between accuracy and speed. We develop a fast pseudodifferential method that takes advantage of the geometric flow of acoustic energy to efficiently handle the highly oscillatory nature of ultrasound waves. Simultaneously, the method accurately incorporates refraction, reflection and attenuation imposed by realistic models of biological media. As a result, simulations of ultrasound wave propagation can be executed orders of magnitude faster than using conventional approaches. Some numerical results will be presented, and limitations discussed. This is joint work with Benjamin Palacios (Universidad Catolica de Chile) and Jesse Chan (Rice University).

4

Tumor Burden Reduction and Immune Microenvironment Modulation in a Preclinical Murine Glioblastoma Model through Laser Interstitial Thermal Therapy

Prazwal Athukuri BS[1], Karina V Moreno BS[1], Yuhui Yang BS[1], Malcolm F McDonald BS[1], Dr. Sungho Lee MD, PhD[2], Dr. Khatri Latha PhD[1], Dr. Anantha Marisetty PhD[1], Dr. Ganesh Rao MD[1]

[1]Baylor College of Medicine, Houston, Texas, USA. [2]Louisiana State University Health, Shreveport, Louisiana, USA

Prazwal Athukuri
Position (at Institution/Hospital/Company)
Medical Student

Karina V Moreno
Position (at Institution/Hospital/Company)
Research Technician III

Yuhui Yang
Position (at Institution/Hospital/Company)
Senior Research Assistant

Malcolm F McDonald
Position (at Institution/Hospital/Company)
MD/PhD Student

Dr. Sungho Lee
Position (at Institution/Hospital/Company)
Neurosurgery Attending

Dr. Khatri Latha
Position (at Institution/Hospital/Company)
Scientist

Dr. Anantha Marisetty
Position (at Institution/Hospital/Company)
Scientist

Dr. Ganesh Rao
Position (at Institution/Hospital/Company)
Department Chair

Abstract

Introduction:

Glioblastoma (GBM), a highly aggressive form of brain cancer, poses significant challenges in its management. Maximal surgical resection has long been considered a standard treatment approach, offering tangible survival benefits. However, the effectiveness of this strategy can be hindered by factors such as tumor location, unusual geometry, or bifrontal involvement, which may limit the feasibility of achieving maximal resection. In response to these challenges, laser interstitial thermal therapy (LITT) has emerged as a promising alternative. LITT utilizes thermal energy to induce cell death, with the advantage of being minimally invasive and suitable for treating deep-seated lesions. Furthermore, its application can be precisely regulated to avoid thermal damage to critical neural structures. Real-time monitoring through magnetic resonance thermometry adds another layer of

control to this innovative treatment modality. Our study seeks to delve into the effects of LITT on GBM using a genetically engineered mouse model. By exploring the potential of LITT in cases where maximal resection is restricted, we aim to contribute to a better understanding of its role in GBM treatment.

Methods:

To simulate the poorly-circumscribed nature of GBM, we developed a preclinical murine model utilizing tumor cells with overexpressed PDGFB and STAT3. Tumor-bearing mice were subjected to LITT or sham treatment, the latter involving the implantation of a laser fiber without activation. Our evaluation focused on multiple time points, specifically 3, 7, 14, and 21 days post-treatment. Bioluminescent live images (BLI) were employed to assess tumor burden, providing dynamic insights into the treatment effects. Additionally, Hematoxylin & Eosin staining (H&E) allowed for a detailed histological characterization of tumor burden. To investigate the immune microenvironment, we utilized immunohistochemistry (IHC) and immunofluorescence (IF) staining.

Results:

The results of our study revealed a consistent reduction in tumor burden in mice treated with LITT across the designated time points. Hypercellular regions indicative of tumor burden on H&E staining consistently decreased, contrasting with the increase observed in sham-treated mice. BLI and Luciferin tagging further confirmed the efficacy of LITT in reducing tumor burden. Notably, the mice treated with LITT exhibited a distinct ablation zone at the probe insertion site, reinforcing the precision of this thermal ablation modality. IHC staining with IBA1 demonstrated significant microglial activation in the resection cavity margin after LITT, indicating a potential impact on the immune microenvironment. IF staining with IBA1 and CD68 revealed increased expression, suggesting enhanced microglial activation and macrophage infiltration in LITT-treated mice compared to sham.

Conclusion:

The observed reduction in tumor burden in LITT-treated mice holds significant promise for the development of a preclinical GBM model. LITT, as a thermal energy ablation modality, demonstrates potential in cases where maximal resection is challenging. Furthermore, the induction of microglial activation and macrophage infiltration suggests a potential avenue for enhancing immunotherapy accessibility, particularly for immune checkpoint inhibitors, to prevent tumor recurrence. Future studies will delve into the infiltration of T cells, NK cells, and antigen-presenting cells, along with assessing the efficacy of immunotherapies in conjunction with LITT through comprehensive survival studies. This combined approach could open new avenues for improved and personalized GBM treatment strategies.

5

Cancer Cell Membrane Camouflaged Gold Nanoshells for Photothermal Therapy of Triple-Negative Breast Cancer

Sara B. Aboeleneen[1], Grace M. Azevedo[2], Avery M. Wolverton[1], Emily S. Day[1,3]
[1]Biomedical Engineering, University of Delaware, Newark, DE, USA. [2]Chemical and Biomolecular Engineering, University of Delaware, Newark, DE, USA. [3]Center for Translational Cancer Research, Helen F. Graham Cancer Center and Research Institute, Newark, DE, USA

Sara B. Aboeleneen
Position (at Institution/Hospital/Company)
Graduate Student

Grace M. Azevedo
Position (at Institution/Hospital/Company)
Undergraduate Student

Avery M. Wolverton
Position (at Institution/Hospital/Company)
Undergraduate Student

Emily S. Day
Position (at Institution/Hospital/Company)
Associate Professor

Abstract

Triple-negative breast cancer (TNBC) accounts for 15-20% of all breast cancer diagnoses. Currently, the only treatment options available for TNBC patients are surgery, radiotherapy, chemotherapy, or a combination of two or more of these treatments, all of which have adverse side effects and lack the ability to specifically target the tumor. Therefore, there is an urgent clinical need to develop effective targeted treatment strategies for TNBC patients. Photothermal therapy (PTT) is a promising cancer treatment in which light-sensitive nanoparticles (NP) are injected into the bloodstream, and once they arrive at the tumor site, an externally applied laser is used to irradiate the NPs, converting light into heat that thermally ablates the tumor. One limitation to PTT is the lack of NP targeting to the tumor. Recent studies suggest that coating NPs with cancer cell-derived membranes can evade the immune system and improve the NP's tumor-targeting ability, so we hypothesized that wrapping light-activated gold nanoshells (NS) with TNBC cell membranes, forming MWNS could enable them to target the tumor for effective PTT treatment. Here, we present the results of *in vitro* and *in vivo* studies confirming the synthesis of MWNS that successfully target TNBC tumors and when activated by an 808nm laser, led to efficient thermal killing of TNBC cells. This work provides a promising biomimetic NP-mediated PTT platform to treat TNBC.

6

Feasibility of volumetric hyperthermia in head and neck cancer using the ExAblate Body MR-guided focused ultrasound system

Kisoo Kim, Pragya Gupta, Kazim Narsinh, Chris J Diederich, Eugene Ozhinsky
University of California San Francisco, San Francisco, CA, USA

Abstract

Background: Magnetic resonance imaging (MRI)-guided focused ultrasound represents a promising technology for non-invasive, precise, and efficient heat delivery to targeted areas of the body and the brain.[1] This technology, operating under MRI guidance, allows for treatment planning, temperature monitoring, and safety assurance. One potential application of this technology is in hyperthermia treatments, which aim to induce various therapeutic effects on tumors through a temperature rise within the range of 39-43°C maintained for a duration of 30-60 min.[2–4] The ExAblate MR-guided focused ultrasound system (Insightec, Haifa, Israel) has received FDA approval and is clinically available in the United States. Despite its approval, there is a limited body of research on the system's utilization for volumetric hyperthermia delivery. This could be attributed to the array configuration limitations affecting off-axis focusing and volume heating, as well as safety constraints requiring slower transducer movement for focal spot repositioning.

The objective of this study was to develop a method for volumetric hyperthermia with the ExAblate Body array by integrating mechanical transducer movement with a sector-vortex based beamforming approach. Acoustic and biothermal simulations were conducted to assess the hyperthermia delivery characteristics of the ExAblate Body array achieved through mechanical scanning and beamforming. An iterative process strategy was proposed for sequentially heating multiple spots within the targeted volume. To validate the sonication strategy, patient-specific simulations were conducted using a head and neck cancer model. Further validation was performed through experiments using a tissue-mimicking phantom.

Methods: The simulation framework was developed to calculate the 3D acoustic intensity distribution for beamforming and scanning strategies, specifically for the ExAblate Body transducer.[5] Based on acoustic and biothermal simulation, multiple positions were sonicated sequentially using mechanical scanning and sector vortex beamforming. The system control in the ExAblate Body system was modified to achieve fast transducer movement and MR thermometry-based hyperthermia control, mechanical transducer movements and electronic sector-vortex beamforming were combined to optimize hyperthermia delivery. Experimental validation was performed in a tissue-mimicking phantom. Finally, patient-specific simulations were performed in a head and neck cancer model to demonstrate the feasibility of hyperthermia in the head and neck.

Results: The developed simulation framework allowed for a parametric study with varying numbers of heating spots, sonication durations, and transducer movement times to evaluate the hyperthermia characteristics for mechanical transducer movement and sector-vortex beamforming. Hyperthermic patterns involving 2-4 sequential focal spots were generated and analyzed. Regarding the distance between spots, for a maximum temperature of 45 °C, 2 spots with a distance of 8-12 mm can achieve average T10 of 43 °C. In terms of the sonication time at each spot, due to a minimum transducer movement

time of 12 s, a sonication time extending beyond 10 s resulted in a larger hyperthermic volume and reduced temperature ripple. To demonstrate the feasibility of volumetric hyperthermia in the system, a tissue-mimicking phantom was sonicated with two distinct spots through mechanical transducer movement and sector vortex beamforming. The heated region was clearly observed during acquisition. The average values of Tmax, T10, Tavg, T90, and Tmin between 217 s and 417 s were measured to be 45.6 °C, 44.9 °C, 43.6 °C, 42.2 °C, and 41.5 °C, respectively. Effective hyperthermia heating (T10) was delivered to an average volume of 67.7 mm^3 for 200 s in the phantom.

Conclusions: This study demonstrated the volumetric hyperthermia capabilities of the ExAblate Body system. The simulation framework developed in this study allowed for the evaluation of hyperthermia characteristics that could be implemented with the ExAblate MRgFUS system. The results of volumetric hyperthermia in a head and neck cancer model will be presented at the conference.

7

Heat shock protein induction as a strategy to inhibit protein aggregation in neurodegenerative diseases

Azemat Jamshidi Parsian MS[1], Robert J Griffin PhD[1], Mousumi Patra PhD[1], Peter Crooks PhD[1], Mahmoud Kiaei PhD[2]
[1]UAMS, Little Rock, AR, USA. [2]RockGen Bio, Little Rock, AR, USA

Azemat Jamshidi Parsian
Position (at Institution/Hospital/Company)
Senior research associate

Robert J Griffin
Position (at Institution/Hospital/Company)
Professor

Mousumi Patra
Position (at Institution/Hospital/Company)
Postdoctoral associate

Peter Crooks
Position (at Institution/Hospital/Company)
professor emeritus

Mahmoud Kiaei
Position (at Institution/Hospital/Company)
CEO

Abstract

Amyotrophic lateral sclerosis (ALS) is a progressive paralytic disorder that characterized by the degeneration of both upper and lower motor neurons. Inclusion bodies, protein misfolding and aggregation are major pathological features that are collectively contributed to neurodegenerative pathways in patients and models of ALS. Molecular chaperones, including heat shock proteins assist in the repair of misfolded, denatured proteins or promote their degradation if irreparable. Chaperones (HSPs in particular) are a relevant choice of therapeutic targets to be activated to block or resolve these pathological pathways in motor neurons. The currently FDA approved agents for treatment of ALS or similar diseases do not target chaperone protein levels but instead mostly treat symptoms of the progressive neural degeneration. Here, we hypothesized that by using mild heating to induce expression of HSPs in various cell types: a) NSC-34 motoneuron cells b) HEK-293 cells transfected with profilin1 c) Wild type and transgenic motor neurons and d) spinal cord lysates from the ALS model G93A mice we could reduce unwanted protein aggregation to establish a potential rationale for using clinical hyperthermia applicators to treat ALS patients. Specifically, we observed that induction of Hsp70 and Hsp90, results in a dramatic clearance of profilin1 (PFN1) aggregates. Further work to establish a method of applying hyperthermia to the spinal column and other aspects of the CNS is ongoing in our laboratories. It seems reasonable to conclude that the clearance of PFN1 aggregates and potentially other protein aggregates by the activation of Hsp70 and Hsp90 could be an important therapeutic opportunity for ALS if an optimized applicator and thermal history monitoring approach can be developed.

8

The real potential of hyperthermia to overcome radiation resistance from tumor hypoxia

Professor Michael R. Horsman PhD
Experimental Clinical Oncology-Dept. Oncology, Aarhus University Hospital, Aarhus, Denmark

Professor Michael R. Horsman
Position (at Institution/Hospital/Company)
Professor of Experimental Radiotherapy, Aarhus University

Abstract

Purpose: Regions of low oxygenation (hypoxia) are a characteristic feature of solid tumors and a major factor in developing resistance to radiation therapy and enhancing metastatic spread. Hypoxia is either chronic, resulting from limitations in oxygen diffusion, or acute, due to transient fluctuations in blood flow. Hyperthermia is believed to overcome hypoxia, but it is unclear whether it actually affects both types. This pre-clinical study was designed to investigate this possibility by monitoring the heat-induced enhancement of radiation response after acute hypoxia had been eliminated.

Methods: A C3H mammary carcinoma, implanted in the right rear foot of CDF1 mice, was used for all experiments. Treatments began when tumors had reached 200 mm^3 in size. Radiation and hyperthermia were administered locally to tumors by placing non-anesthetized mice in specially constructed jigs that restrained the animals, but allowed the tumor bearing foot to be exposed and loosely attached to the jig with tape. The tumor bearing leg could then be submerged in a heated water bath. The radiation (230 kV X-rays) treatments involved giving a range of single doses (20-70 Gy), with the water bath temperature maintained at 25^{O}C. When combined with hyperthermia (42.5 ^{O}C or 43.5^{O}C for 1-hour), the radiation was either applied in the middle of the heating period (simultaneous treatment) or 4-hours prior to heating (sequential treatment). Mice receiving an intraperitoneal injection with nicotinamide (1000 mg/kg) did so 30-minutes prior to irradiation. The response endpoint was local tumor control at 90 days and involved producing full radiation dose-response curves for each treatment condition, from which logit analysis allowed us to calculate the TCD50 dose (radiation dose inducing tumor control in 50% of animals). A Chi-squared test ($p<0.05$) was used for statistical comparisons.

Results: The TCD50 dose (± 95% confidence intervals) for radiation alone was 54 Gy (52-56). A sequential radiation and heat treatment significantly reduced this TCD50 dose to 48 Gy (45-51) when heating at 42.5^{O}C and to 32 Gy (29-36) with a higher temperature of 43.5^{O}C. With a simultaneous radiation and heat (42.5^{O}C only) treatment, the TCD50 dose was 21 Gy (19-23). Nicotinamide significantly reduced the radiation TCD50 dose to 44 Gy (42-46). It further significantly reduced the TCD50 doses obtained with radiation and heat to 35 Gy (33-37) and 23 Gy (20-27) for a sequential treatment with 42.5^{O}C and 43.5^{O}C, respectively, and to 13 Gy (11-15) for a simultaneous treatment at 42.5^{O}C.

Conclusion: Heating tumors simultaneously with radiation, or sequentially (4-hours) after irradiating, significantly enhanced radiation response. These enhancements have often been associated with hyperthermia primarily eliminating the radiation resistant hypoxic cell population. However, nicotinamide, a drug that prevents acute hypoxia from occurring and has no effect on chronic hypoxia, significantly enhanced the effect seen with either temperature (42.5 or 43.5^{O}C) when given sequentially (4-hours) after irradiating. It also enhance a simultaneous radiation and heat (42.5^{O}C) treatment. These results suggest that hyperthermia primarily eliminated cells that were from the chronically hypoxic population and had little or no effect on acutely hypoxic cells.

Supported by a grant from the Danish Cancer Society.

9

Photothermal Treatment of Infected Melanoma Using Silver Nanoparticles

Marco Benavides-Taylor[1], Spencer Phillips MS Biomedical Engineering[1,2], Dr. Sijia Liu PhD Chemistry[1], Scott Northrup BS Biochemistry[1], Dr. Nicole Levi PhD Biomedical Engineering and Science[1,2]
[1]Wake Forest University Department of Plastic and Reconstructive Surgery, Winston Salem, NC, USA. [2]Wake Forest University Biomedical Engineering Graduate Program, Winston Salem, NC, USA

Marco Benavides-Taylor
Position (at Institution/Hospital/Company)
Research Assistant

Spencer Phillips
Position (at Institution/Hospital/Company)
Graduate Student/Researcher

Dr. Sijia Liu
Position (at Institution/Hospital/Company)
Research Fellow

Scott Northrup
Position (at Institution/Hospital/Company)
Lab Technician III

Dr. Nicole Levi
Position (at Institution/Hospital/Company)
Associate Professor

Abstract

Introduction

Melanoma has recently been discovered to harbor intracellular bacteria, which affects their migration and metabolism. Silver nanoparticles (AgNPs) are used clinically for their antimicrobial benefits, and they can be tailored for photothermal therapy (PTT). The present work evaluates AgNPs fabricated for PTT as a strategy to eliminate both melanoma cells and intracellular bacteria.

Methods

AgNPs were made using the seed-mediated method. Human melanocytes (CRL-4059) and SK-Mel-3 and SK-Mel-28 melanoma cell lines were infected with Staphylococcus aureus (Xen40). Cell and bacteria viability were measured following incubation with AgNPs and exposure to 800 nm light to generate heat.

Results

AgNPs have a triangular shape, and average size of 105nm. Laser powers of 3 and 5W were applied to 10 and 25 µg/mL AgNPs for 60s and 36s, respectively, for laser fluency of 180J. Heat generating ability of 10 µg/mL concentration was roughly 30°C increase for both powers, and 25 µg/mL concentration saw a temperature increase of approximately 50°C for both powers. Cytotoxicity of 0, 10, 25, 50, 100, and 250 µg/mL AgNPs were calculated for both non-infected and infected cells. Infected CRL-4059 cells were more sensitive at

concentrations below 100 µg/mL. Non-infected SK-Mel-3 cells saw greater reduction than infected SK-Mel-3 cells at all concentrations. All infected cell saw greater viability reduction than non-infected cell lines, with SK-Mel-3 having the largest reduction. Concentrations of 0, 10, 25, 50, 100, and 250 µg/mL were tested using PTT at 5W for 36s on SK-Mel-3, and infected cells were more resistant to PTT than non-infected. While maintaining fluency of 180J, different powers and application times were tested. Infected cells were more resistant across groups, with the 5W 36s group seeing the greatest viability reduction, and thus was used for all subsequent experiments. Cell counts and CFUs/cell were found after PTT, and regardless of the cell line, the resultant number of infected cells were larger than their non-infected counterparts. SK-Mel-28 saw the greatest reduction of CFUs/cell while CRL-4059 had the least. Cell regrowth of SK-Mel-3 after PTT was also evaluated using clonogenics, and non-infected were more susceptible to AgNPs alone. However, applying PTT mitigates survival of infected cells. When PTT was applied, regrowth after 1 week was decreased for both non-infected and infected cell lines as concentration increased to 25 µg/mL.

Conclusion

AgNPs are more cytotoxic to melanoma cells when combined with PTT. Additionally, infected cells are more resistant to both AgNPs and hyperthermia alone, but this can be overcome by increasing the thermal dose.

10

Improved Phototherapeutic Combination Nanomedicine

Mr. Adeniyi Oyebade[1], Mrs. Mujeebat Bashiru[1], Sara Mateen[1], Dr. Nawab Ali[1], Dr. Robert Griffin[2], Dr. Adegboyega K Oyelere[3], Dr. Noureen Siraj[1]
[1]University of Arkansas, Little Rock, AR, USA. [2]University of Arkansas for Medical Sciences, Little Rock, AR, USA. [3]Georgia Institute of Technology, Atlanta, Georgia, USA

Mr. Adeniyi Oyebade
Position (at Institution/Hospital/Company)
PhD student

Mrs. Mujeebat Bashiru
Position (at Institution/Hospital/Company)
PhD student

Dr. Nawab Ali
Position (at Institution/Hospital/Company)
Professor

Dr. Robert Griffin
Position (at Institution/Hospital/Company)
Professor

Dr. Adegboyega K Oyelere
Position (at Institution/Hospital/Company)
Professor

Dr. Noureen Siraj
Position (at Institution/Hospital/Company)
Professor

Abstract

Herein, we report the synthesis and characterization of combination ionic materials from a chemotherapeutic drug (chemo), and two different NIR dyes (NaICG and NaIR820) as a photothermal therapeutic drug. Ionic nanomedicines (INMs) were derived from ionic materials (IMs) via a facile reprecipitation method which produces carrier-free nanoparticles (INMs). Photophysical properties of INMs were studied in detail. The phototherapeutic efficiency of the combination drugs was examined by investigating the light-to-heat conversion efficiency. The improved photophysical properties of the combination nanomedicines in comparison to their parent compounds significantly enhanced INMs' photothermal efficiency. *In vitro* dark and light toxicity studies were also carried out. *In vitro* dark and light cellular studies showed enhanced cytotoxicity (lower IC_{50}) as compared to the chemo drug, revealing the significance of nanoparticle modification upon alteration of the counterions. Importantly, the results from combination index and improved *in vitro* cytotoxicity reveal a great potential synergy between chemo and photothermal agents in the newly developed combination nanomedicines based on Chemo and NIR dyes.

11

Comparing Temperature-Dependent and Constant Thermophysical Properties in Focused Ultrasound Simulations

Christian Valencia Narva B.Sc, PhD Christopher R Dillon PhD
Brigham Young University, Provo, Utah, USA

Christian Valencia Narva
Position (at Institution/Hospital/Company)
Graduate Research Assistant

PhD Christopher R Dillon
Position (at Institution/Hospital/Company)
Assistant Professor

Abstract

INTRODUCTION High intensity focused ultrasound (HIFU) has proven effective in tumor treatment through both thermal ablation and hyperthermia. HIFU simulations may enhance treatment planning in ways that will shorten treatment times, increase safety, and improve efficiency. Numerical methods predicting temperature distribution and thermal dose often assume constant thermophysical properties of the tissue, neglecting temperature dependencies. The study investigates how constant versus temperature-dependent thermal conductivity, specific heat capacity, and perfusion impact HIFU ablation and hyperthermic temperature distributions, thermal doses, and computation time.

METHODS The simulations predict HIFU heating of liver tissue initially at 37 °C. Two heating scenarios are tested. First, thermal ablation is applied to 9 different focal locations (3x3 grid with 4 mm spacing in a plane perpendicular to the FUS beam) that are heated with 30 W for 30 s followed by a 30-second cooling period for each location (9 minutes total simulated time). Second, mild hyperthermia was simulated with low-power (3.3 W) simultaneous heating at all 9 focal locations, representing the rapid and sequential electronic steering of the ultrasound beam. This study simulates mild hyperthermia for 15 minutes, sufficient time to reach a steady-state temperature distribution. The temperature distributions for both heating scenarios are calculated using two versions of an explicit finite difference time-domain (FDTD) solver of the Pennes bioheat transfer equation (PBTE). The first version employs constant thermophysical properties with values taken from the literature. In contrast, the second version incorporates thermal conductivity, specific heat capacity, and perfusion that vary with temperature. Temperature-dependent property models are sourced from Guntur and Choi (Ultrasound Med Biol, 2013), and Prakash and Diederich (Informa Healthcare, 2012).

RESULTS: In the context of thermal ablation, the maximum temperature at each focal location reaches an average of 59.2°C, with the constant-property solver exhibiting a slightly higher value by approximately 0.4°C. Additionally, volume-averaged maximum temperatures in a cubic region (91.125 mm^3) centered at the focal location were 48.1°C and 47.5 °C for the constant-property and temperature-dependent solvers, respectively. Thermal dose volumes for a cumulative equivalent minutes at 43 °C (CEM_{43}) exceeding 240 mins were 109.25 mm^3 and 93.75 mm^3 for the constant-property and temperature-dependent solvers, respectively. The computation time needed for these simulations was 21.1 mins for the constant-property solver and 32.7 mins for the temperature-dependent solver.

For the mild hyperthermia scenario, the average temperature rise of the 9 locations for the constant-property and temperature-dependent solvers were 5.8 °C and 4.5 °C, respectively.

In addition, the steady-state volume exceeding 41 °C for the constant-property and temperature-dependent solver were 2512.9 mm^3 and 571.1 mm^3, respectively. The computation time required for the constant-property solver was 40.4 mins and 62.0 mins for the temperature-dependent solver.

CONCLUSIONS: For the thermal ablation model, the results highlight subtle differences in peak temperatures (0.4 °C) for constant versus temperature-dependent solvers. However, there are substantial differences in the volume of tissue with a CEM_{43} exceeding 240 mins (16.5% different). In terms of computation time required, the temperature-dependent solver requires about 50% more time than the constant property solver. Trends observed for the ablation model also applied to the hyperthermia model. However, for the hyperthermia scenario, the constant-property solver has an average temperature increase 29% greater than the temperature-dependent solver. Additionally, the total volume with temperatures greater than 41 °C for the constant-property solver is nearly 3.4 times greater than for the temperature-dependent solver. This is because perfusion plays an important role for the temperature-dependent model in the range temperature of mild hyperthermia. In conclusion, incorporating temperature-dependent properties changes the temperature distributions in ways that could impact HIFU therapy outcomes.

12

Photothermal Silicone Nanocomposites for Eradication of Staphylococcus aureus Biofilms

Erica Vargas MS, Dr. Nicole Levi PhD
Wake Forest University School of Medicine, Winston-Salem, NC, USA

Erica Vargas
Position (at Institution/Hospital/Company)
graduate student at Wake Forest University School of Medicine

Dr. Nicole Levi
Position (at Institution/Hospital/Company)
Associate Professor, Plastic and Reconstructive Surgery, Wake Forest University School of Medicine

Abstract

Many implantable medical devices are comprised of silicone and their infection due to the presence of bacterial growth post-implantation can be difficult to treat. Standard treatment involves prolonged courses of antibiotics or removal of the implant. These infections start with planktonic bacteria (free-floating bacteria) entering the body and overtime, bacteria can grow in an optimal environment rich in polymers, polysaccharides, extracellular DNA, and water. These individual components make up a complex structure known as a biofilm and bacteria within this structure are more susceptible in growing resistance to antibiotics.

Staphylococcus aureus is one of the most common bacterial strains associated with biofilm growth on medical devices. This project evaluated using photothermal treatment (PTT) to disrupt *S. aureus* biofilms via nanoparticle infused medical-grade silicone.

The main objective of this project was to evaluate the effects of PTT on *S. aureus* Xen 29 and Xen 40 biofilms grown on nanoparticle infused medical grade silicone. Xen 29 and Xen 40 biofilms were grown on silicone and silicone infused with (10mg/g) of Poly[4,4-bis(2-ethylhexyl)cyclopenta[2,1-*b*;3,4-*b*'] dithiophene-2,6-diyl-*alt*-2,1,3-benzoselenadiazole-4,7-diyl] (PCPDTBSe) and were subject to 800 nm, from a continuous wave photodiode laser with various powers and times. The effects were quantified by measuring colony forming units per milliliter (CFU/mL). Additionally, individual structures that make up the biofilm such as bacteria, polysaccharides, and extracellular DNA, were characterized following PTT with a variety of fluorescent staining reagents. SYTO 9 was used to characterize live cells, Propidium Iodide (PI) was used for dead cells, Wheat Germ Agglutinin (WGA) 555 was used for polysaccharides, and TOTO 3 was used for extracellular DNA. Regrowth of biofilms was determined using crystal violet biomass analysis.

The nanoparticle infused silicone could generate heat rapidly ($\Delta T = 26.5°C$) with 800 nm stimulation at 300 J/cm^2, using either 3W or 5W. However, 1W applied for 300s only had a $\Delta T = 18°C$, resulting in a less than 1 log reduction of Xen 29 and 3 log reduction of Xen 40. Silicone without nanoparticles exhibited minimal heating, and was not effective at reducing biofilms, or altering biofilm regrowth following treatment. Xen 29 had complete eradication using 3W, 100s and Xen 40 had complete eradication using 3W, 100s or 5W, 60s. Effective parameters for reducing CFUs/ mL also halted biofilm regrowth. These laser powers and times show that over time the nanoparticle silicone can generate temperatures high enough to kill viable bacteria, and damage to the biofilm components to impede biofilm regrowth. Compared to silicone, the nanoparticle treated silicone had significant reductions in viability of live cells, polysaccharides, and DNA content, based on fluorescent imaging. PI-stained biofilm on the nanocomposite silicone indicated more dead cells than live cells after

treatment than silicone. These images further confirm that the integrity of the individual structures was successfully diminished following photothermal treatment. Overall, our results conclude that photothermal elimination of biofilms is effective using heat-generation using infrared absorbing nanoparticles in silicone, and effectiveness depends upon time of laser application and not only laser fluence, or temperature. Unexpectedly, we observed differences in the response of bacterial biofilms to PTT, with Xen 29 being more resistant to thermal injury. A benefit of nanocomposite PTT for eliminating pathogenic biofilms is that the technique damages the structural components of biofilms, which can impede biofilm regrowth.

13

Summary of the Radiofrequency Hyperthermia Safety Study (RHYSS)

Nicole Levi PhD[1], Dr. Lucian Vlad MD[1], Dennis Clark BS[2], Shawn Clark BS[2]
[1]Wake Forest University School of Medicine, Winston-Salem, NC, USA. [2]Thermofield, Nashville, TN, USA

Nicole Levi
Position (at Institution/Hospital/Company)
Associate Professor in Plastic and Reconstructive Surgery at Wake Forest University School of Medicine

Dr. Lucian Vlad
Position (at Institution/Hospital/Company)
Associate Professor in Plastic and Reconstructive Surgery at Wake Forest University School of Medicine

Dennis Clark
Position (at Institution/Hospital/Company)
CEO at Thermofield

Shawn Clark
Position (at Institution/Hospital/Company)
CTO at Thermofield

Abstract

Introduction

Mild Hyperthermia (MH) has been used for thousands of years to help decrease pain, improve blood flow to tissues, and aid lymphatic drainage. Although the complete mechanisms are not yet understood, there is evidence that MH may be beneficial for wound healing, most likely via temporary increases in blood perfusion. Despite these observations MH has been slow to be established and adopted for routine use in wound care, possibly due to wide variations in technical specifications of heating devices, and challenges managing impaired tissue.

Methods

Our study evaluated the safety and tolerability of Thermofield radiofrequency device for improving blood flow to the lower limb. This is a novel approach to MH by using a lightweight, portable radiofrequency system that induces heat in the exposed tissue topically with a controlled feedback loop to maintain a specific and precisely controlled temperature, without the need for a water bolus interface. A key feature of the device is feedback temperature control to ensure safety.

We enrolled 20 healthy volunteers, with cohorts ranging in ages from 18-30, 31-40, 41-50, 51-60, and 61+. We also accounted for variances in calf circumference, and the device was used on the right calf only, while the left served as a control for image analysis. Patients were treated weekly for 45 minutes for a total of 4 weeks, and followed up 4 weeks after the final treatment. Ten participants were treated with 42°C and ten participants were treated with 40 °C. Tissue blood perfusion was measured by laser scanning doppler and skin temperature was measured using infrared thermography. Subjective pain scores and photographs of the treated area were also documented weekly.

Results

Blood perfusion increased from 170% up to 756% with an average of 432% as measured within 5 minutes post-treatment. Subjects treated with 40 °C had an average increase of 372.7% and subjects treated with 42 °C had an average increase of 502%. Skin temperature for subjects treated with 40°C had an average increase of 6.5 °C and subjects treated with 42°C had an average increase of 7.2 °C. There was an average 4.3°C increase at a 1 cm depth. Subjective pain scores (0 is no pain and 10 is the worst) were 0 (zero) except for 1 participant reported score 1 on week 3 and one participant reported score 2 with each treatment. Three of the subjects treated with 42 °C were noticed to have minor skin erythema.

Conclusion

This study demonstrates safety and good tolerability of the Thermofield radiofrequency hyperthermia device, especially using 40 °C for once weekly application. The device is compact, easily portable, and heats tissue rapidly to a depth of a few centimeters. The major conclusion of the study is that this new device can safely produce increased blood perfusion, which is critical for aiding in the healing of chronic soft tissue wounds. A major finding was that the device increased blood perfusion well, even in older patients, which represent a large majority of lower limb maladies. No complications were noted at this temperature and the patient satisfaction was high. We propose that the Thermofield device will be a beneficial addition for the management of complex soft tissue healing, and may offer additional benefits in pain mitigation, or augment clinical standards of care, which we will explore in a developing clinical trial.

15

Design and characterization of a clinical AMF system for uniform heating of prosthetic knee implants.

Varun Sadaphal Ph.D.[1], Bibin Prasad Ph.D.[1], Suri Le[2], Robert Oakley[2], Mikel Serralde[3], Isaiah Baker[4], Andrei Mitrofan[4], Jared Smothermon[3], Kevin McCoy[3], Jeff Garret[2], John Tepper M.S.[1], Rajiv Chopra Ph.D.[1,4]
[1]Solenic Medical, Addison, Texas, USA. [2]Cobalt Product Solutions, Plano, Texas, USA. [3]Aava Technologies, Plano, Texas, USA. [4]8Fold Mfg, Addison, Texas, USA

Varun Sadaphal
Position (at Institution/Hospital/Company)
Senior Engineer

Bibin Prasad
Position (at Institution/Hospital/Company)
Senior Scientist

Suri Le
Position (at Institution/Hospital/Company)

Robert Oakley
Position (at Institution/Hospital/Company)

Jared Smothermon
Position (at Institution/Hospital/Company)
Vice President

Kevin McCoy
Position (at Institution/Hospital/Company)
President

Jeff Garret
Position (at Institution/Hospital/Company)
Principle

John Tepper
Position (at Institution/Hospital/Company)
Senior VP Engineering

Rajiv Chopra
Position (at Institution/Hospital/Company)
CTO

Abstract

Treating prosthetic joint infection (PJI) involves highly-invasive surgical procedures with great impact on quality of life for patients. PJI occur due to biofilm formation around the implant. This process sets up an altered microenvironment for bacteria to thrive unhindered by the body's natural immunologic protective response and antibiotic treatment. Studies have reported that heat can reduce biofilm on implant surfaces and can also increase its sensitivity to antibiotics. AMF provides a method for non-invasive targeted heating of metal implants without surgical intervention. Although promising, its application encompasses numerous engineering challenges. This study explores design challenges to generate a system capable of efficiently delivering a therapeutic dose of AMF to a primary knee implant and the development of a clinical device for human trials. Based on prior in-vitro, large animal, and computational studies, a complex AMF coil pattern generating 5 mT at 200 kHz

was required to reach 75°C average surface temperature within 2 min on the knee implant with uniform distribution. Construction of the system required electrical currents on the order of 200 A, specialized litz wire, use of resonance and matching circuits, handling of up to 10 KV peak circuit voltage, dynamic tracking of thermal resistive changes of tank circuit, and a means to position the coil accurately around the knee. The magnetic field of constructed system was measured and validated against simulated magnetic field calculations. The surface temperature distribution of clinical knee implants was measured with infrared imaging, and found to agree within <10% with equivalent simulations. Overall, this study shows successful engineering of a clinical system for AMF heating of prosthetic knee implants, and it is in the process of obtaining approval for human feasibility studies.

16

Preliminary analysis and challenges with simulation and verification of thermoembolization

Rohan P. Amare Ph.D.[1], David T Fuentes Ph.D.[1], Danielle L. Stolley Ph.D.[1], Megan C Jacobsen Ph.D., DABR[1], R. Jason Stafford Ph.D.[1], Rick Layman Ph.D.[1,2], Emily A. Thompson Ph.D.[1], Erik N.K. Cressman MD, Ph.D., FSIR[1]
[1]UT MD Anderson Cancer Center, Houston, Texas, USA. [2]UT Health Graduate School of Biomedical Sciences (UT-GSBS), Houston, Texas, USA

Rohan P. Amare
Position (at Institution/Hospital/Company)
Postdoctoral Fellow,
Department of Imaging Physics - Research, Division of Diagnostic Imaging
The University of Texas MD Anderson Cancer Center

David T Fuentes
Position (at Institution/Hospital/Company)
Associate Professor,
Department of Imaging Physics - Research, Division of Diagnostic Imaging
The University of Texas MD Anderson Cancer Center

Danielle L. Stolley
Position (at Institution/Hospital/Company)
Research Scientist,
Flow Cytometry & Cellular Imaging Core Facility
Department of Leukemia
The University of Texas MD Anderson Cancer Center

Megan C Jacobsen
Position (at Institution/Hospital/Company)
Assistant Professor,
Department of Imaging Physics - Research, Division of Diagnostic Imaging,
The University of Texas MD Anderson Cancer Center

R. Jason Stafford
Position (at Institution/Hospital/Company)
Professor,
Department of Imaging Physics,
Division of Diagnostic Imaging
The University of Texas MD Anderson Cancer Center

Rick Layman
Position (at Institution/Hospital/Company)
Associate Professor, Department of Imaging Physics, Division of Diagnostic Imaging, The University of Texas MD Anderson Cancer Center, Houston, TX

Associate Member, Division of Medical Physics, MD Anderson Cancer Center - UT Health Graduate School of Biomedical Sciences (UT-GSBS), Houston, TX

Emily A. Thompson
Position (at Institution/Hospital/Company)
Medical Physics Fellow
Department of Imaging Physics
The University of Texas MD Anderson Cancer Center

Erik N.K. Cressman
Position (at Institution/Hospital/Company)

Associate Professor,
Department of Interventional Radiology, Division of Diagnostic Imaging,
The University of Texas MD Anderson Cancer Center

Abstract

Thermoembolization is a novel treatment method in which a reagent undergoing exothermic chemical reaction provides thermal and chemical embolization. The reagent is delivered endovascularly to a target such as hepatocellular carcinoma. Due to the chemical and thermal ablation nature of the treatment, the vasculature rapidly reaches stasis upon delivery of the reagent to the target tissue. Determining the correct amount of reagent, location and speed of delivery is important for designing appropriate treatment delivery protocols. Computational simulations of thermoembolization can aid clinical study to predict where the damage would occur as well as how much. This presentation will discuss the equations, algorithms, and analysis for thermoembolization simulation.

A Gaussian mixture model was applied to segment the vessels as the source of the exothermic reaction. A Hessian based filter provided the priors for the mixture model segmentation. A centerline extraction was applied to the vessel segmentation generating a NIFTI dataset of centerline pixels. An algorithm to connect the neighboring centerline pixels, identify terminal endpoints and any discontinuities is developed. This algorithm provides a 1D pipe network of the segmented vasculature generated from the extracted centerline pixels. Each centerline pixel acts as a pressure node and the 1D pipe element connects two pixels as vessel. The blood flow in this 1D vessel is modeled using Hagen-Poiseuille's equation, and mass conservation is applied at each pressure node. Thus, the total number of unknowns was the same as the total number of centerline pixels in the segmented vasculature. The linear system of mass conservation equations at each pressure node, with pressure as the unknowns was solved using direct solver.

Since the centerline pixels were extracted directly from the CT scans, there was a direct pixel to pixel correlation between the imaging data and simulation results. Numerical simulations were validated in a porcine animal model. The observed contrast enhancement was used as a reference for the expected mass transport. Simulation showed good agreement with the observed mass transport in imaging. Current directions for further model validation will also be presented.

17

Human cadaver validation study to quantify the AMF heating on a primary prosthetic knee implant and surrounding tissues

Dr Bibin Prasad PhD[1], Dr Varun Sadaphal PhD[1], Luke Gritter[2], Joshua Thomas[2], Jose Guzman[1], John Tepper[1], Haley Alegria[1], Dr Rajiv Chopra PhD[1]
[1]Solenic Medical, Inc., Addison, TX, USA. [2]AltaSim Technologies, Colombus, OH, USA

Dr Bibin Prasad
Position (at Institution/Hospital/Company)
Senior Scientist

Dr Varun Sadaphal
Position (at Institution/Hospital/Company)
Senior Engineer

Luke Gritter
Position (at Institution/Hospital/Company)
Principal Engineer

Joshua Thomas
Position (at Institution/Hospital/Company)
Senior Engineer

Jose Guzman
Position (at Institution/Hospital/Company)
Vice President of Strategic Marketing

John Tepper
Position (at Institution/Hospital/Company)
Senior Vice President of Engineering & Manufacturing

Haley Alegria
Position (at Institution/Hospital/Company)
Senior Project Manager

Dr Rajiv Chopra
Position (at Institution/Hospital/Company)
CTO and Executive Vice President of R&D

Abstract

Metal implant infections are a devastating problem due to the formation of biofilm which impairs the effectiveness of antibiotics and leads to surgical replacement as definitive treatment. Exposing implants to Alternating Magnetic Fields (AMF) generates surface heating where biofilm tends to reside. However, the use of AMF heating on implants to eradicate biofilm must be accurate and safe to surrounding tissues, in order to be practical. In this study the validation of AMF heating in a knee implant and surrounding tissues is investigated using Solenic's AMF treatment device (Sola 2) on a human cadaver and digital knee models. Real time temperature measurements using fiber optic sensors were performed on a primary knee implant and surrounding tissues including, medial and lateral collateral ligaments, patella, muscle, and skin. Simulations were performed on a cadaver equivalent digital knee model to compare the temperatures that were measured from the cadaver. To ensure safety due to the AMF treatment thermal dose levels on surrounding tissues were calculated based on CEM43 and Arrhenius tissue damage models. Results show <10% of uncertainty variation between simulations and experiments. Using the treatment strategy of achieving an average surface temperature of 75°C in single 80s

exposure, no significant irreversible tissue damage was observed to surrounding tissues. This heating scheme has also been shown to be effective at eradicating biofilm in our *in vitro* and *in vivo* studies. Overall, this study indicates accurate heating and safe implementation of AMF treatment in clinics for primary knee implants.

19

Unveiling the Therapeutic Potential of Brain-Guided Whole-Body Hyperthermia: Insights from a Pilot Biomarker Study on Inflammation, Immune Modulation, and Angiogenesis in Noninvasive Cancer Treatment

Professor David M Smadja[1,2], Doctor Lisbeth Cortina[3], Doctor Rafal Bonet-Vazquez[3], Doctor Alberto F Chocron[3,4], doctor Mohammad Hosseine-Farid[5], Mr. Andrew J Lopez[3], Doctor M. Marc Abreu[3,6]

[1]Paris Cité university, Paris, paris, France. [2]AP-HP, European Georges Pompidou hospital, Paris, paris, France. [3]Clinical Sciences Division, BTT Medical Institute, Aventura, florida, USA. [4]Research Service, Miami Veteran Administration Medical Center, Miami, Florida, USA. [5]College of Computing and Engineering, Nova Southeastern University, Fort Lauderdale, florida, USA. [6]Department of Biomedical Engineering and Medical Physics, BTT Medical Institute, Aventura, Florida, USA

Professor David M Smadja
Position (at Institution/Hospital/Company)
Professor of Hematology

Doctor Lisbeth Cortina
Position (at Institution/Hospital/Company)
Laboratory Supervisor

Doctor Rafal Bonet-Vazquez
Position (at Institution/Hospital/Company)
Laboratory Assistant

Doctor Alberto F Chocron
Position (at Institution/Hospital/Company)
Research Assistant

doctor Mohammad Hosseine-Farid
Position (at Institution/Hospital/Company)
Assistant Professor

Mr. Andrew J Lopez
Position (at Institution/Hospital/Company)
Clinical Researcher

Doctor M. Marc Abreu
Position (at Institution/Hospital/Company)
Medical Director

Abstract

Background: Hyperthermia has emerged as a promising therapy for cancer, with potential effects on platelet function, inflammation, and cytokine production. Whole-body hyperthermia treatment utilizes the brain-eyelid thermal tunnel (BTT), pioneered at Yale University, which enables non-invasive, continuous monitoring of brain temperature and optimizes heat transfer between brain and eyelid, resulted in the development of brain-guided WBH (BgWBH).

Purpose: To investigate the alterations in white blood cell count, hemoglobin levels, platelet count, sedimentation rate, and cytokine/growth factors indicative of angiogenesis

and/or inflammation 24 hours after BgWBH treatment in a focused cohort of 16 cancer patients.

Methods: After obtaining informed consent, BgWBH was administered using the FDA-approved Abreu-BTT-700 system and BTT radiant-heat equipment involving a heat chamber enclosing the patient's body and head inductor delivering heat to the brain via BTT. During hyperthermia, non-sedated patients were exposed to far-infrared heat, aiming to achieve their brain and body temperature to 41.5°C (SD ±0.3°C) for 35 minutes (SD ±8 minutes). Continuous monitoring included heart rate, respiratory rate, oxygen saturation, body core temperature (measured with tympanic probe), and skin temperature at eight sites (precordium, forehead, and right and left arms, hips, and calves) besides blood pressure every 5 minutes. The infusion pump provided hydration as needed. Brain temperature was measured using the noninvasive FDA-approved C1-eyelid surface probe. Biological assessment was performed on the peripheral blood of sixteen consecutive cancer patients both before and 24 hours after undergoing a single BgWBH treatment. The selected cases had an average age of 62 years (SD ±12.5 years) and included four cases of prostate cancer, three of breast cancer, two of lymphomas, two of pancreatic cancer, one of sarcoma, one of colon cancer, one of ovarian cancer, one of lung cancer, and one of uterine cancer. Vascular endothelial growth factor A (VEGF-A) levels were examined in platelet-poor plasma, while C-reactive protein (CRP), tumor necrosis factor alpha (TNF-α), soluble interleukin-2 receptor (sIL-2R) and interleukin-10 (IL-10) were assessed in serum. We conducted a Wilcoxon matched-pairs signed-rank test to assess the comparison of biological parameters before and after BgWBH treatment.

Results: Evaluation of white blood cells, hemoglobin and platelet demonstrated no significant difference before and after BgWBH treatment (respectively with a P-value=0.53; 0.09 and 0.11). The sedimentation rate used as a non-specific marker of inflammation associated to CRP and TNF-α were all significantly decreased after BgWBH treatment (with respectively a P-value=0.003; 0.0004 and 0.004). Interleukin-10 (IL-10) has been evaluated for its anti-inflammatory properties that may contribute to an immunosuppressive environment, potentially aiding tumor growth. IL-10 was not significantly modified after BgWBH treatment (with a P-value=0.16). The IL-2 receptor (IL-2R) plays a crucial role in the immune system and several malignant cells express high levels of IL-2 receptors giving rise to high sIL-2R levels in serum. Measuring soluble IL-2R levels has been proposed recently as a diagnostic and prognostic tool that could provide insights into the patient's treatment efficacy or disease progression. sIL-2R was significantly decreased after BgWBH treatment (with a P-value=0.0002). Finally, VEGF-A, a well know angiogenic growth factor was found to significantly decrease after BgWBH treatment (with a P-value=0.003).

Conclusion: All in all, our findings demonstrated a noteworthy reduction in both specific and non-specific biomarkers associated with inflammation, immune modulation, and angiogenesis following BgWBH treatment. This discovery implies that BgWBH establishes an inhibitory environment conducive to suppressing tumor growth and angiogenesis. To substantiate our findings, additional research and clinical trials are essential, setting the stage for the potential incorporation of BgWBH into clinical practice for cancer treatment.

20

Lymph node metastases in resected pancreatic ductal adenocarcinoma (PDAC) as predictor of survival in the randomized HEAT study: a preliminary report

Dr Felix Oliver Hofmann MD[1], Dr Markus Albertsmeier MD[1], Prof Jens Werner MD[1], Mr Michael Schmidt[2], Prof. Stefan Boeck MD[3], Prof Lars Lindner MD[3], Prof. Rolf Issels MD PhD[3]
[1]Dept. of Surgery, University Hospital, Munich, Germany. [2]Dept. of Statistics (IBE), University, Munich, Germany. [3]Dept. of Medical Oncology, University Hospital, Munich, Germany

Abstract

Background:

Lymph node involvement (LN) is a major prognostic factor of survival in pancreatic ductal adenocarcinoma (PDAC). In the HEAT study, regional hyperthermia with cisplatin added to gemcitabine (GPH) compared to gemcitabine (G) in resected PDAC did not significantly improve disease-free survival (DFS) with a borderline trend of improved overall survival (OS) (Issels et al. EJC 2023). To analyze the prognostic accuracy of N0/N1 tumors, different LN parameters in the HEAT study population have been tested.

Methods:

In 109 randomized patients who underwent pancreatoduodenectomy between April 2012 to April 2018, we assessed the prognostic value of the LN status (N0/N1) according the AJCC 7 edition and the number of examined lymph nodes (ELN) and of positive lymph nodes (PLN) according the AJCC 8th edition. Exploratory analyses of DFS and OS were performed. All Confidence Intervals (CIs) are two-tailed with 90% confidence level. All p-values are one-sided. Cut points were determined by ROC method.

Results:

In 109 randomized patients (N0: 32 patients; N1:77 patients), the median number of ELN was 22.0 (interquartile range: 12.5-28) and the median number of PLN was 1 (interquartile range: 0-3). After median follow-up of 60 months, recurrence occurred in 86 patients (N0: 23 versus N1:63). There was a difference of DFS in favor of the N0 group (N0 vs N1; HR, 0.68; 90% CI, 0.46-1.00; p=0.051).Median OS was 33.8 (N0) vs 24.8 months (N1) (HR 0.68; 90% CI, 0.45-1.02; p=0.059). High number of ELN (cut point ≥ 18 vs < 18) was associated with improved median OS (28.9 versus 23.6 months (Kaplan-Meier p=0.027). Low number of PLN (cut point < 3 vs ≤ 3) was associated with improved median DFS (12.6 versus 11.2 months (Kaplan-Meier p=0.045).

Conclusions:

This study demonstrates that - in addition to the N0/N1 category - the number of ELN and the number of PLN are parameters in predicting survival for patients with resectable PDAC in the HEAT study. Uni- and multivariate analyses including additional risk factors and testing the impact of treatment are ongoing.

22

Ultrasound guided interstitial photothermal therapy for treating neuroblastoma

Grace E Olsson B.S.[1], Rohan V Patil B.S.[1], Samantha J Chin B.S.[1], Katharine N Rus B.S.[1], Dr. Elizabeth E Sweeney PhD[1], Dr. Karun V Sharma PhD, M.D.[2], Dr. Rohan Fernandes PhD[1]
[1]George Washington University, Washington, District of Columbia, USA. [2]Children's National Hospital, Washington, District of Columbia, USA

Grace E Olsson
Position (at Institution/Hospital/Company)
Research assistant at the George Washington University

Rohan V Patil
Position (at Institution/Hospital/Company)
Research assistant at the George Washington University

Samantha J Chin
Position (at Institution/Hospital/Company)
PhD candidate at the George Washington University

Katharine N Rus
Position (at Institution/Hospital/Company)
Research assistant at the George Washington University

Dr. Elizabeth E Sweeney
Position (at Institution/Hospital/Company)
Assistant Research Professor

Dr. Karun V Sharma
Position (at Institution/Hospital/Company)
Director of Interventional Radiology at Children's National Hospital

Dr. Rohan Fernandes
Position (at Institution/Hospital/Company)
Associate Professor at the George Washington University

Abstract

Neuroblastoma is an aggressive solid tumor most frequently observed in childhood and is associated with poor outcomes despite various available treatment strategies (e.g. chemotherapy, radiation therapy). Photothermal therapy (PTT) is a promising strategy to treat tumors such as neuroblastoma using a nanoparticle-based photothermal agent. Prussian blue nanoparticles (PBNPs), as studied by our lab, are optimal nanoparticles to use as photothermal agents as they have limited toxicity and are FDA-approved to treat radioactive poisoning. When irradiated with a near infrared wavelength laser, the PBNPs absorb the light and convert it to heat, causing thermal ablation, tumor cell death, and local as well as abscopal immune effects. Our earlier findings reveal that PBNP-based PTT (PBNP-PTT) is an effective strategy for treating neuroblastoma *in vivo* when the laser light is administered superficially, but this approach, while successful in laboratory settings, is associated with translational limitations. Specifically, superficially administered lasers are typically unable to penetrate the entire tumor depth, and may deliver heterogeneous thermal doses across tumor tissue, thereby generating variable cytotoxicity, suboptimal tumor regression, which ultimately drives tumor recurrence. Interstitial PTT (I-PTT) is a promising alternative that comprises a laser diffuser placed intratumorally using a catheter to administer PTT from the “inside out”. In this context, ultrasound-based image guidance can be used to accurately position the laser diffuser within a tumor, facilitating more

consistent laser delivery, which may provide more effective treatment responses. Motivated by the potential benefits of using ultrasound-guided I-PTT as a precise and effective therapy for neuroblastoma, in this study we assess the effect of ultrasound-guided I-PTT on neuroblastoma tumor control compared to controls.

In order to test feasibility of the study, 2% agar gel phantoms were injected with PBNPs and the laser fiber was inserted using ultrasound guidance. Optimal needle and fiber position was achieved by direct visualization with an ultrasound probe. Building on these phantom studies, we conducted a pilot study in a TH-MYCN derived 9464D syngeneic model of neuroblastoma. In this pilot study, 15 C57BL/6 mice were inoculated with 1e6 9464D neuroblastoma tumor cells in 100 µL of 1:1 PBS/Matrigel in the flank. Once tumors became palpable (at least ~5 mm in each dimension), the mice were randomized into three groups (n=5/group). Tumor volumes for each animal were normalized relative to their initial volume at the day of treatment to monitor tumor progression. Five mice were treated with ultrasound guided I-PTT (US I-PTT), five mice were given I-PTT treatment without ultrasound guidance (blinded), and five mice were left untreated. Mice were regularly visualized by the Vevo 3100 ultrasound system to monitor tumor growth and progression in B-mode cross-sectional 2D images. For all groups, tumors were confirmed with ultrasound imaging by identifying a hypoechoic region characteristic of the tumor. For the mice in the US I-PTT group, hypoechoic tumor structures served as landmarks for optimal needle guidance during treatment. On day 8 post-treatment, the normalized tumor volume for the US I-PTT group (0.503 ±0.367) was significantly smaller than both the blinded treatment group volume (4.20 ±1.09) and the control group (6.64 ±1.82). Additionally, the one-way ANOVA test demonstrated a statistically significant difference in mean value for each experimental group (0.003). Together, these proof-of-principle results demonstrate the value of using ultrasound guidance for I-PTT treatment and the potential of this approach to provide a more accurate and effective treatment for neuroblastoma. Despite these results, through both t-test and one-way ANOVA, there was no statistical significance seen after day 8 post-treatment. Ongoing studies and future studies will be dedicated to increasing sample sizes, analyzing animal survival post-treatment and assessing tumor immune characteristics post-treatment via flow cytometry and immunohistochemistry.

23

Nanoparticle-Based Photothermal Therapy Generates Multi-Targeted T Cells for Glioblastoma Therapy

Danielle E Schmidt[1], Palak Sekhri[2], Erin E Grundy[3,4], Samantha Chin[5,3], Josh Ghofrani[5,3], Katherine B Chiappinelli[4], Catherine M Bollard[5,2], Carlos E Sanchez[5], C. Russell Y Cruz[5,2], Elizabeth E Sweeney[5,6], Rohan Fernandes[5,3,7]

[1]George Washington Cancer Center, School of Medicine and Health Sciences, Washington DC, District of Columbia, USA. [2]Center for Cancer and Immunology Research, Children's National Hospital, Washington DC, USA. [3]The Integrated Biomedical Sciences Program, School of Medicine and Health Sciences, Washington DC, USA. [4]Department of Microbiology, Immunology, and Tropical Medicine, Washington DC, USA. [5]George Washington Cancer Center, School of Medicine and Health Sciences, Washington DC, USA. [6]Department of Biochemistry & Molecular Medicine, School of Medicine and Health Sciences, Washington DC, USA. [7]Department of Medicine, School of Medicine and Health Sciences, Washington DC, USA

Katherine B Chiappinelli
Position (at Institution/Hospital/Company)

Abstract

The goal of this study is to investigate the use of nanoparticle-based photothermal therapy to generate multi-antigen, targeted T cells for glioblastoma (GBM). GBM is a deadly cancer that impacts >13,000 patients per year. Adoptive T cell therapy (ATCT) is a promising immunotherapeutic approach that uses autologous or allogeneic T cells to target and lyse tumor cells. While chimeric antigen receptor (CAR) T cells have shown promising results in treating hematological malignancies, they have had limited efficacy against solid tumors. GBM is particularly hard to treat with current ATCT approaches because it is notably heterogeneous among patients and within a patient's tumor. Because CAR T cells and other ATCTs are designed based on previously identified antigens, GBM cells that do not express the chosen target can resist therapy and cause recurrence. To address these mechanisms of treatment failure, we have developed a novel tumor-specific T cell expansion platform that uses Prussian blue nanoparticle-based photothermal therapy (PBNP-PTT). Here, we describe the use of PBNP-PTT to generate T cells specifically targeted to GBM U87 cell lines as well as primary GBM tumor samples from patients. To generate "PTT-T" cells, we administer PBNP-PTT at a specific thermal dose to elicit cytotoxicity and immunogenic cell death in GBM cells. Then, the PBNP-PTT-treated tumor cells are co-cultured with dendritic cells (DCs) and T cells to facilitate the expansion of T cells designed against multiple antigens in GBM in an agnostic and personalized manner. Our recently published papers illustrated that several healthy donor-derived GBM-specific T cells are specific and cytotoxic against target cells both *in vitro* and in orthotopic animal models *in vivo*. GBM-specific T cells generated by PBNP-PTT exhibited selective expansion of a subset of TCR clones and increased cytotoxic phenotype as measured by TCR sequencing and flow cytometry. Despite these promising results, the translation of this PBNP-PTT-based ATCT product is limited by a lengthy manufacturing period (23 days) and the cumbersome and harsh handling of DCs. To improve the manufacturing process, which has implications for speed of product availability and production cost, we performed optimization studies which demonstrated that *ex vivo* stimulation of T cells by DCs for 12 days, rather than 20 days, produced comparable cytotoxicity and shortened the overall manufacture time to 15 days from 23. Additional optimizations included direct delivery of naïve T cells to the DC-tumor co-culture in order to limit handling of DCs, which yielded 100% cytotoxicity of the GBM-specific T cell product at

various effector cell to target cell ratios. These preliminary findings suggest both the improved efficacy and efficiency of our product after the optimization studies. Together, our findings demonstrate the promise of our nanoparticle-based photothermal therapy to generate potent T cells for treating GBM, which has the potential to expand the pool of targeted antigens and provide advantages over other ATCTs.

24

A multiphysics multiscale model of photobiomodulation therapy for hearing preservation

Mason Forshage MSc[1], Ricardo Rodriguez BSc[2], Fateme Esmailie PhD[2]
[1]University of North Texas, Dentin, TX, USA. [2]University of North Texas, Denton, TX, USA

Fateme Esmailie
Position (at Institution/Hospital/Company)
Assistant Professor

Abstract

Introduction:

Hearing loss is one of the most common human medical conditions that happens due to aging, congenital conditions, genetic issues, and exposure to noise or ototoxic drugs. More than 30% of adults above 65 suffer from some degree of hearing difficulty in the United States [National Center for Health Statistics. Percentage of any difficulty hearing for adults aged 18 and over (95% confidence intervals), United States, 2019—2022]. Despite the success of hearing aids and cochlear implants in improving the patient's life quality, these treatments face some challenges, including high cost, risk of damaging remaining hearing ability, limitation in restoring all features of natural sound perception, and risk of post-operation infection in cochlear implants. Hearing loss prevention mitigates the need for cochlear implants and hearing aids and provides individuals with a healthier, sustainable life.

Medication, hypothermia, hyperthermia, and photobiomodulation therapy (PBMT) have been studied as possible methods to prevent hearing loss. Hypothermia and medications may lead to adverse events such as interruption of necessary free radical accumulation, coagulation mechanism, impaired immune function, longer hospitalization, cardiac events, and wound infection. The near-infrared (NIR) light that is used in photobiomodulation can be absorbed by the cochlear fluid, cause mild hyperthermia, and lead to triggering the release of heat shock proteins (HSP). Even though this mechanism can boost the effectiveness of photobiomodulation, it also may lead to intracochlear thermal damage. Therefore, a thermal model can ensure the thermal safety of PBMT.

Methods:

We integrated our finite element heat transfer and fluid dynamics model of the cochlea with Monte-Carlo ray tracing and finite difference biological reaction models to find the combination of wavelength, intensity, and duration of photo-thermal therapy that prevents hearing loss. This combination depends on the source of hearing damage, the size of the cochlea and temporal bone, and the diameter of the NIR laser. The most common wavelength of near-infrared light used in PBM is in the range of 800-1000 nm, which can penetrate human tissues up to 5 mm.

Heat transfer within human tissues is determined by the Pennes Equation and includes accumulation term, conduction, convection (in the form of perfusion and other biological fluid flows), radiation, metabolic heat generation, and any other heat source. We estimated the maximum value of each term in Pennes Equation by applying the concept of thermal dose and limiting the maximum safe temperature to 43^{o}C. In PBMT, metabolic heat generation is subject to change due to the release of ATP and HSP. The heat source in PBMT is the absorbed light, and the perfusion rate is subject to change in PBMT.

We used conservation of mass equations for the reaction that leads to the release of HSPs as they are listed in [Szymańska, Z. & Zylicz, M. Mathematical modeling of heat shock protein synthesis in response to temperature change. *J Theor Biol* 259, 562–569 (2009)]. This model consists of nine ordinary differential equations, which were solved using the Runge-Kutta method. The impact of temperature on these chemical reactions will be added using the fraction of protein denaturation. Similarly, we defined a system of ode equations for predicting the electron transport and ATP synthesis. The equilibrium constants are functions of temperature. PBMT impacts the release of ATP by providing energy to open ion channels without causing a measurable increase in temperature.

Conclusion:

We modeled this phenomenon by incorporating the impact of light wavelength on the reaction's equilibrium constants. We developed a multiscale multiphysics computational model that can be used to understand the impact of integrated mechanisms of photobiomodulation and hyperthermia on hearing loss prevention and avoiding potential adverse events. We validated the results with *In-Vitro* models.

25

Computational modeling of magnetic nanoparticle hyperthermia to predict the spatial distribution of intratumoral temperatures: Preliminary study

Mahesh Nandyala[1,2], Ahmed A El-Gendy[3], Chengyue Wu[1,4,5,6,2], R Jason Stafford[1], John D Hazle[1], Thomas E. Yankeelov[7,8,9,10,2,1], David Fuentes[1]

[1]Department of Imaging Physics, Division of Diagnostic Imaging, The University of Texas M.D. Anderson Cancer Center, Houston, Texas, USA. [2]Oden Institute for Computational Engineering and Sciences, The University of Texas at Austin, Austin, Texas, USA. [3]Department of Physics, University of Texas at El Paso, El Paso, Texas, USA. [4]Department of Breast Imaging, Division of Diagnostic Imaging, The University of Texas M.D. Anderson Cancer Center, Houston, Texas, USA. [5]Department of Biostatistics, The University of Texas M.D. Anderson Cancer Center, Houston, Texas, USA. [6]The Institute for Data Science in Oncology, The University of Texas M.D. Anderson Cancer Center, Houston, Texas, USA. [7]Department of Biomedical Engineering, The University of Texas at Austin, Austin, Texas, USA. [8]Department of Diagnostic Medicine, The University of Texas at Austin, Austin, Texas, USA. [9]Department of Oncology, The University of Texas at Austin, Austin, Texas, USA. [10]Livestrong Cancer Institutes, The University of Texas at Austin, Austin, Texas, USA

Abstract

Introduction

The objective of this study is to predict the spatial distribution of intratumoral temperatures during magnetic hyperthermia treatment using computational modeling. Magnetic nanoparticle hyperthermia has shown promise in cancer treatment due to its ability to locally induce cell death within tumors. However, it is important to understand the temperature changes and their spatial distribution during treatment to optimize therapeutic results and minimize damage to surrounding tissues.

Methods

Experimental: In vivo specific absorption rates were estimated via surface temperature measurements during hyperthermia on subcutaneous tumors in mice using an alternating magnetic field (AMF) generator. The mice are placed in a double-hole coil animal bed, and the temperature sensor is attached to the tumor surface. The exposure time was 20 min under AMF of H=150Oe and f=164kHz. The temperature versus time (Txt) was collected, and SAR was calculated from the initial slope of the Txt curve.

Computational: A steady-state Pennes' bio-heat transfer model, coupled with the estimated specific absorption rates, was used to predict the tumor temperature distribution. Assuming the uniform distribution of nanoparticles within a volume equal to injected nanofluid, we predicted the rise in intratumoral temperature. By representing experimental mice in a 3D computational model and solving the mathematical model with a Dirichlet boundary condition on the surface touching the animal bed and a convective boundary condition on the remaining surface steady-state temperature distribution was predicted. The mathematical model was implemented in the finite element-based software package COMSOL Multiphysics. The accuracy of prediction is evaluated by comparing it to the experimental measurement of tumor surface temperature.

Results

The in vivo experiments showed a 2.6±0.1°C increase in tumor surface temperature, while our computational modeling predicted a rise of 3.096 ±0.172°C (mean±95%CI) for different physiological conditions (varying blood perfusion and metabolic heat generation rates), showing a reasonable match between the model and experiment.

Discussion and Conclusion

This initial work demonstrates the model may be able to simulate the spatial distribution of intratumoral temperatures with varying physiological parameters, which is difficult to obtain experimentally. Additional experiments are needed to improve and validate the computational accuracy. However, the computational model has the potential to optimize and guide how magnetic hyperthermia can be applied to cancer treatment.

Keywords: Magnetic nanoparticles, Hyperthermia, Bio-heat transfer, Finite elements, Temperature elevation.

26

Systemic exposure after thermoembolization in a swine model

Dr. Erik N.K. Cressman PhD, MD, Dr. Danielle L. Stolley PhD, Dr. Waldemar Priebe PhD, Edd Felix MS, Steve Parrish BS
MD Anderson Cancer Center, Houston, TX, USA

Dr. Erik N.K. Cressman
Position (at Institution/Hospital/Company)
Associate Professor

Dr. Danielle L. Stolley
Position (at Institution/Hospital/Company)
Research Scientist

Dr. Waldemar Priebe
Position (at Institution/Hospital/Company)
Professor

Edd Felix
Position (at Institution/Hospital/Company)
Research Scientist

Steve Parrish
Position (at Institution/Hospital/Company)
Senior Medical imaging Technologist

Abstract

Introduction: Thermoembolization is an experimental, minimally invasive, catheter-directed therapy for unresectable tumors. It was designed to use local chemistry to address incomplete treatment seen with existing methods such as chemoembolization or radioembolization. It is an exothermic procedure due to the energy release on reaction of an acid chloride or other strong electrophile. A way to combine heat, local chemical ablation, ischemia, and a high local drug concentration would be an appealing line of investigation if a drug remained in the target area as hypothesized. A key question is how much of a delivered dose escapes from the target zone and thus could cause off-target toxicity. We report here on our initial experience in vivo with thermoembolization using 2-propylpentanoyl chloride, measuring plasma levels of the reaction product valproate.

Materials and Methods:

Experiments were conducted under an IACUC-approved protocol. Domestic swine (n=3) under general anesthesia had 5F access sheaths placed in the common femoral artery for delivery and vein for sampling. Imaging was performed to define anatomy at baseline. Under fluoroscopy, a 2.7F microcatheter was advanced through a reverse-curve base catheter seated at the origin of the celiac artery to select a single lobar hepatic artery. Baseline labs (liver panel, blood count) were drawn. Timed blood draws (5 mL each) were started 2 minutes prior to thermoembolization and continued at intervals for 2h following delivery. The embolic solution consisted of 400-600 µL of freshly prepared 2-propylpentanoyl chloride at 1 mol/L in ethiodized oil. Plasma was isolated and frozen for later analysis. Animals were recovered, and 3-7 days later, again under anesthesia, an intravenous bolus dose of sodium valproate (20 mg/kg) was administered as a positive control. Starting 2 minutes prior to the dose as before, labs and timed blood draws for

plasma were obtained. Analyses for valproate were done by LC/MS in triplicate and plotted against known standards used to generate a standard curve.

Results: Animals tolerated the procedure well. Experimental samples showed either no spike or a barely detectable rise in concentration and immediate return to baseline. Positive controls from intravenous dosing showed the expected early spike in plasma concentration which rapidly decreased with time.

Conclusion: Based on the extremely low levels of valproate detected in experimental samples, thermoembolization confines a delivered dose primarily to the target vascular bed with little to no systemic exposure. The multiplexed effects rapidly and durably disrupt perfusion in the target tissue. Accordingly, 2-propylpentanoyl chloride based thermoembolization has potential as a therapeutic strategy for treatment of solid tumors.

29

Evaluation of the value of invasive versus skin temperature measurements as predictive hyperthermia parameters for locoregional tumor control in locoregional recurrent breast cancer patients treated with postoperative re-irradiation and hyperthermia

Drs. Paola Tello Valverde MSc[1,2], Dr. Petra Kok PhD[1], Drs. Willemijn Kolff MD[1], Prof. Dr. Ben Slotman MD, PhD[2], Dr. Hans Crezee PhD[1]

[1]Amsterdam UMC, location University of Amsterdam, Department of Radiation Oncology, Amsterdam, North Holland, Netherlands. [2]Amsterdam UMC, location Vrije Universiteit Amsterdam, Department of Radiation Oncology, Amsterdam, North Holland, Netherlands

Drs. Paola Tello Valverde
Position (at Institution/Hospital/Company)
PhD Candidate and Clinical Epidemiologist

Dr. Petra Kok
Position (at Institution/Hospital/Company)
Principal Investigator

Drs. Willemijn Kolff
Position (at Institution/Hospital/Company)
Radiation Oncologist

Prof. Dr. Ben Slotman
Position (at Institution/Hospital/Company)
Professor and Chairman of Department of Radiation Oncology

Dr. Hans Crezee
Position (at Institution/Hospital/Company)
Research Physicist and Principal Investigator

Abstract

ABSTRACT:

Hyperthermia is used for treatment of locoregional recurrent (LRR) breast cancer. Hyperthermia at 40-43°C acts synergistically with ionizing radiation and chemotherapeutic agents. To achieve this temperature goal it is important that superficial hyperthermia device has the ability to penetrate the target location depth and to have extensive well-documented thermometry with multiple sensor thermocouple probes. Cooling with a circulating water bolus during the treatment is applied to augment the penetration depth. There is a debate whether invasive intratarget and skin surface temperature measurements have a relationship with locoregional tumor control (LRC). We therefore investigated the association of various invasive and skin hyperthermia parameters with LRC for patients with LRR breast cancer treated with postoperative re-irradiation and hyperthermia.

METHODS:

This historical cohort study included 112 women with LRR breast cancer who were treated between 2010-2017 with postoperative re-irradiation 8x4Gy (n=34) or 23x2Gy (n=78), combined with 4-5 weekly hyperthermia sessions. Superficial hyperthermia was given with

microstrip applicators operating at 434MHz with a penetration depth of circa 4cm (Medlogix, Rome, Italy). Both intratarget guided invasive thermometry and extensive skin surface thermocouple thermometry were employed to monitor and measure tumor target temperatures in each session. For each patient seven-sensor copper-constantan thermocouple probes (Volenec RD Inc., Hradec Králové, Czech Republic) were placed invasively (8 ± 5 sensors) for intratarget monitoring, and similar probes were placed on the skin surface (80 ± 30 sensors). Based on Weibull univariate and multivariate stepwise backward regression analysis, the highest invasively and skin surface measured thermal dose CEM43°CT_{50} (median cumulative equivalent minutes at 43°C) and average T_{50} (median cumulative temperature in °C) were selected to analyze relationships between thermal dose or temperature and LRC. Tumor location breast/chest wall, lymph node involvement and age were also included in the model. Additionally, Pearson correlation coefficient analysis between invasive and skin surface hyperthermia parameters was performed.

RESULTS:

Twenty-four patients (21.4%) developed an infield recurrence; with a median time to recurrence of 3.4 years (interquartile range (IQR) 2.7-4.6 years). Median highest hyperthermia session CEM43°CT_{50} for invasive and skin surface were 7.2 minutes (IQR 3.4-15.9) and 2.8 minutes (IQR 2.0-4.3), respectively. For average T_{50}, the median invasive and skin temperatures were 40.7°C (IQR 40.0-41.3) and 40.6°C (IQR 40.3-40.8), respectively. Univariate and multivariate analysis showed no association between skin surface temperature parameters and LRC (P=0.131; P=0.215, respectively), but invasive intratarget temperature parameters did show a significant association with LRC (P=0.015; P=0.021, respectively). Pearson correlation analysis showed no significant association between the intratarget and skin temperature parameters. The close proximity of the water bolus is likely to be a major reason for the absence of correlation between skin temperature measurements and LRC.

CONCLUSION:

Invasively intratarget thermometry was and skin thermometry was not significantly associated with LRC in patients with LRR treated with postoperative re-irradiation combined with superficial hyperthermia. These results are relevant for the clinical practice when it comes to treatment delivery and stressed once again the paramount value of invasive thermometry.

30

Reducing chemotherapeutic toxicity by thermosensitive liposomal drug delivery combined with extracorporeal blood filtration

Dr. Danforth A Newton[1], Dr. Pratikshkumar Patel[1], Dr. A. Marissa Wolfe[1], Dr. Anjan Motamarry[2], Dr. Krishna K Ramajayam[3], Dr. Dieter Haemmerich[1,4]
[1]Medical Univ. of South Carolina, Charleston, SC, USA. [2]AstraZeneca, Boston, MA, USA. [3]Unchained Labs, Pleasanton, CA, USA. [4]Clemson Univ., Clemson, SC, USA

Dr. Danforth A Newton
Position (at Institution/Hospital/Company)
Staff Scientist

Dr. Pratikshkumar Patel
Position (at Institution/Hospital/Company)
Post-doctoral fellow

Dr. Krishna K Ramajayam
Position (at Institution/Hospital/Company)

Abstract

Background/rationale: Systemic toxicities from chemotherapeutic agents limit the dosage and potential effectiveness of many cancer treatments. For widely-used doxorubicin, toxicities can occur during treatment (e.g., hematological effects) and long after (e.g., permanent cardiovascular damage). Incorporation of such drugs into thermosensitive liposomal nanoparticles (TSL) allows delivery of high doses directly to solid tumors upon heat-stimulated release within the tumor vasculature. This approach results in rapid drug escape from tumor capillaries and should decrease extraneous doxorubicin delivery to non-tumor tissue. We hypothesize that remaining circulating doxorubicin concentration could further be reduced by extracorporeal filtration following TSL treatment, with measurable reduction of systemic toxicity.

Methods: In a pilot study to demonstrate feasibility and potential efficacy of this approach, brown Norway rats (n=5 to date) were subjected to baseline cardiovascular measurements by ultrasound before surgically inserting jugular vein and carotid artery catheters with external, back-mounted ports. For treatment animals, extracorporeal circulation (ECC), driven by a peristaltic pump, was started 30-min post-injection of TSL-encapsulated doxorubicin (7 mg/kg) to transport blood from the carotid catheter through a 43^{o}C heating element to release dox, then through a column containing activated charcoal, before returning to the animal through the jugular catheter. ECC continued for 1 hr, with blood collection both before and after the column every 15 min (for plasma chemistry, cell counts and dox quantification). Control animals were subjected to the same surgery and TSL-dox injection, but no ECC. After treatment, animals were followed for 6 wks by weekly blood sampling, cardiac imaging (echocardiography of left ventricular function), and vascular imaging (vascular ultrasound to quantify changes in pulse propagation velocity, an early biomarker of cardiac chemo-toxicity). Measured parameters were compared between groups of animals using t-tests and ANOVA.

Results: After experimental optimization, the ECC setup was shown to be feasible, with no observed detrimental effects. Between 20-30% of circulating doxorubicin was removed by the filtration column in test rats, but the treatment did not result in significant reduction of major plasma electrolyte or protein concentrations. All measured blood chemistry parameters had returned to base level ranges by the day after the treatment, and animals were able to complete the 6-week study. There were no significant differences with post-experimental blood cell counts between test and control animals (neutrophils, total WBCs and RBCs returned to base ranges within 2 weeks post-treatment). While ECC test animals showed little change throughout the study in abdominal aortic pulse propagation velocity (PPV), control animals demonstrated an average of 49% increase in PPV ($p=0.036$, ctrl vs exp at wk 6).

Conclusions: A method for extracorporeal removal of circulating doxorubicin released from thermosensitive liposomes was determined to be safe and effective in rats. Aortic stiffening, an early indicator of long-term doxorubicin-induced cardio-toxicity, was reduced in treated animals. Further optimization of this approach could increase efficacy of drug removal, and increased statistical power may reveal additional discernable effects of this treatment.

31

Computer modeling and image processing to study hemodynamics in congenital heart defects

Charles Puelz[1], Dan Lior[1], Justin Weigand[1], Mette Olufsen[2], Alyssa Taylor-LaPole[2]
[1]Baylor College of Medicine and Texas Children's Hospital, Houston, Texas, USA. [2]North Carolina State University, Raleigh, North Carolina, USA

Abstract

This talk will focus on our recent efforts to develop computer modeling and image processing techniques for the study of hemodynamics in the Fontan circulation, a common post surgical physiology for children born with a single ventricle. The clinical questions of this study are related to the effect of the Norwood surgically reconstructed aorta on peripheral blood flow, perfusion, and other quantities that exist outside of the imaged thoracic region. We will describe approaches to register MRA images of the vessel anatomy with 4Dflow images of the time-resolved blood velocity field. We will also discuss methods to incorporate these images into the calibration of vessel network computer models for the prediction of peripheral perfusion and other clinical variables outside of the imaged region.

32

Preventing Local Recurrence Following Surgical Tumor Resection With Thermosensitive Liposomes

Dr. Pratikshkumar R Patel[1], Dr. Danforth A Newton[1], Dr. David Wang[1], Dr. Dieter Haemmerich[1,2]

[1]Medical Univ. of South Carolina, Charleston, SC, USA. [2]Clemson Univ., Clemson, SC, USA

Dr. Pratikshkumar R Patel
Position (at Institution/Hospital/Company)
Post-doctoral fellow

Abstract

Background: Residual cancer cells following surgical tumor excision are responsible for local cancer recurrence, posing a significant challenge. To address this, we developed a method for delivering a large chemotherapy dose to the surgical margin. After tumor resection, we administered thermosensitive liposomes (TSL) loaded with doxorubicin (Dox), followed by exposure of the surgical cavity to infrared laser hyperthermia. The goal was to eliminate residual cancer cells to prevent local tumor recurrence.

Method: The efficacy of our approach was evaluated in a mouse model using luciferase-labeled human RH-30 rhabdomyosarcoma cells. First, *in vitro* cytotoxicity of Dox in RH-30 Luc cells was determined by incubation with Dox for 1 hr, drug removal, then luminescence imaging of cells after 24 hr of culture. In mouse studies, RH30 Luc cells were subcutaneously injected into two groups of athymic nude mice (n=4/group) to form tumors (5-8 mm). Tumors were then partially removed, leaving a small fraction (~1-2 mm) behind to simulate an incomplete surgery with residual cancer cells. In the surgery control group (S), the surgical incision was closed after surgery without further treatment. In the treatment group (SDH), immediately after resection (with surgical cavity still accessible), TSL-Dox (5 mg/kg) was administered intravenously. The region of the remaining tumor fragment in the surgical cavity was then exposed to laser hyperthermia (43°C for 30 min), to locally deliver Dox to the remaining cancer cells. The laser hyperthermia was carried out inside an *in vivo* imaging system for luminescence imaging of tumor and fluorescence imaging of Dox. After treatment, mice were followed bi-weekly with luminescence imaging and tumor size measurement, until any recurrent tumors reached 10 mm in size.

Results: The cytotoxicity study with the RH-30 Luc cell line found an LD50 of 1.6 µg/ml for Dox after 24 hr. For mice in the SDH group, in 2 mice tumors disappeared without recurrence before the 90-day study endpoint. A 3rd mouse hasn't shown any recurrence after 61 days and is still being followed. The 4th mouse developed a tumor and was sacrificed 44 days post-treatment when tumor size reached the endpoint. In contrast, all 4 mice in the control group (S) experienced local recurrence, with an average of 15.25±6.73 days to reach their tumor size endpoint. Mean survival time was significantly longer for animals in the SDH group (p=0.005).

Conclusions: We present a novel method for eradication of residual cancer cells after surgery. The combination of TSL-Dox and laser hyperthermia enabled targeted chemotherapy delivery to the surgical margin, preventing local recurrence in 3 out of 4 mice. This therapy has potential clinical application in cancer types with high local recurrence rates, such as certain soft tissue sarcoma or pancreatic cancer.

33

Engineering syngeneic murine glioma-specific T cells using nanoparticle-based photothermal therapy

Katharine N Rus BS[1], Danielle E Schmidt BS[1], Grace E Olsson BS[1], Rohan V Patil BS[1], Russell Y Cruz M.D., Ph.D.[2], Elizabeth E Sweeney Ph.D[1,3], Rohan Fernandes Ph.D[1,4,5]

[1]George Washington Cancer Center, School of Medicine and Health Sciences, George Washington University, Washington, District of Columbia, USA. [2]Center for Cancer and Immunology Research, Children's National Hospital, Washington, District of Columbia, USA. [3]Department of Biochemistry & Molecular Medicine, School of Medicine and Health Sciences, George Washington University, Washington, District of Columbia, USA. [4]The Integrated Biomedical Sciences Program, School of Medicine and Health Sciences, George Washington University, Washington, District of Columbia, USA. [5]Department of Medicine, School of Medicine and Health Sciences, George Washington University, Washington, District of Columbia, USA

Katharine N Rus
Position (at Institution/Hospital/Company)
Research assistant

Danielle E Schmidt
Position (at Institution/Hospital/Company)

Grace E Olsson
Position (at Institution/Hospital/Company)

Russell Y Cruz
Position (at Institution/Hospital/Company)

Abstract

The prognosis for patients with glioblastoma (GBM) remains dismal, with a relative five-year survival rate of 7.5%, a consequence of extensive intertumoral heterogeneity and other factors. Hence, there is an urgent need for personalized novel therapies for this patient population that directly address cellular heterogeneity in each patient. Adoptive T cell therapy (ATCT) has been successful in treating hematological malignancies, and is currently under investigation for solid tumor therapy. In contrast to existing chimeric antigen receptor (CAR) T cell and/or antigen-specific T cell approaches which require known targets, and responsive to the need for targeting a broad repertoire of antigens in GBM, we have described the first use of immunostimulatory photothermal nanoparticles to generate tumor-specific T cells. Using partially HLA-matched healthy donor peripheral blood mononuclear cells (PBMCs), we recently published that Prussian blue nanoparticle-based photothermal therapy can be used to generate multi-targeted GBM-specific T cells that are effective against GBM cell lines both *in vitro* and *in vivo*. Although these studies are promising, they do not reflect the envisioned clinical scheme of developing an autologous ATCT using PBNP-PTT. Further, the *in vivo* studies were performed using xenografts in immunodeficient NSG mice. Thus, there is a need to establish an autologous or syngeneic model with which to test the PBNP-PTT-based ATCT platform in an immunocompetent murine system. This will enable us to rigorously evaluate the therapeutic potential of this ATCT platform, especially in the context of an intact and immunosuppressive tumor microenvironment. Here, we seek to describe the generation of syngeneic tumor-specific T cells using PBNP-PTT.

To this end, we subjected whole murine GL261 glioma cells (syngeneic to C57BL/6 mice) to PBNP-PTT to induce immunogenicity of the tumor cells. Syngeneic dendritic cells (DCs) and T cells were isolated from the bone marrow and spleens of healthy C57BL/6 mice, respectively. DCs were then cultured with IL4 and GM-CSF for three days. Next, we cultured the PBNP-PTT-treated GL261 cells with DCs for 4 hours and cultured the DCs in maturation cytokines overnight. The following day, these primed DCs were co-cultured with the splenic T cells and supplemented with IL6, IL7, IL12, IL15 to promote the expansion of GL261-specific T cells.

In proof-of-concept studies, we demonstrated that when PBNP-PTT was administered at a thermal dose to induce the immunogenicity of GL261 cells, we expanded GL261-specific murine T cells, that had a mixed population of CD4+ and CD8+ cells. Upon co-culture with target GL261 cells, GBM-specific T cells secreted IFN-ɣ in a specific and dose-dependent manner. At an E:T ratio of 1:1, T cells expanded using PBNP-PTT secreted IFN-ɣ two-fold compared to T cells alone, suggesting that the T cells were specifically activating in response to the target cells. These findings provide proof-of-concept data supporting the potential of using PBNP-PTT in a syngeneic murine model to stimulate and expand tumor-specific T cells *in vitro*. Ongoing investigation is testing the cytolytic functionality of PBNP-PTT-derived glioma-specific T cells in cytotoxicity assays, and evaluating the efficacy of the T cells to delay tumor growth and improve survival in GL261 tumor-bearing mice. These studies in syngeneic murine models aim to inform the development of a novel PBNP-PTT-based autologous ATCT approach for patients with GBM.

34

Magnetic Nanoparticle Hyperthermia Therapy: Past, Present and Future

Associate Professor Ahmed A. El-Gendy PhD
University of Texas at El Paso, El Paso, TX, USA

Associate Professor Ahmed A. El-Gendy
Position (at Institution/Hospital/Company)
Associate Professor of Physics at University of Texas at El Paso

Abstract

Hyperthermia is a therapeutic anti-cancer treatment which raises the temperature of tumor tissue in-vivo. This method applies the fact that a cancer cell-killing effect is caused when a temperature above 41-42 ^{o}C is maintained in the target volume. At higher temperatures, the effect is called 'thermoablation'. However, for the past decades, hyperthermia was struggling to be one of the most successful cancer therapy due to non-localization of the induced heating power leading to damage of the surrounded normal cells. After the revolution of nanotechnology, new applications have been revealed in particular nanomedicine including drug delivery, agents for magnetic resonance imaging and the possibility of internalizing small nanomaterials to the tissue becomes possible. With the new field, scientist gave hyperthermia another chance to be successful as cancer therapy by using nanoparticles that can be internalized to the tumors to produce localized efficient heat inside the tumor cells and to minimize the damage of the normal cells due to non-localized heat. However, many parameters were needed to be optimized such as biocompatibility of the nanoparticles with the tissue, physical/chemical properties, size control, aggregation due to the large surface to volume ratio. If not optimized, those parameters lead to 1) lack of efficient induced heating power to the tumor tissue, 2) excess heat and side effect to the surrounded normal tissues, and 3) lack of successful targeting to the tumors. These factors were and still the main obstacles for the clinical use of hyperthermia until this moment.

In recent years, great progress has been made in this respect and nano-sized materials with novel properties have already found or exhibit at least a great potential for applications in the fields of, e.g., optics, magnetism, electricity, catalysis, and biomedicine. Because of their novel magnetic properties, magnetic nanoparticles offer attractive potentials not only for fundamental science value but also for technological innovations. One possible field of application of magnetic nanomaterials is their usage in biology and medicine. The applicability of such methods relies on the fact that magnetic fields only very weakly interact with organic materials and do not cause known side effects. Once magnetic nanoparticles are internalized in a particular organic environment such as, e.g., the human body, external magnetic fields can be applied in order to address these magnetic agents. In general, external static magnetic fields can fix ferromagnetic nanoparticles at a precise position, gradient fields can move them and alternating magnetic fields will yield heating of the nanoparticles. It is the latter effect that opens a completely new route for anti-cancer therapies: Once internalized in tumor tissue, such a heating effect can be utilized for so-called 'magnetic nanoparticles hyperthermia' (MNH).

When aiming at realizing hyperthermia as independent cancer therapy, however, much research is required to be done on the laboratory scale to preclinical stages. Therefore, the talk focusses on summarizing the work have been done in hyperthermia in the past and highlighting the present and the future directions to make hyperthermia is the future and most efficient cancer therapy.

35

Clinical Estimation of Hyperthermia Treatment Effectiveness: The Importance of Adequate Perspective

John Pearce PhD[1], Jack Hoopes DVM, PhD[2]
[1]The University of Texas at Austin, Austin, TX, USA. [2]Dartmouth College, Hanover, NH, USA

John Pearce
Position (at Institution/Hospital/Company)
Temple Foundation Professor Emeritus
Chandra Family Department of Electrical & Computer Engineering

Jack Hoopes
Position (at Institution/Hospital/Company)
Professor of Radiation Oncology, Surgery and Engineering
Director, Center for Comparative Medicine,
Director, Imaging and Irradiation Resource
Geisel School of Medicine /Dartmouth Cancer Center/Thayer School of Engineering

Abstract

For many decades the assessment of hyperthermia treatment effectiveness has relied on calculation of CEM @ 43 C. This results in a single number that gets larger without providing additional perspective on the likelihood of a successful treatment. While some indication of the probability of loss of clonogenicity among CHO (and analogous) cells can be extracted, there are many different CA cell types and other indicators of thermally-initiated irreversible changes in cells that suggest some cells are more robust against thermal stress than the CHO (and the like) cells. Some assays of thermal damage and cell death closely follow the single-step irreversible reaction kinetics at the root of a CEM calculation, but many important ones do not, particularly those that depend on functional protein cascades. Indeed, in the original CEM clonogenicity data there is a time-delay at 43 C of around 60 minutes during the slowly-developing shoulder region before the constant rate region develops, the region from which the CEM time-scaling ratio R_{CEM} was derived.[1] An initial time-delay shoulder region is a common characteristic of many intrinsic cell death processes, but not all.

For example, SN12 cells appear to be much more thermally-robust than most other CA cell lines. Different assays in the same cell line can exhibit substantially different kinetic responses to thermal stress. Some assays follow single constituent Arrhenius kinetics (an exponential decay curve) quite well, while others do not. Even so, an excellent estimate of overall cell alterations can be obtained by adding a temperature-dependent time delay to the first-order constant rate region.[2]

We suggest that improved estimates of the expected spectrum of possible cellular responses is provided by including several plainly different thermodynamically-independent kinetic models of cell alterations in a single model simulation. Some pathologic evaluation of the particular CA cells under treatment can be combined to give a clearer picture of the likely treatment effectiveness than can be obtained from a single CEM number alone, even in a 3D rendition of the treatment space. We present the specific example of mNP heating of mouse fore-shoulder tumors to support the hypothesis.[3]

1. Pearce JA. "Comparative analysis of mathematical models of cell death and thermal damage processes", *International Journal of Hyperthermia*, **v29**, n4, pp262-280, June 2013.

2. Pearce J.A., “Improving Accuracy in Arrhenius Models of Cell Death: Adding a Temperature-Dependent Time Delay,” *J. of Biomechanical Engineering*, **v137**, no. 12, pp. 121006, 2015.

3. Pearce J.A., Petryk AA, Hoopes, PJ. “Numerical Model Study of *In Vivo* Magnetic Nanoparticle Tumor Heating”, *IEEE Transactions on Biomedical Engineering*, **v64**, n12, pp.2813-2823, 2017.

36

Brain-Guided Whole-Body Hyperthermia as Pre-Treatment Strategy for Enhancing Efficacy and Safety of Chemotherapy in Breast Cancer through Tumor Reduction and Normalization of Cellular and Molecular Risk Factors

Dr. M Marc Abreu MD[1,2], Dr Mohammad Hosseine-Farid PhD[3], Dr. Alberto F Chocron MD[4,5], Dr David M Smadja MD, PhD[6,7], Dr Victor Spitz MD[4], Eng Jorge Velar MS[2], Dr David G Silverman MD[8]

[1]Clinical Sciences Division, BTT Medical Institute, Aventura, Florida, USA. [2]Department of Biomedical Engineering and Medical Physics, BTT Medical Institute, Aventura, FL, USA. [3]College of Computing and Engineering, Nova Southeastern University, Fort Lauderdale, FL, USA. [4]Clinical Sciences Division, BTT Medical Institute, Aventura, FL, USA. [5]Research Service, Miami Veteran Administration Medical Center, Miami, FL, USA. [6]Université de Paris, INSERM, Innovative Therapies in Hemostasis, Paris, France. [7]Hematology Department, AP-HP, Georges Pompidou European Hospital, Paris, France. [8]Department of Anesthesiology, Yale University School of Medicine, New Haven, CT, USA

Dr. M Marc Abreu
Position (at Institution/Hospital/Company)
Medical Director

Dr Mohammad Hosseine-Farid
Position (at Institution/Hospital/Company)
Assistant Professor

Dr. Alberto F Chocron
Position (at Institution/Hospital/Company)
Clinical Researcher

Dr David M Smadja
Position (at Institution/Hospital/Company)
Professor

Dr Victor Spitz
Position (at Institution/Hospital/Company)
Senior Clinical Researcher

Eng Jorge Velar
Position (at Institution/Hospital/Company)
Senior RD Engineer

Dr David G Silverman
Position (at Institution/Hospital/Company)
Professor

Abstract

BACKGROUND: In 2023, an estimated 43,170 deaths are anticipated from the most common cancer in US women, breast cancer. Our hyperthermia treatment utilizes the brain-eyelid thermal tunnel (BTT), pioneered at Yale University, which enables non-invasive, continuous monitoring of brain temperature and optimizes heat transfer between brain and eyelid DOI:10.22541/au.160225723.36016917/v1. **PURPOSE:** To enhance standard breast cancer therapy through pre-treatment with brain-guided whole-body hyperthermia (BgWBH)

utilizing brain temperature monitoring via BTT (Brain°) and Brain°-titrated hyperthermia to reduce tumor burden and normalize cancer signaling molecules. **CASE REPORT:** An otherwise healthy 62-year-old female from Canada referred to the BTT Medical Institute in Florida, presented with left nipple inversion and palpable axillary lymph node. Upon examination, a 3 cm breast mass was palpated. Mammogram revealed spiculated left mass measuring 2.4 cm with nipple retraction and heterogeneous calcifications. Left breast core biopsy diagnosed Invasive Ductal Carcinoma HER2+/ER+/PR+. Patient chose BgWBH before undergoing standard oncologic treatments. **METHOD:** After obtaining informed consent, BgWBH was administered using the FDA-approved Abreu-BTT-700 system and BTT radiant-heat equipment involving a heat chamber enclosing the patient's body and head inductor delivering heat to the brain via BTT. During hyperthermia, non-sedated patient was exposed to far-infrared heat, aiming to achieve Brain° of 41.5°C for 20 minutes followed by 41.8°C for 10 minutes. Continuous monitoring included heart rate, respiratory rate, oxygen saturation, body core temperature (measured with tympanic probe), and skin temperature at eight sites (precordium, forehead, and right and left arms, hips, and calves) besides blood pressure every 5 minutes. Infusion pump provided hydration with normal saline as needed. Brain° was obtained using noninvasive FDA-approved C1-eyelid surface probe. Patient received three treatments spanning one-month, with the final session on November 22nd, 2023. Chemotherapy commenced shortly thereafter on November 28th in Canada. **RESULTS:** Pre-treatment laboratory assessments revealed cancer growth risk factors at the cellular level [mild leukopenia (4400/uL) with increased percentage of CD3-/CD16-CD56+NK cells (26%)] and at molecular level [increased DHEA-Sulfate levels (148 mcg/dl), Alpha-Fetoprotein tumor marker (AFP-TM) (6.3 ng/ml), Interleukin-4 (4.7 pg/ml) and Interleukin-10 (5.9 pg/ml)]. Patient evidenced mild cognitive impairment [score of 25 on Montreal Cognitive Assessment (MoCA)] and micrographia. In pretreatment breast MRI, a left subareolar mass measured 3.5 x 2.6 x 3.6 cm, constituting an impressive 127.5% increase over the preceding 45 days. Left lymph node measured 5.61 mm. Final breast MRI after BgWBH exhibited a remarkable 19.2% tumor volume reduction (3.2 x 2.6 x 3.2 cm) and 8.1% lymph node size decrease (5.25 mm). Remarkably, BgWBH led to cellular and molecular normalization including leukocytes (5300/uL), percentage of CD3-/CD16-CD56+NK cells (17%), DHEA-Sulfate (112 mcg/dl), AFP-TM (6.0 ng/ml), Interleukin-4 (<2.2 pg/ml), and Interleukin-10 (<2.8 pg/ml). There was restoration of cognitive function (normal MoCA of 27), normalization of handwriting, 30 to 56% increases in right arm, left arm, right leg, left leg, right palmar and left palmar strength and 48.8% increase in endurance. **CONCLUSION:** BgWBH, a safe and well-tolerated modality, showed efficacy in reducing tumor size and lymph node involvement in aggressive breast cancer besides restoring cognitive and motor functions. Normalization of AFP-TM, typically linked to liver cancer—a frequent metastatic site in breast cancer—suggests potential therapeutic effect on latent liver malignancies. Normalization of leukocytes bolsters immune response, potentially decelerating breast cancer progression and counteracting chemotherapy-induced leukopenia, enhancing chemotherapy safety. When combined with normalization of DHEA-S, Interleukin-4, and Interleukin-10, which play roles in reducing inflammation and breast cancer growth, supports trials for BgWBH as preparatory measure to enhance efficacy and safety of chemotherapy and immunotherapy. This aligns with prior research indicating that hyperthermia can be an adjuvant treatment of chemotherapy and immunotherapy.

37

In Vivo 3D Hybrid fat-water MR Thermometry via Simultaneous Proton Resonance Frequency Shift and T_1 Measurement

Nicholas Richards, Michael Malmberg, Samuel I Adams-Tew, Henrik Odéen PhD, Dennis Parker PhD, Allison Payne PhD
University of Utah, Salt Lake City, Utah, USA

Abstract

Introduction

A significant advantage of MR-guided focused ultrasound (MRgFUS) is the ability to monitor temperature change during treatment. The proton resonance frequency (PRF) shift method provides clinically relevant temporal and spatial resolution but is not sensitive to temperature changes in fat. While it is known that measuring T_1 changes can measure temperature change in fat, this has not been used clinically.

A hybrid MR thermometry sequence has been developed to simultaneously measure temperature using both the PRF and T_1 thermometry methods. PRF shift is calculated at each time point while ΔT_1 is calculated using a single reference image with the variable flip angle method in a stack-of-stars sampling method (SR-VFA-SoS). The SR-VFA-SoS sequence has previously been evaluated under phantom and non-heating conditions, demonstrating the ability to simultaneously measure 3D PRF and T_1 changes. This work evaluates the SR-VFA-SoS approach for predicting thermal ablation in MRgFUS in an in vivo rabbit model through comparison of thermal biomarkers to post-treatment images and histology data.

Methods

In vivo experiments (New Zealand white rabbits, N=4) were performed in a 3T MRI scanner (Prisma, Siemens) using an MRgFUS system. Sequential volumetric sonications (40s, 27-31W acoustic power, N=9) were performed in a grid pattern centered at the perirenal fat-paraspinal muscle interface (Figure A). Hybrid thermometry data was acquired during sonications using the SR-VFA-SoS sequence with a pseudo-Golden Angle view angle increment and 377 total projections. Two baseline acquisitions at a lower flip angle were acquired prior to each sonication, followed by five total dynamic acquisitions at a higher flip angle acquired before, during, and after heating. Additional MR images were acquired before and after MRgFUS ablation.

Reconstruction of the SR-VFA-SoS images were performed using a k-space weighted image contrast method to leverage oversampling at the center of radial projections. Temporal resolution for the T_1 and PRF shift temperature data was 1.71 s. Temperature and ΔT_1 data was acquired at 1.5 × 1.5 × 2 mm (zero-fill interpolated to 0.75 × 0.75 × 2 mm). Images were segmented into muscle and fat based on water- and fat-fractions. Hybrid thermometry and cumulative thermal dose (CTD) maps were formed by using PRF thermometry data for muscle voxels and ΔT_1 for fat voxels (Figure B). The ΔT_1 data was converted to temperature using a previously experimentally derived conversion factor of 7.3 ms/°C.

The volume of hyperintense regions of contrast-enhanced post-treatment images was calculated and compared with the volume of the associated PRF shift only and hybrid SR-VFA-SoS thermometry CTD maps.

Muscle and fat tissue from the treated area were excised for histology. Tissue samples were fixed, processed, embedded, sectioned, and stained with H&E. A compound light

microscope was used to assess tissue damage in sonicated regions.

Results

PRF-only and hybrid PRF and ΔT_1-based temperature changes were successfully calculated for all sonications. Peak temperature rises from 23.6 to 32.0 °C were observed for individual sonications. CTD maps based on PRF-only thermometry accurately monitored thermal damage in muscle but, as expected, did not measure any thermal damage in fat. CTD maps calculated from hybrid PRF and ΔT_1-based temperature changes measured thermal damage in both muscle and fat, qualitatively aligning with hypointense regions in post-treatment images. Histology confirmed thermal damage in sonicated regions of both muscle (Figure C) and fat (Figure D).

Conclusion

This work demonstrates the capability of the SR-VFA-SoS method for predicting thermal ablation using simultaneous PRF shift and ΔT_1 measurement in vivo. CTD maps calculated from the SR-VFA-SoS thermometry more accurately predicted thermal damage in heterogeneous tissue volumes than CTD maps calculated from PRF shift-only thermometry. Predicted thermal damage was confirmed via histological samples taken from the treatment site.

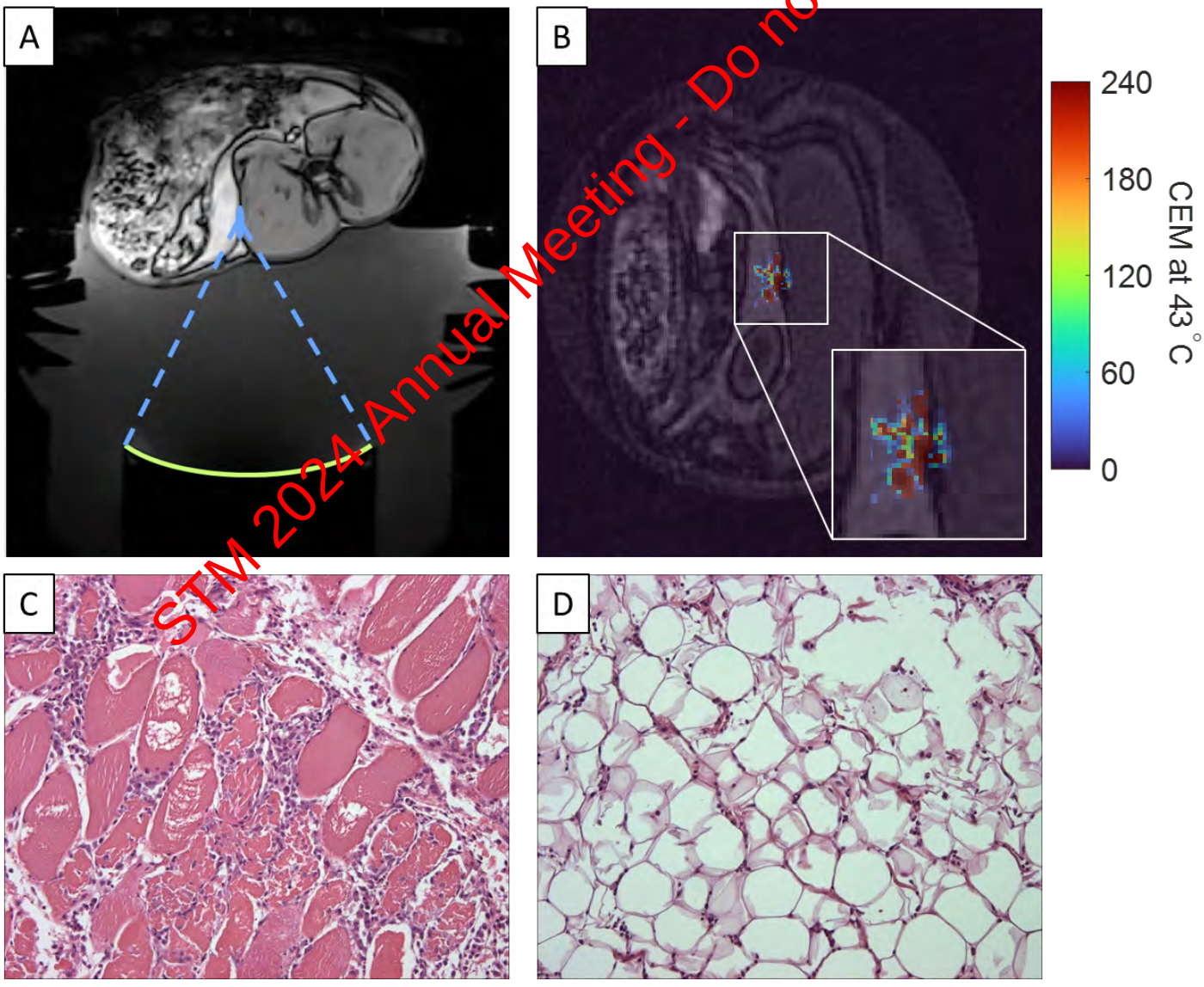

38

Absolute magnetic resonance imaging thermometry in the breast using interleaved echo planar spectroscopic imaging

Allison Payne, Dennis L Parker, Peyton Wong, Duane Blatter, Seong-Eun Kim, Henrik Odéen
University of Utah, Salt Lake City, UT, USA

Allison Payne
Position (at Institution/Hospital/Company)
Associate Professor

Abstract

Introduction

MR thermometry is used to monitor and evaluate thermal treatment such as focused ultrasound and laser interstitial thermal therapy. Many MR parameters have a temperature dependence and have been investigated for thermal monitoring. Most of these approaches can only measure change in temperature. However, spectroscopic approaches have been shown to be able to measure absolute temperature changes by using the temperature insensitive resonance frequency of one proton pool as a reference for another, temperature sensitive, proton pool. Typically, MR spectroscopy and spectroscopic imaging approaches have low spatial and temporal resolution and are not well suited for thermal therapy monitoring. The goal of this work is to implement and evaluate a new interleaved echo planar spectroscopic imaging pulse sequence for absolute MR thermometry in the breast.

Methods

A multi-echo gradient recalled echo pulse sequence (iEPSI) as modified to allow acquisition of up to 32 mono- or bi-polar echoes. In addition, the sequence was modified to allow interleaving multiple sets of the 32 echoes to effectively achieve a smaller echo spacing. In this work each set of spatial phase encodings the excitation and echotrain readout is repeated 6 times with a time shift of 0.4 ms relative to the RF excitation between each interleave. Each set of measurements (positive lobe and negative lobe) are then interleaved and sorted in echo-time order to yield effective FID measurements with dwell times of 0.4 ms, and 38.4 ms total FID duration. These values yield a frequency bandwidth of 2500 Hz and a spectral resolution of 26 Hz. Experiments were performed in ex vivo breast fat samples and, after local IRB approval and informed consent, in one healthy volunteer in a dedicated breast MR guided FUS system. The breast fat samples were cooled and heated between 3-35 °C in water bath setup. Spatial and temporal resolution for imaging were 1.5x1.5x3 mm3/31 s and 1.5x1.5x2 mm^3/261 s for ex vivo and in vivo measurements, respectively. These results were compared to a stock vendor single voxel PRESS spectroscopy (SVS) sequence. All experiments were performed at 3T (Prisma and Vida, Siemens) and data were processed using custom Matlab scripts.

Results

Measured spectra from single voxels using SVS (10 mm^3 voxel) and the described iEPSI pulse sequence (1.5x1.5x2 mm^3 voxel) in the ex vivo breast fat sample demonstrated that the fat and water peaks can be detected using both approaches. Accurate comparison between the measured frequency spectra as a function of time as the temperature agreed

with gold standard fiberoptic probe measurements. The figure shows in vivo feasibility in a healthy volunteer. Both fat and water peaks can be detected in both fibroglandular and fat tissue. The detected frequency spacing can be extrapolated across the full breast demonstrating the spatial monitoring potential of the presented iEPSI technique.

Discussion and Conclusions

An efficient approach to acquire high resolution spectroscopic images using an interleaved echo-planar imaging-type pulse sequence has been developed and evaluated for absolute temperature measurements. Compared to SVS the acquired spectra are naturally noisier, considering the voxel size is less than 1/200, however the clinical impact of this information could be high for all thermal therapies. To improve quality of the iEPSI spectra more advanced peak-finding algorithms, filtering methods, and spatial and temporal averaging could be performed. In vivo absolute temperature measurements will potentially be highly impactful to MRI guided by providing accurate absolute temperatures for thermal dose calculations or other thermal biomarkers.

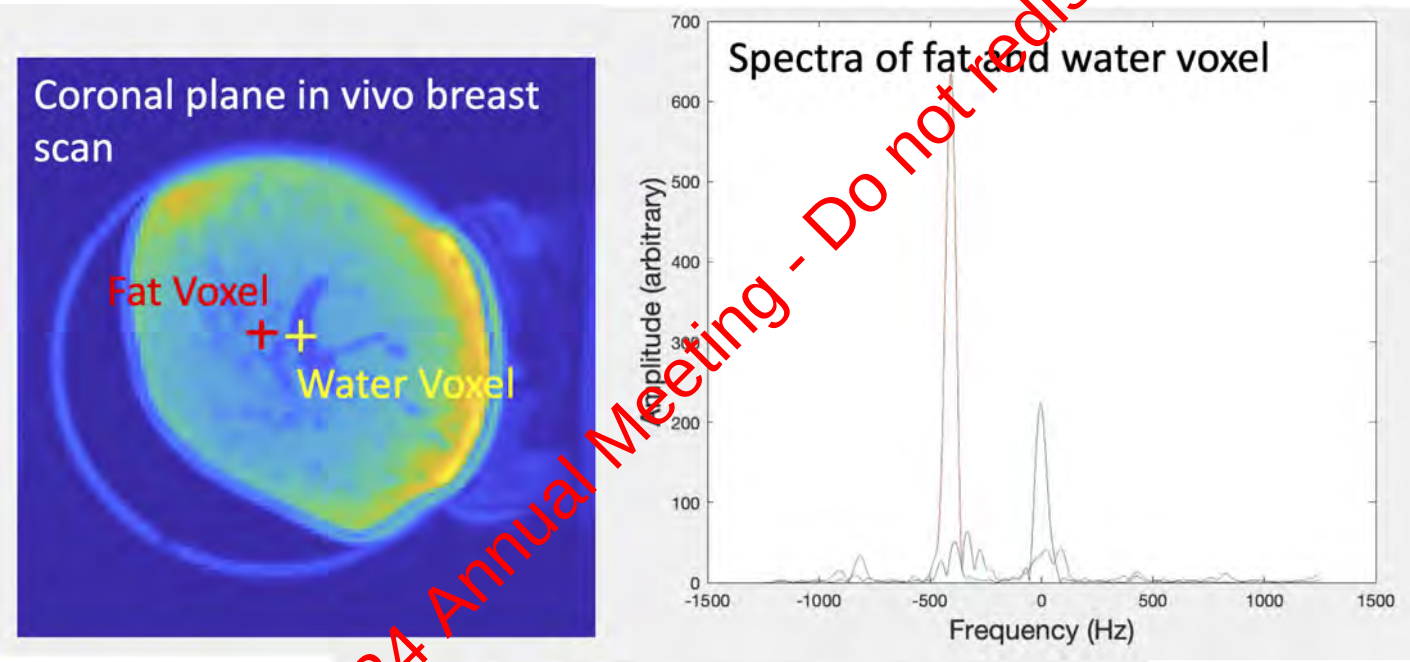

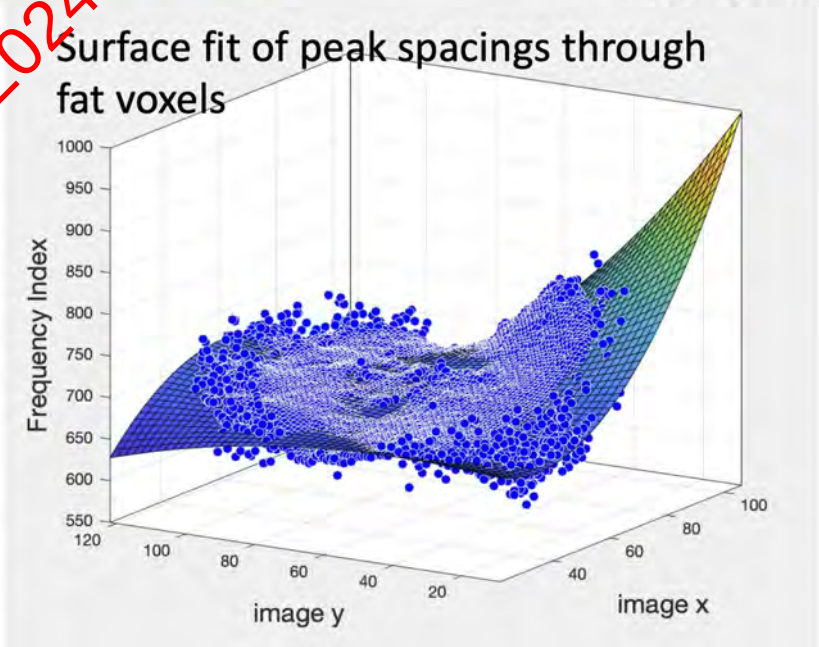

39

Quantum computing based image segmentation for treatment planning applications

Rachel Glenn[1,2], Tucker Netherton[1], Beatrice Riviere[3], Adrian Celaya[1,3], Eugene Koay[1], David Fuentes[1,3]

[1]MD Anderson, Houston, TX, USA. [2]UT Health, Houston, TX, USA. [3]Rice University, Houston, TX, USA

Rachel Glenn
Position (at Institution/Hospital/Company)
Master's Student

Tucker Netherton
Position (at Institution/Hospital/Company)
Assistant Professor, Department of Radiation Physics, Division of Radiation Oncology, The University of Texas MD Anderson Cancer Center, Houston, TX

Beatrice Riviere
Position (at Institution/Hospital/Company)
Professor in the Department of Computational and Applied Mathematics at Rice University

Eugene Koay
Position (at Institution/Hospital/Company)
Associate Professor, Department of Radiation Oncology, Division of Radiation Oncology, The University of Texas MD Anderson Cancer Center, Houston, TX

David Fuentes
Position (at Institution/Hospital/Company)
Associate Professor, Department of Imaging Physics - Research, Division of Diagnostic Imaging, The University of Texas MD Anderson Cancer Center, Houston, TX

Abstract

Image segmentation is an important step for hyperthermia treatment planning. Tissue properties vary between organs. Thus, accurate image segmentation influences the expected energy absorption in the target tissue. Neural networks are the current state of the art for image segmentation. However, we are currently at a new frontier of quantum computing maturing for medical applications and image processing. In this study, we provide three different examples of quantum algorithms for image processing in the area of auto-contouring. Each of the three algorithms falls under the three different areas that quantum is impacting medical diagnostics and treatment planning, including: quantum inspired algorithms, gate-based quantum computers, and quantum annealing. These examples help provide insight and understanding for those wanting to begin research in quantum computing. The quantum algorithm's performance was evaluated using the Sorensen-Dice coefficient. The median Dice coefficient for the AI-based method was 0.9167, for a hybrid classical/quantum gate-based method was 0.9232, a quantum-annealing based methods was 0.2710, and a quantum inspired network was 0.1989. The results show that quantum algorithms have need for improvement if they are to be used for auto-contouring in the clinic.

To compare the three different algorithms against a neural network-based segmentation approach, we used a dataset consisting of 33-patients with magnetic imaging data of the abdomen. Imaging was acquired from multiple scanners. Preoperative abdominal images were obtained using a liver protocol comprised of a pre-contrast phase, a venous phase (60-

80 seconds after injection of intravenous contrast material), and a delayed phase (15 minutes after contrast injection).

41

Multigrid Inspired Deep Learning Architectures for Medical Imaging Segmentation

Mr. Adrian Celaya MA[1,2], Dr. Rachel Glenn PhD[2], Dr. Beatrice Riviere PhD[1], Dr. David Fuentes PhD[2]

[1]Rice University, Houston, TX, USA. [2]The University of Texas MD Anderson Cancer Center, Houston, TX, USA

Mr. Adrian Celaya
Position (at Institution/Hospital/Company)
Ph.D. Student

Dr. Rachel Glenn
Position (at Institution/Hospital/Company)
Master's Student

Dr. Beatrice Riviere
Position (at Institution/Hospital/Company)
Noah Harding Chair and Professor of Computational Applied Mathematics and Operations Research

Dr. David Fuentes
Position (at Institution/Hospital/Company)
Associate Professor, Department of Imaging Physics - Research, Division of Diagnostic Imaging

Abstract

SHORT ABSTRACT – Accurate medical imaging segmentation is critical for precise and effective medical interventions. However, despite the success of convolutional neural networks (CNNs) in medical image segmentation, they still face challenges in handling fine-scale features and variations in image scales. These challenges are particularly evident in complex and challenging segmentation tasks, such as the BraTS multi-label brain tumor segmentation challenge. In this task, accurately segmenting the various tumor sub-components, which vary significantly in size and shape, remains a significant challenge, with even state-of-the-art methods producing substantial errors. Therefore, we propose two architectures, FMG-Net and W-Net, that incorporate the principles of geometric multigrid methods for solving linear systems of equations into CNNs to address these challenges. Our experiments on the BraTS 2020 dataset demonstrate that both FMG-Net and W-Net outperform the widely used U-Net architecture regarding tumor subcomponent segmentation accuracy and training efficiency. These findings highlight the potential of incorporating the principles of multigrid methods into CNNs to improve the accuracy and efficiency of medical imaging segmentation.

INDEX TERMS – Deep learning; segmentation; multigrid methods

MOTIVATION – Medical imaging segmentation is an essential task in medical imaging analysis that involves dividing an image into regions of interest based on anatomical or pathological features. It is crucial in various clinical applications, including disease diagnosis, treatment planning, and surgical guidance. Deep learning-based methods, specifically CNNs, have emerged as powerful tools for medical imaging segmentation. Specifically, the U-Net architecture and its variants have achieved state-of-the-art results in several imaging segmentation challenges. However, deep learning architectures like the U-Net still face challenges in preserving fine structures and handling significant variations in

image scales. We look to GMMs, well-established techniques used in scientific computing to solve problems with multiple scales to address these issues efficiently.
HYPOTHESIS – We hypothesize that by capitalizing on the principles of GMMs, we can reduce the number of parameters in existing CNNs and design novel architectures to address the limitations of CNNs in handling fine-scale features and variations in image scales.
METHODS AND RESULTS – GMMs and CNNs construct a series of grids at appropriate resolutions to resolve specific frequencies (GMMs) or learn appropriate features (CNNs). The V-cycle, W-cycle, and FMG-cycle are different implementations of GMMs, with varying complexities. The U-Net architecture is nearly identical to the V-cycle. However, The W-cycle and FMG-cycle are more complex and computationally intensive, but they offer superior convergence properties by performing more complex operations at each intermediate grid level. We propose the FMG-Net and W-Net architectures based on the FMG and W-cycle GMMs.
CONCLUSION – Our results with our proposed FMG and W-Net architectures indicate that incorporating the principles of GMMs into CNNs for medical imaging segmentation is beneficial in their design. However, future work will focus on further testing our methods and exploring questions such as the interpretability and explainability of our methods.

42

Investigating the Influence of Tumor Viscosity and Density on MNP’s SAR

Dr. Irma Shamatava Ph.D, Dr. Fridon Shubitidze Ph.D
Dartmouth College, Hanover, NH, USA

Dr. Irma Shamatava
Position (at Institution/Hospital/Company)
Research Scientist

Dr. Fridon Shubitidze
Position (at Institution/Hospital/Company)
Professor of Engineering,

Abstract

The viscosity and density of the tumor microenvironment play crucial roles in affecting both tumor behavior and treatment efficacy. These properties differ significantly among various cancer types and even within the same cancer, influenced by the composition of the tumor microenvironment. For example, breast tumors have varying degrees of stiffness throughout their mass, with some areas being more rigid than adjacent normal tissue due to the denseness of the extracellular matrix and fibrous tissue presence. Tumor viscosity impacts cellular movement, nutrient distribution, and the delivery of therapeutic agents, thereby hindering the migration of immune cells and drugs, reducing immune responses, and lessening the effectiveness of treatments. Pancreatic tumors, characterized by their dense and fibrous stroma, exemplify how a high-viscosity microenvironment can obstruct cancer development as well as drug delivery. In response to these challenges, nanotechnology-based localized treatments like magnetic nanoparticle (MNP) hyperthermia therapy, have emerged. This minimally invasive approach involves delivering MNPs to tumor cells, activating them with an external alternating magnetic field (AMF). The MNPs convert the external AMF energy into heat through magnetic hysteresis, Neel and Brownian relaxations, and the physical rotation of MNP within surrounding medium. This results desirable localized temperature in targeted tumor areas selectively. While MNP hyperthermia has shown promising results in preclinical models, optimizing and translating this therapy for clinical application requires a thorough understanding of how a tumor's viscosity and density influence MNP's Specific Absorption Rate (SAR). This understanding can be used to improve MNP and drug delivery, to modify the tumor microenvironment, and to enhance overall cancer treatment outcomes. This paper presents SAR data for MNPs, which generate heat using magnetic hysteresis and physical rotation mechanisms, in different viscous and dense environments, and analyzes the relationship between MNP SAR and tumor microenvironmental factors like viscosity and density.

43

Combining spatially fractionated radiation, immunotherapy, and hyperthermia in a head and neck tumor model

Samir V. Jenkins, Azemat Jamshidi-Parsian, Ruud P.M. Dings, Robert J. Griffin
University of Arkansas for Medical Sciences, Little Rock, AR, USA

Abstract

Spatially fractionated radiation therapy offers the potential to spare both normal tissues and immune cells in residence within the tumor, which may enable improved retention of immunological memory, activity, and increased frequency of tumor remission. This treatment can be further augmented by the incorporating immune checkpoint inhibitor (ICI) therapies, which allow the immune system to further eliminate the tumor. Thermal therapy is also associated with stimulation of the immune system and increased radiation sensitivity via increased oxygenation and inhibition of DNA repair. We thus hypothesized that combined hyperthermia and radiation might significantly increase degree and frequency of response to ICI. Murine head and neck tumors (SCCVII) were implanted in immunocompetent (C3H) mice and treated with combinations of spatially fractionated radiation, ICI, and mild hyperthermia. In vitro clonogenic assays revealed that hyperthermia caused a significant decrease in proliferative capacity when applied before or following radiation therapy. Our spatial fractionation system (GRID) used a honeycomb pattern with a peak dose of 20 Gy and a valley dose of 3 Gy. Peak fields were 2 mm in diameter spaced 3 mm apart center to center. GRID alone did not significantly affect tumor growth relative to untreated controls. Addition of treatments of ICI, specifically anti-PD1 and anti-CTLA-4 applied immediately following radiation and 3, 6, and 9 days after GRID led to tumor regression in more than 60% of tumors. Interestingly, application of 1 hour of localized hyperthermia at 42.5 °C immediately following GRID radiation and ICI resulted in a slower rate of tumor regression and a lower percentage of tumor response. However, application of hyperthermia immediately prior to GRID radiation and ICI resulted in a similar rate of volume reduction as with GRID and ICI alone, but an overall increase in the percentage of responsive tumors. Mice that demonstrated full remission were re-challenged by inoculation of the same tumor cell line, which resulted in delayed growth of the new tumor, but did not prevent tumor re-establishment. The combination of GRID and ICI also led to significant necrosis within the tumor and scattered infiltration of CD45+ cells. The final response, histological analysis, and growth delay numbers will be reported from ongoing studies.

44

Validating a computational model for convection heat transfer during transcranial focused ultrasound therapies

Chris Paul, Alex Edwards, Steven P Allen PhD, Christopher R Dillon PhD
Brigham Young University, Provo, UT, USA

Chris Paul
Position (at Institution/Hospital/Company)
Undergraduate Research Assistant

Alex Edwards
Position (at Institution/Hospital/Company)
Undergraduate Research Assistant

Steven P Allen
Position (at Institution/Hospital/Company)
Assistant Research Professor of Electrical and Computer Engineering

Christopher R Dillon
Position (at Institution/Hospital/Company)
Assistant Professor of Mechanical Engineering

Abstract

Focused ultrasound thalamotomy is a novel therapy that uses sound waves to kill neurons in the thalamus, treating conditions such as essential tremor and tremor-dominant Parkinson's disease. However, the treatment can result in high temperatures at the skull-brain interface, leading to damaged tissues within or near the skull. Currently, this risk is reduced by keeping stationary chilled water around the skull during treatments. However, many patients are still unable to receive treatment due to unfavorable subject-specific characteristics, including low skull density ratio. Our long-term goal is to increase the number of potential patients by exploring how convective water flow around the skull might improve cooling efficiency.

We have developed a finite-difference time-domain (FDTD) numerical solver to simulate convection heat transfer from water flow around the skull during focused ultrasound therapies. To validate model performance, we have designed a laboratory experiment to imitate focused ultrasound thalamotomy.

The experimental setup consists of a hemispherical 3D-printed (PLA) skull containing a brain surrogate, placed into a mock transcranial focused ultrasound transducer. Heating is achieved by pumping hot water at a constant temperature across the inside of the brain surrogate. Both the temperature and flow rate of the chilled water between the skull and mock transducer will be varied across experimental trials. Thermocouple temperatures are recorded throughout the setup.

Beyond model validation, these data will be used to quantify convection heat transfer between the skull and chilled water bath. Determining the quality of this predictive model and the potential impact of convective flow over the skull are important steps to reducing the risk of skull lesions and improving the lives of additional focused ultrasound thalamotomy patients.

46

Numerical feasibility of delivering deep hyperthermia to lateral tumors opposite to metallic hip implants

Dario B. Rodrigues[1], Mattia De Lazzari[2], Carolina Carrapiço-Seabra[3], Ulf Lamprecht[4], Manfred Schmidt[5], Dietmar Marder[6], Sergio Curto[3], Hana Dobsicek Trefna[2], Jason K. Molitoris[1]

[1]University of Maryland School of Medicine, Baltimore, MD, USA. [2]Chalmers University of Technology, Göteborg, Sweden. [3]Erasmus MC Cancer Institute, Rotterdam, Netherlands. [4]University Hospital Tübingen, Tübingen, Germany. [5]University Hospital Erlangen, Erlangen, Germany. [6]Cantonal Hospital Aarau, Aarau, Switzerland

Abstract

Introduction: Approximately 2% of cancer patients (38,000/year in USA) treated with radiation therapy have metallic hip implants. These implants are a contraindication for deep hyperthermia (DHT) due to the potential induction of hot spots that can cause tissue thermal damage. We hypothesize that heating lateral tumors on the opposite side of metallic hip implants is possible via power and phase steering methods to minimize temperature around the implant to safe levels.

Methods: We tested our hypothesis via a numerical approach, using the BSD Sigma 60 (Pyrexar Medical, USA) DHT applicator model, the VHP-Female model v2.2 (NEVA BioElectromagnetics, USA) with the Austin-Moore metal implant on the right femur, and a representative 86 mL tumor model. Two target locations were analyzed: bladder and left femur. Specific absorption rate (SAR, W/kg) and temperature were computed using COMSOL, IT'IS tissue properties database v4.0, and tumor properties retrieved from the ESHO computational guideline (PMID:34581246). Antenna settings were optimized to reach T90=40°C and a maximum temperature (Tmax) of 44°C in target. Power and phase were optimized for each of the independent four Sigma 60 amplifiers that control a pair of antennas located on the top (T), bottom (B), right (R), and left (L) sides of the applicator.

To validate the numerical model, we built a 60-cm long cylindrical phantom with 25-cm diameter and 8-mm thick plastic wall filled with a muscle-mimicking gel. This gel was made of wallpaper paste powder (40 g/L), salt (3.5 g/L), and deionized water, resulting in dielectric properties of ε_r = 65.7 and σ = 0.60 S/m at 90 MHz. Temperature probes were inserted in closed-tip catheters secured by custom-built holders positioned inside the cylinder. We performed thermal mapping to capture temperature along the center longitudinal axis and transverse plane. The heating time was 10 min at 1000 W. Three phantoms were manufactured for repeatability testing.

Results: When targeting the centrally-located target (bladder), the Tmax was observed at the end of the implant stem, reaching ablative temperatures of 62°C at steady state (reached within 30min) and SAR values of 485 W/kg vs. 189 W/kg in target. No hot spot was observed in the femoral head implant. For this configuration, we used a setting of 100 MHz with 100% relative power in all amplifiers. When targeting the tumor in the left hip, we optimized the relative power to 16% (R), 50% (T,B), and 100% (L) at 100 MHz. For this case, there was no hot spot observed in the hip implant, with maximum SAR values in the femur/implant interface of 61 W/kg vs. 558 W/kg in target.

The experimental results showed good repeatability with Tmax varying ±0.5°C (longitudinal thermal map) and ±0.8°C (transverse thermal maps) for a temperature increase of 10.8°C at the phantom center at 10 min. These results showed a very good correlation within 1°C

with the equivalent computational model, which is expected given the ~1cm uncertainty associated with the probe position.

Conclusion: Numerical simulations demonstrate the potential to expand the pool of patients that can benefit from hyperthermia to include patients with lateral tumors opposite to metallic hip implants. However, so far this conclusion is valid for our case study only, which used 3D hyperthermia treatment planning (HTP). The current HTP standard of care oversimplifies patient anatomy to 2D homogenous media. Only with 3D patient-specific HTP, can DHT be safely assessed for patients with metallic hip implants. Future work includes using anatomical phantoms with different hip implants and thermometry along the metal surface to characterize hot spots and further validate our HTP approach.

47

Trial in progress: First-in-human phase I study of THE001 combined with regional hyperthermia in patients with locally advanced or metastatic soft tissue sarcoma

Prof. Dr. Lars H Lindner MD[1,2], Dr. Dorit Di Gioia MD[1], Gesa Schuebbe[1], Dr. Saeed Ghani MD[3], Dr. Martin Hossann[2], Dr. Zuzana Haramiova[2], Dr. Frank Hermann[2], Prof. Dr. Peter Reichardt MD[3]

[1]University Hospital, LMU Munich, Munich, Germany. [2]Thermosome GmbH, Martinsried, Germany. [3]Helios Klinikum Berlin-Buch and Medical School Berlin, Berlin, Germany

Prof. Dr. Lars H Lindner
Position (at Institution/Hospital/Company)
Head of Sarcoma Medical Oncology (SarKUM) and Head of Hyperthermia Unit of the Medical Clinic III

Dr. Dorit Di Gioia
Position (at Institution/Hospital/Company)
Senior physician

Gesa Schuebbe
Position (at Institution/Hospital/Company)
Senior physician

Dr. Saeed Ghani
Position (at Institution/Hospital/Company)
Senior physician

Dr. Zuzana Haramiova
Position (at Institution/Hospital/Company)
Clinical Research Project Manager

Dr. Frank Hermann
Position (at Institution/Hospital/Company)
Chief Medical Officer

Prof. Dr. Peter Reichardt
Position (at Institution/Hospital/Company)
Head Physician Oncology and Palliative Medicine

Abstract

Objective

Doxorubicin (DOX) is the most relevant chemotherapeutic agent for the treatment of soft tissue sarcomas (STS). Because DOX is known to induce immunogenic cell death, combination therapies of DOX with immune checkpoint inhibitors have gained interest. Regional hyperthermia (RHT) has been shown to improve survival in locally advanced high-risk STS when combined with DOX-based chemotherapy, and stimulates the tumor microinvironment to enhance antitumour immune activity. THE001 is a thermosensitive liposomal formulation of DOX based on phosphatidyldiglycerol as the key membrane component. After intravenous administration, THE001 releases DOX in the bloodstream once the temperature in the target area is above 40°C. The application of THE001 plus RHT resulted in preclinical models in up to 15-fold higher DOX concentrations in the tumor and is expected to improve clinical treatment efficacy.

Methods

THE001 in combination with RHT is being evaluated in an open-label, non-randomized, dose-escalation study in patients with locally advanced or metastatic STS (NCT ID: NCT05858710). The study explores ascending doses of intravenous THE001 monotherapy in 21-day cycles to identify the maximum tolerated dose (MTD). From cycle 2, RHT is performed simultaneously. THE001 study began enrolling patients in April 2023 and is conducted at the LMU Klinikum and the Helios Klinikum Berlin Buch. Dose level 1 has been completed without DLT. Recruitment to dose level 2 began in January 2024. Adverse events are assessed according to CTCAE v5. Tumor response is determined according to RECIST 1.1 and Choi criteria and safety findings reviewed by an independent Data Safety Monitoring Board, which will determine the MTD. Key Phase 1 eligibility criteria include 1) locally advanced (unresectable) or metastatic STS for which treatment with DOX monotherapy is appropriate, and 2) pretreatment with DOX combination chemotherapy (DOX/ifosfamide or DOX/dacarbazine) achieved at least stable disease; for patients who received DOX in an adjuvant setting, local recurrence free interval of >6 months is required, 3) progressive disease not suitable for surgery after 3a) only one further line of chemotherapy (including tyrosine-kinase inhibitor) if the RHT field targets the clinically relevant tumor manifestation/s (e.g., locally advanced or multifocal intraabdominal STS; diffuse metastatic STS in which RHT of a tumor manifestation [e.g., liver] is considered relevant although other systemic metastases are present that do not endanger the patient), or 3b) two or more further lines of chemotherapies (including TKI) for patients with metastatic STS and a tumor manifestation suitable for RHT. Further clinical evaluations of THE001 plus RHT are planned in follow-on studies, e.g. in patients with unresectable localized STS as monotherapy and in combination with ifosfamide (undifferentiated pleomorphic sarcoma) or dacarbazine (leiomyosarcoma) in neoadjuvant therapy of patients with locally-advanced high-risk STS.

48

Evaluation of the efficacy of laser interstitial thermal therapy for biopsy-proven radiation necrosis over a one-year follow-up.

Dr. Mohammed A Azab MD, Dr. Issa Lahirish MD, Dr. Alireza Mohammadi MD
Cleveland Clinic, Cleveland, Ohio, USA

Dr. Mohammed A Azab
Position (at Institution/Hospital/Company)
Clinical fellow

Dr. Issa Lahirish
Position (at Institution/Hospital/Company)
Clinical fellow

Dr. Alireza Mohammadi
Position (at Institution/Hospital/Company)
Associate Professor of Neurosurgery

Abstract

Background

Laser interstitial thermal therapy (LITT) has substantial evidence for efficacy in the setting of radiation necrosis (RN) for patients with primary or secondary brain tumors. However, the long-term control, and synchronous use of other therapies as steroids and bevacizumab remains questionable.

Objective: To evaluate the efficacy, safety, of LITT over 12-months follow-up period of patients with biopsy proven RN treated with LITT.

Methods

This is a single-institution retrospective study of 36 patients treated with LITT for RN from 2012-2023. A same session frozen section biopsy was performed in all patients. Age, sex, tumor type, preoperative MRI (Magnetic Resonance Imaging) T1 with contrast and T2 follow-up volumes over 3,6,12 months, Karnofsky Performance Scale (KPS) over 12 months of all patients were retrospectively analyzed. Concurrent therapies with steroids, or bevacizumab and time to steroid independence were recorded.

Results

Our study includes **36** patients, **22** females **(61%**), and 14 males (**39%**). The most common brain tumor was a metastasis from a primary non-small cell lung cancer (NSCLC) (25.0%). All the patients had a biopsy proven RN and were treated with LITT (Neuroablate). Six patients (17%) received bevacizumab while 30 patients (83%) had steroid therapy before undergoing LITT. The median preoperative MRI T1 volume was **5.2,** while at 3,6,12 months

were **4.6**, **3.1** and **2.1**cc, respectively. The median preoperative MRI T2 volume was **37.3** cc, while at 3,6,12 months were **25.9**, **25** and **14**cc, respectively. The median time to corticosteroid tapering after LITT was **14** days. Only three patients (**8%**) had complications following LITT. Baseline treatment with steroids or bevacizumab before LITT did not impact the overall mortality (HR= 0.95, 95% CI= 0.12 - 7.42), (HR= 1.00, 95% CI= 0.98 - 1.5) respectively. Through a 12-months follow-up, the median KPS remained at 80. We had recurrence in three patients (8.3%), over 12 months. All three patients were treated with bevacizumab, which did not impact the mortality.

Conclusions

Although LITT has been an effective therapy for patients with RN, the long-term volumetric analysis has not been fully studied. Our current results suggest local control over a follow-up time of 12 months with only three recurrences over a one year. Moreover, it enhanced steroids independence which could improve overall survival.

49

Regional deep hyperthermia in combination with platinum-based chemotherapy in children and adolescents with with relapsed or refractory non-testicular germ cell tumors: long-term results from a non-randomised, open-label, phase 1/2 trial.

Ruediger Wessalowski MD[1], Dominik Schneider MD[2], Oliver Mils[1], Katrin Harder[1], Dirk Klee MD[3], Christiane Matuschek MD[4], Christiane Staude MD[5], Christian Vokuhl MD[6], Stefan Schönberger MD[7], Gabriele Calaminus MD,[8]

[1]Heinrich-Heine-University, Medical Faculty, Department of Pediatric Oncology, Hematology and Clinical Immunology, Düsseldorf, NRW, Germany. [2]Clinic of Pediatrics, Dortmund, NRW, Germany. [3]Heinrich-Heine-University, Medical Faculty, Department of Pediatric Radiology, Düsseldorf, NRW, Germany. [4]Heinrich-Heine-University, Medical Faculty, Department of Radiation Oncology, Düsseldorf, NRW, Germany. [5]Heinrich-Heine-University, Medical Faculty, Department of Pediatric Surgery, Düsseldorf, NRW, Germany. [6]University Hospital Bonn, Section of Pediatric Pathology, Department of Pathology,, Bonn, NRW, Germany. [7]University of Duisburg-Essen, University Children's Hospital, Department of Pediatrics III, Essen, NRW, Germany. [8]University Hospital Bonn, Division of Pediatric Hematology and Oncology, Bonn, NRW, Germany

Gabriele Calaminus
Position (at Institution/Hospital/Company)

Abstract

Background:
Despite treatment with novel therapies and autologous stem-cell transplant (auto-SCT) consolidation, outcomes in children and adolescents with relapsed or refractory non-testicular germ cell tumors remain poor, underlining the need for more effective therapies. We wanted to determine whether patients with refractory or recurrent germ cell tumors could achieve an objective response to the tumor with PEI chemotherapy and regional deep hyperthermia as salvage treatment.

Methods:
This single-arm prospective trial was done at the Heinrich-Heine-University of Düsseldorf and enrolled patients aged 25 years or younger with diagnosed and histologically confirmed relapsed or refractory non-testicular malignant germ cell tumors following standard cisplatin-based chemotherapy. PEI chemotherapy consisted of cisplatin 40 mg/m^2 administered intravenously on days 1 and 4; etoposide 100 mg/m^2 intravenously on days 1-4; and ifosfamide 1800 mg/m^2 intravenously on days 1-4 plus concomitant 1-hour regional deep hyperthermia (41-43°C) on days 1 and 4. Patients received three to four treatment courses at 21-day intervals until residual tumor resection was possible; they subsequently received one or two additional courses of PEI-regional deep hyperthermia. Local radiotherapy was given for incompletely resected tumors. The primary endpoint was the proportion of patients who had an objective response as assessed with Response Evaluation Criteria in Solid Tumors version 1.0 guidelines. Secondary endpoints were the event-free survival and overall survival after 5 years.

Results:
107 patients aged 5 months to 24 years (median 3 years and 2 months) with refractory or

recurrent malignant germ cell tumors (32 patients with poor response, 51 patients with first relapse, 24 patients with multiple relapses) were enrolled in this study. We identified 67 yolk sac tumors, thirteen embryonic carcinomas, one choriocarcinoma, two dysgerminomas and 24 unfavorable teratomas by histological analysis. Of the 87 patients with sufficient clinical and radiological data to assess response, 69 (83%) objectively responded to treatment (31 patients in complete remission and 38 in partial remission). The 5-year event-free survival rate was 67% and the 5-year overall survival rate was 75%.

Interpretation:
The long-term results confirm that a multimodal strategy that includes PEI chemotherapy plus regional deep hyperthermia and tumor resection with or without radiation can successfully treat children and adolescents with refractory or recurrent non-testicular germ cell tumors. In this success story, the long-term prognosis of patients with an unfavorable response or a first relapse shows nearly the same results as patients receiving first-line therapy.

Funding:
Deutsche Krebshilfe e. V. , Bonn, Elterninitiative Kinderkrebsklinik Düsseldorf e. V.

.

50

Tumor Immunomodulatory Effects of Mild Hyperthermia, Thermal Ablation, and Histotripsy from Focused Ultrasound: A Comparative Analysis.

Akansha Singh Ph.D, Ashish Ranjan DVM, Ph.D
UT Southwestern Medical Center, Dallas, TX, USA

Akansha Singh
Position (at Institution/Hospital/Company)
Assistant Professor

Ashish Ranjan
Position (at Institution/Hospital/Company)
Professor

Abstract

Introduction: Focused ultrasound-mediated mild hyperthermia (40-42°C; HY), thermal ablation (>60°C; AB) and boiling histotripsy-based mechanical ablation (HT) can target tumor cells and modulate tumor immune microenvironment, thereby enhancing tumor cell eradication. Despite their potential, limited information exists regarding relative benefits of immune alterations induced by each modality under similar conditions, resulting in confusion regarding the most suitable approach for tumor immunomodulation. To bridge this knowledge gap, we conducted a comparative study, evaluating FUS-mediated HY, AB, and HT in a bilateral B16F10 melanoma mouse model and characterized infiltrated immune cell phenotypes and assessed gene expressions related to tumor immunogenicity, sensitivity, stromal factors, and inhibitory metabolic pathways.

Method: Female C57BL6 mice bearing bilateral B16F10 melanoma tumors in flank region were randomized into four groups(n=8/group): 1) Untreated control, 2) HY, 3) AB, and 4) HT. A single FUS treatment was administered to the primary tumors (~100mm^3) using an Alpinion HIFU system with the following parameters: HY: DC-50%, PRF-20 pulses/s, Power-20W, Time-120s, tumor coverage-100%; AB: DC-50%, PRF-20 pulses/s, Power-90W, Time-30s, tumor coverage-<20%; HT: DC-1%, PRF-5 pulses/s, Power-600W, Time-20s, tumor coverage-<20%. Treated and untreated (abscopal) tumors volume was measured daily. Three days post-treatment treated tumors(n=3/group) were isolated, and total RNA was extracted for nCounter PanCancer IO360 panel analysis. Eight days post-treatment, remaining 5 mice/group were euthanized, treated and untreated tumors were isolated and processed for flow cytometry analysis.

Results: HY induced 21% reduction in tumor growth at treated site, while AB led to 52% reduction, and HT exhibited the most substantial effect with an 81% reduction. At the abscopal site, tumor growth delays of 28%, 30%, and 40% were observed with HY, AB, and HT, respectively. Among 749 genes analyzed using nCounter, HY-treated tumors exhibited upregulation of 110 genes compared to control tumors baseline. Notably, *cdc20* gene, associated with tumor metastasis, and *rad51* gene, essential for proper DNA repair, were suppressed. AB-treated tumors showed significant upregulation of 100 genes, primarily clustered into 'response to external biotic stimulus,' and 'regulation of NK cell chemotaxis, with downregulation of *hdac3* and *elob* genes associated with cancer progression. HT-treated tumors displayed upregulation of 258 genes clustered into 'immune effector

process’, 'regulation of TNF production' and ‘toll-like receptor signaling’. Meanwhile, genes associated with tumor progression, *aldoc*, *cd276*, and *hdac3*, were downregulated. HT led to downregulation of genes associated with angiogenesis, metabolic stress, matrix remodeling, and metastasis, which remained unchanged with HY. Concurrently, AB treatment significantly upregulated Wnt signaling genes, which decreased with HT treatment. Flow cytometry analysis of treated and abscopal tumors revealed no significant change in immune cell populations with HY compared to the control, except for an increase in neutrophils (CD45+LY6G+). Consistent with gene expression analysis, AB treatment increased the presence of NK cells (50%), exhausted CD8 T cells (~48%), and Treg (~62%) in treated tumors. However, this increase was also associated with a higher infiltration of cytotoxic T cells, exhausted T cells, and PMN-MDSCs in untreated tumors. HT treatment resulted in significantly higher concentrations of cytotoxic T cells (GranzymeB+ & IFNγ+) in both treated and untreated tumors compared to all other groups. Additionally, CD11c+ Dendritic cells (~68%) and CD11b+ macrophages (~39%) were more abundant in HT-treated tumors, with a higher number of DC-1 (CD11c+ CD11b- CD8a+ SIRPα-) infiltrating both treated (~38%) and abscopal (~61%) sites compared to the control. NK cells in HT-treated mice exhibited a cytotoxic phenotype (NKG2D^{Hi}NKG2A^{Lo}; IFNγ^{Hi}TIM3^{Lo}PD-1+), whereas in AB-treated mice, exhausted NK cells (NKG2A^{Hi}NKG2D^{Lo}; IFNγ+TIM3^{Hi}PD-1^{Hi}) were observed.

Conclusion: While all FUS modalities modulate tumor's immunogenic properties, under similar conditions, HT exhibits relatively superior immunogenicity compared to HY and AB. Further, utilizing clinically relevant tumor models can offer additional insights into our observed findings.

51

Epigentic modulation by hyperthermia on dysbiotic tumor vasculature

Hailey Kristian B.Sc., Dr. Robert J. Griffin Ph.D., Dr. Samir V. Jenkins Ph.D., Dr. Ruud P.M. Dings Ph.D.
UAMS, Little Rock, AR, USA

Abstract

Bacteria colonize many parts of the body, and the crosstalk between the microbiota and the host is crucial to various developmental and physiological processes. Consequently, a growing body of literature supports the idea that microbial imbalance, dysbiosis, affects disease susceptibility and progression. In cancer, although certain types of dysbiosis are known to induce local effects in the gastrointestinal (GI) tract and associated tumors, we have shown that distal, non-GI tract solid tumors also show accelerated progression during dysbiosis due to a vascular immune suppression in the tumors. Epigenetic changes have been increasingly recognized as drivers in carcinogenesis, yet the epigenetic events and regulation during antibiotic-induced dysbiosis are unknown. The balance of histone acetylation and deacetylation plays a critical role in the regulation of gene expression and thereby cellular processes. Therefore, we assessed which histone deacetylases (HDACs) are expressed and their abundance in endothelial cells of various sources with or without dysbiotic stress and/or local hyperthermia to understand the utility of thermal medicine to promote normal functioning of the vasculature in dysbiotic patients. We found that inherent HDAC expression levels and their receptors (GPR41, GPR43, and GPR109a) differed among endothelial cells from different origins. Moreover, that hyperthermia (60 min of either 41.5 °C or 43 °C) influenced the HDAC and receptor levels differentially. Specifically, HDACs 2, 3, 5, 7, and 10 were suppressed in dysbiotic tumor vasculature and hyperthermia was able to increase some HDACs up to 2-fold. Although further studies are warranted, these results demonstrate that hyperthermia exerts epigenetic effects and is capable of overcoming the dysbiosis-induced phenotype. Since anti-cancer treatment with HDAC inhibitors has shown promise in the clinic but is hindered by systemic toxicities, localized hyperthermia may become a viable alternative in the future.

52

Beyond Newton's Law of Cooling in nanoparticle heating: a device-independent procedure.

Sergiu Ruta[1], Yilian Fernández-Afonso[2], Samuel Ewan Rannala[3], María del Puerto Morales[4], Sabino Veintemillas-Verdaguer[4], Carlton Jones[5], Lucía Gutiérrez[2], David Serantes[6], Roy William Chantrell[3]

[1]Sheffield Hallam University, Sheffield, United Kingdom. [2]Universidad de Zaragoza, Zaragoza, Spain. [3]University of York, York, United Kingdom. [4]Instituto de Ciencia de Materiales de Madrid, Madrid, Spain. [5]nanoTherics Ltd, Warrington, United Kingdom. [6]Universidade de Santiago de Compostela, Santiago de Compostela, Spain

Abstract

Estimates of nanoparticle heating performance, usually reported in terms of the *Specific Loss Power* (SLP) obtained from the temperature variation *vs*. time curve, ΔT(t), are often found to vary significantly when carried out in different laboratories and/or different devices. Such diversity may strongly hamper the use of the particles for applications relying on accurate heating, therefore calling for improvements in the way of assessing the heating performance. We discuss in this work that such diversity may be strongly influenced by the fact that the basic-physics model upon which most estimates are based, the so-called *Newton's law of cooling*, in general may not apply for the dynamical situation of nanoparticle heating. The main reasons are i) temperature profiles during heating and cooling are not the same, and ii) different heat dissipation channels may coexist. We report an alternative approach, based on the general heat diffusion equation, which focuses the analysis of the peak of the ΔT(t) curve, so that the role of both limiting aspects is reduced. Our approach is supported by theoretical and computational calculations to increase the reliability and reproducibility of SLP determination. Furthermore, the new methodological approach is experimentally confirmed using as an example magnetic hyperthermia experiments performed using 3 different devices located in 3 different laboratories. In addition, the application of this peak analysis method (PAM) to a rapid succession of stimulus on/off switches that result in a *zigzag*-like ΔT(t), which we term the zigzag protocol, allows evaluating possible variations of the SLP values with time or temperature.

53

PID Control with Automated Laser Probe Positioning applied to Laser Interstitial Thermal Therapy

Yash Lad Masters, Nageshwar Arepally Masters, Mr. Shreeniket Pawar Masters, Ma'Moun Abu-Ayyad Ph.D., Anilchandra Attaluri
Pennsylvania State University, Middletown, Pennsylvania, USA

Yash Lad
Position (at Institution/Hospital/Company)
Graduate Research Assistant

Nageshwar Arepally
Position (at Institution/Hospital/Company)
Graduate Research Assistant

Mr. Shreeniket Pawar
Position (at Institution/Hospital/Company)
Graduate Research Assistant

Ma'Moun Abu-Ayyad
Position (at Institution/Hospital/Company)
Associate Professor

Anilchandra Attaluri
Position (at Institution/Hospital/Company)
Associate Professor

Abstract

Laser interstitial thermal therapy (LITT) is a minimally invasive surgical technique used for treating brain malignancies such as Glioblastoma Multiforme (GBM). Current LITT systems require physicians' input for pullback of the laser probe during the treatment to achieve optimal thermal dose coverage. The goal of this study is to design an automated laser probe positioning system based upon temperature feedback to deliver target thermal dose. A cascaded proportional-integral-derivative (PID) controller with a fuzzy logic controller was designed using integrated system dynamics and finite element simulations. The PID controller was constrained to prevent tumor boundary temperature from exceeding 57 [°C]. Fuzzy logic controller was used for pulling back the laser probe once the thermal dose at the corresponding probe reaches the setpoint value. The cascade controller was designed using co-simulations in MATLAB Simulink® and COMSOL Multiphysics©. Deidentified patient dataset were imported into COMSOL Multiphysics©, to perform bioheat transfer simulations. The computational domain consists of Skull, CSF general, brain tissue (gray & white matter), CSF ventricles, and tumor. The laser probe was modelled as a cylindrical geometry with a diameter of 1.65 [mm] and height of 105 [mm]. Arrhenius thermal damage feedback was used as input to Fuzzy logic to control the pullback of the laser probe. Simulation results show that approximately 80% of the tumor has thermal damage greater than 70-80% for treatment time of 2500 [s] with controlled temperature. With a cascade PID-fuzzy logic control, the temperature within the tumor boundary does not exceed 57 [°C]. Hence, we can conclude that a PID controller combined with a fuzzy logic controller can be used to achieve planned thermal dose coverage, without damaging surrounding healthy tissues. Since there is a significant need of a feedback control strategy for the pullback control as well as thermal dose control during LITT treatments, a cascaded PID control with fuzzy logic control system can be used to automate the LITT treatments.

54

HYPER: Pre-Clinical Device for Spatially-Confined Magnetic Particle Hyperthermia

Hayden Carlton PhD[1], Matthias Weber PhD[2], Maximillian Peters[2], Nageshwar Arepally[3], Yash Lad[3], Anshul Jaswal[3], Robert Ivkov PhD[1,4], Anilchandra Attaluri PhD[3], Patrick Goodwill PhD[2]

[1]Johns Hopkins School of Medicine, Baltimore, MD, USA. [2]Magnetic Insight, Alameda, CA, USA. [3]The PA State University, Harrisburg, PA, USA. [4]Johns Hopkins University, Baltimore, MD, USA

Hayden Carlton
Position (at Institution/Hospital/Company)
Postdoctoral Researcher

Nageshwar Arepally
Position (at Institution/Hospital/Company)
Graduate Student

Yash Lad
Position (at Institution/Hospital/Company)
Graduate Student

Anshul Jaswal
Position (at Institution/Hospital/Company)
Graduate Student

Robert Ivkov
Position (at Institution/Hospital/Company)
Professor

Anilchandra Attaluri
Position (at Institution/Hospital/Company)
Associate Professor

Patrick Goodwill
Position (at Institution/Hospital/Company)
CEO/CTO

Abstract

Purpose: To develop a prototype pre-clinical device that confines magnetic nanoparticle heating to a volume and location selected by the user.

Introduction: Magnetic nanoparticle hyperthermia is a thermal therapy for cancer that exploits hysteresis heating of magnetic nanoparticles exposed to alternating magnetic fields (AMFs). Several properties govern the magnitude of temperature rise from nanoparticle heating within tissue, including nanoparticle structure, magnetic field intensity, and the duration of heating. A major challenge with magnetic nanoparticle hyperthermia is spatially confining the heat within the tumor and limiting the temperature rise in healthy tissue beyond the tumor boundary. Here, we demonstrate the performance of a prototype pre-clinical device, designated HYPER, designed to confine magnetic nanoparticle heating in mouse models to a volume and location defined by the user.

Methods: Spatial confinement of nanoparticle heating with the HYPER relies on the same physical principles that govern magnetic particle imaging (MPI). Within the HYPER chassis, two opposing permanent magnets of equivalent strength create a region of zero magnetic

field, or field free region (FFR), in the space between them. The size and position in 3D of the FFR is controlled by the position and relative separation of the magnets. A radiofrequency coil placed within the FFR creates an AMF, which encompasses any sample within the FFR (340kHz, 0-15 mT) causing moment reversal to generate heat, while moments of nanoparticles outside the FFR are fixed by the static field, unable to reverse and contribute to heating. Cameras enable the user to visually select the FFR location and size within a graphic user interface that relays instructions to actuators. To verify FFR adjustment functionality, we heated a small vial of magnetic nanoparticles (Synomag®-D70, micromod Partikeltechnologie, GmbH, Rostock, Germany; Lot#: 09122104-02) at varying FFR sizes and locations within the coil. Sample temperature was measured using a fiber optic thermal probe. Also, we used a fillable mouse phantom (BioEmission Technology Solutions, Athens, Greece) with two compartments: ‘lower tumor’ (204 mm3) and ‘liver’ (1164 mm3), which are approximately 3 cm apart to further demonstrate potential control in a geometry-relevant phantom. After filling the regions of the mouse phantom with the same nanoparticles, we centered the FFR on the tumor and heated for 300 s, then centered on the liver and heated for another 300 s, while monitoring the temperature in both.

Results: The results of the first experiment verified that the size of the heated region within the coil varied inversely with magnet separation in all three dimensions. Since the HYPER contains only one set of opposing magnets along the x-axis, the FFR was notably more constrained in the x-dimension. Additionally, when heating the mouse phantom in the second experiment, we observed only a 0.6°C rise in the liver compartment when we focused the FFR on the tumor compartment, which observed a 4.9°C rise.

Conclusions: We confirmed that the HYPER prototype enables spatially-confined magnetic nanoparticle heating in three dimensions in space. The size and location of the heated region can be adjusted automatically for individual treatment planning and different nanoparticle-rich regions within the same AMF-generating coil can be heated independently from one another.

55

Impact of tumor volume and radiation dose on tumor control rates in recurrent breast cancer patients treated with hyperthermia and radiation

Mark L Solter[1], Cole Billena[2], Peng Qi[2], Chirag Shah[2], Jennifer S Yu[2]

[1]Cleveland Clinic Lerner College of Medicine, Case Western Reserve University, Cleveland, OH, USA. [2]Department of Radiation Oncology, Taussig Cancer Institute, Cleveland Clinic, Cleveland, OH, USA

Mark L Solter
Position (at Institution/Hospital/Company)
Medical student at Cleveland Clinic Lerner College of Medicine, Case Western Reserve University

Abstract

Background: Given the poor response rates and cumulative toxicity in the management of recurrent breast cancer, exploring additional therapeutic strategies is imperative. Concurrent hyperthermia (HT) with radiation (RT) improves locoregional control through radiosensitization, promotion of reoxygenation, and modulation of the tumor microenvironment. Studies suggest that the overall response rate to thermoradiotherapy correlates with tumor volume when relatively low RT doses (20 Gy) are used, but the impact of tumor volume on local control using higher RT doses remains unclear

Methods: Our institutional registry was queried for patients treated with recurrent breast cancer from 2011 to 2023. 73 patients with 81 lesions were identified. Dosimetric, clinical, and toxicity data were collected, and lesions were stratified by quartiles of tumor volume. Fisher exact test was used for univariate analysis. Actuarial data was summarized using Kaplan-Meier and cumulative incidences curves.

Results: Three patients were male, and 68 were female. Median age at the start of treatment was 66 years. Median follow-up was 15.5 months. 69% of lesions were hormone receptor positive (estrogen and/or progesterone), 14% had HER2 amplification, and 21% had triple negative breast cancer. 82% received prior radiation therapy. Radiation was delivered to a median dose of 32 Gy [IQR 30, 40] and a median fractionation of 10 [IQR 8,13]. The most common scheme for radiation delivery was biweekly. Hyperthermia was given to 43 degrees °C for 60 minutes per session typically twice a week before radiotherapy. Tumor volumes ranged from 30.28 cm3 to 6388.05 cm3 [IQR 316.59, 2168.09].

By lesion, there were 41 (51%) complete responses (CR), 21 (26%) partial responses (PR) , 11 (13%) stable disease, and 8 (10%) progressive disease. Overall, there were 16 (20%) instances of local recurrence. Local progression free survival rates at 12 and 24 months were 80.7% and 75.8%, respectively. Cumulative incidence rates at 12 and 24 months were 15.3% and 18.8%. Overall response rate (ORR) was not significantly different between tumor volume quartiles (p = 0.658). Overall response rates for the 1st, 2nd, 3rd, and 4th quartiles of tumor volume were 13 (76%), 13 (76%), 12 (71%), and 13 (81%) respectively. Tumor control rates when >30 Gy radiation was used did not show a dose-dependent effect.

Acute Grade 2 or less toxicities included 63 (78%) instances of radiation dermatitis , 32 (40%) of fatigue , 32 of pain (40%), 21 (26%) of hyperpigmentation, 8 (10%) of lymphedema , 7 (9%) of pruritus, 6 (7%) of dysphagia, and 4 (5%) of nausea. There were no Grade 3+ toxicities except for Grade 3 radiation dermatitis occurring in 3 patients (4%).

Long-term toxicities included 7 (9%) patients with ulceration, 6 (7%) hyperpigmentation, 6 (7%) fibrosis, and 3 (4%) telangiectasias. One patient experienced chronic pain, and one experienced radiation recall when treated with sacituzumab govitecan.

Conclusion: Combining HT and RT yields excellent locoregional control while maintaining a favorable long term side effect profile, even in the context of re-irradiation. RT doses >30 Gy provided equivalent response rates and durable local control across a wide range of tumor volumes. Thermoradiotherapy is an attractive option for patients with recurrent breast cancer irrespective of their tumor volume.

56

Magnetic Nanoparticle Hyperthermia Integrated Interstitial Photodynamic Therapy for Tumor Treatments

Yash Lad M.Sc.[1], Emily Oakley Ph.D.[2], Anilchandra Attaluri Ph.D.[1], Gal Shafirstein D.Sc.[2]
[1]Pennsylvania State University, Middletown, Pennsylvania, USA. [2]Roswell Park Comprehensive Cancer Center, Buffalo, New York, USA

Yash Lad
Position (at Institution/Hospital/Company)
Graduate Research Assistant

Emily Oakley
Position (at Institution/Hospital/Company)
Post Doctoral Research Affiliate

Anilchandra Attaluri
Position (at Institution/Hospital/Company)
Associate Professor

Gal Shafirstein
Position (at Institution/Hospital/Company)
Professor of Oncology, Director of PDT Clinical Research

Abstract

Interstitial Photodynamic Therapy (iPDT), which involves the activation of a light-sensitive cancer killing drug, has shown promising results in the treatment of locally advanced head and neck, lung, and breast cancers. Nevertheless, a significant limitation arises when addressing intricate tumor margins close to vital structures (i.e. major blood vessels), as the depth of light penetration is restricted at these intricate sites to avoid vascular damage. Here we present a retrospective, computational study examining the application of magnetic nanoparticle hyperthermia (MNPH) following iPDT to target and treat tumor margins that were not effectively treated with iPDT alone. A three-dimensional (3-D) computed-aided (CAD) tumor geometry was reconstructed from segmentations of computed tomography (CT) scans acquired of a locally advanced tumor implanted in the neck of a rabbit. The 3D CAD geometry was imported into a commercial finite element analysis (FEA) software where the intratumoral light propagation during I-PDT was computed. In total, 11 iPDT light probes were required to illuminate the tumor margins with our effective light regimen for I-PDT (i.e. ≥ 8.6 mW/cm2 and ≥ 45 J/cm2 at the tumor margins). CT scans post light probe insertion into the rabbit tumor were acquired and our FEA model was updated to compute the actual light delivered during I-PDT. The reconstructed FEA simulation for iPDT revealed the presence of ineffective light treatment at the tumor margins. Using the same rabbit tumor 3D CAD geometry, a retrospective computational study was conducted in which magnetic nanoparticles (MNP) were injected into the areas with untreated margins. Two distribution zones were created based on the tumor geometry. A volumetric heat source of 4×106 [W/m3] was applied to the MNP. A fuzzy logic control algorithm was implemented based on feedback from two temperature measuring probes at the tumor boundary. Tumor boundary temperature was constrained at 43 [°C] using the fuzzy logic controller. Bioheat transfer simulations demonstrated that the temperature at the boundary of the tumor was controlled within the range of 42-45 [°C] using a fuzzy logic control algorithm. The simulation results indicate that the combination of iPDT and MNPH leads to a higher level of damage (5-10%) to the tumor, in comparison to iPDT alone. Therefore, iPDT followed by

MNPH may offer a more effective framework for treating locally advanced head and neck cancer.

57

Using MPI to Guide Thermal Simulations for Hyperthermia Treatment

Hayden Carlton PhD[1], Nageshwar Arepally[2], Sean Healy[3], Anilchandra Attaluri PhD[2], Robert Ivkov PhD[1,4]

[1]Johns Hopkins School of Medicine, Baltimore, MD, USA. [2]The PA State University, Harrisburg, PA, USA. [3]Georgia Tech University, Atlanta, GA, USA. [4]Johns Hopkins University, Baltimore, MD, USA

Hayden Carlton
Position (at Institution/Hospital/Company)
Postdoctoral Researcher

Nageshwar Arepally
Position (at Institution/Hospital/Company)
Graduate Student

Sean Healy
Position (at Institution/Hospital/Company)
Graduate Student

Anilchandra Attaluri
Position (at Institution/Hospital/Company)
Associate Professor

Robert Ivkov
Position (at Institution/Hospital/Company)
Professor

Abstract

Purpose: To develop and verify a clinically translatable, image-guided, *in silico* protocol for planning magnetic nanoparticle thermal therapies.

Introduction: Magnetic nanoparticle hyperthermia offers the ability to heat the interior of solid tumors remotely using magnetic fields. Magnetic nanoparticle heating, however, presents numerous technical challenges that limit widespread adoption. One such challenge is characterizing the intratumor nanoparticle distribution, which directly influences energy delivery and thermal dose absorbed by the cancerous tissue. Magnetic particle imaging (MPI) presents a solution to this challenge. MPI, a tracer imaging modality, directly measures the magnetic moment reversal of magnetic nanoparticles within a region of interest. The signal from these particles can be measured *in vivo*, co-registered with anatomical imaging, and used to map the distribution of nanoparticles within tissue. In this study, we developed and verified a protocol for incorporating this MPI data directly into thermal simulation software to be used for *in silico* thermal treatment planning.

Methods: The first step of the protocol was to co-register the MPI scans with anatomical imaging in order to establish a common datum. For analyzing the imagery, we used the research version of the Mimics Innovation Suite (Materialise Software, Leuven, Belgium). The tumor scan was then segmented to create a 3D mesh, to which the MPI signal was indexed. This mesh, with the indexed MPI signal, was then used to simulate the intratumor heat transfer. We used COMSOL® Multiphysics 6.2 (Burlington, MA) advanced numerical methods software for all heat transfer simulations. Two physics modules were used: Heat Transfer in Solids and Magnetic Fields, to simulate transient intratumor heating, as well as the Electromagnetic Heating multiphysics module. Verification of our *in silico* methodology

consisted of pilot-scale, *in vivo* imaging and heating trials in a 4T1 murine tumor model. All animal studies were approved by our Institutional Animal Care and Use Committee. We grew subcutaneous 4T1 tumors in five, 8-10 week old female BALB/c mice. When the tumors reached a size of 100-500 mm^3, nanoparticles were intratumorally injected to a target concentration of 2 mg Fe / cm^3 tumor (Synomag®-S90, micromod Partikeltechnologie, GmbH, Rostock, Germany). Immediately after injection, the mice were sacrificed. The tumors were then imaged with MPI (Magnetic Insight, Inc., Alameda, CA, USA) and microCT (Perkin-Elmer, Shelton, CT). After imaging, the tumors were heated with an alternating magnetic field, where two fiber optic probes measured temperature at the tumor center and the rectum. We then performed MPI-guided simulations for comparison against the experimental data. Recorded tumor temperatures were reported as a volumetric maximum, minimum, and average of the entire tumor geometry.

Results: The developed method was successful in incorporating the MPI data into thermal simulations. Upon completion of the pilot study, we observed excellent agreement between the experimentally measured intratumor temperatures and the respective simulations. For smaller tumors (100-300 mm^3), only a difference of 1-2°C was shown between the experimental and the average simulated tumor temperatures. As the tumors increased in size, this temperature difference increased commensurately. The heterogeneous distributions of nanoparticles at the injection site caused large thermal gradients to appear across the tumor geometry, thus accentuating the error associated with a lumped mass assumption and single temperature probe placement. However, the experimental temperatures still fell within the max/min temperature bounds shown in the simulation.

Conclusions: Agreement between the experimental and simulated tumor temperatures in the pilot study verified the functionality of our MPI-guided simulation protocol. Treatment outcome for large tumors can be further improved through the usage of multi-point thermometry for improved thermal characterization.

58

Why do magnetic nanoparticles heat under the Brezovich criteria conditions? Past the uniaxial-anisotropy assumption: critical role of the magnetocrystalline anisotropy.

Daniel Faílde[1], Víctor Ocampo-Zalvide[2], David Serantes[2], Òscar Iglesias[3]
[1]Centro de Supercomputación de Galicia (CESGA), Santiago de Compostela, Spain. [2]Universidade de Santiago de Compostela, Santiago de Compostela, Spain. [3]Universitat de Barcelona, Barcelona, Spain

Abstract

Careful determination of the heating performance of magnetic nanoparticles (MNPs) under AC fields is critical for magnetic hyperthermia applications. However, most interpretations of experimental data are based on the uniaxial-anisotropy assumption, which discards the intrinsic magnetocrystalline anisotropy (under the assumption that the former dominates). We show in this work that such premiss, generally valid for large field amplitudes, does not hold for small field/frequency values; specifically, we focus on the so-called Brezovich criteria. By means of a computational model, we show that the intrinsic magnetocrystalline anisotropy, which in first instance can be correlated with particle aspect ratio, plays a critical role in defining the heat output. Our results call therefore for an improvement in the theoretical models used to interpred magnetic hyperthermia performance.

59

Multi-applicator microwave ablation with directional and omni-directional antennas: feasibility study in normal porcine liver in vivo

Nooshin Zeinali[1], Austin Pfannenstiel[2], Clay Hallman[1], Haileigh Avellar[1], Brandon Plattner[1], David Hodgson[1], Jude Conley[2], Jan Sebek[1], Francois H. Cornelis[3], Rahul Anil Sheth[4], Punit Prakash[1]

[1]Kansas State University, Manhattan, KS, USA. [2]Precision Microwave Inc., Manhattan, KS, USA. [3]Memorial Sloan Kettering Cancer Center, New York, NY, USA. [4]University of Texas MD Anderson Cancer Center, Houston, TX, USA

Nooshin Zeinali
Position (at Institution/Hospital/Company)
Ph.D. candidate in the Department of Electrical and Computer Engineering, Kansas State University

Francois H. Cornelis
Position (at Institution/Hospital/Company)

Punit Prakash
Position (at Institution/Hospital/Company)

Abstract

Objective

Directional microwave antennas are under development and may offer operators an added degree of freedom to tailor ablation profiles. The objective of this study was to experimentally evaluate ablation zone volumes in porcine liver *in vivo* following dual-antenna microwave ablation (MWA) combining a directional and omnidirectional antenna.

Methods

MWA was delivered to sites within normal porcine liver *in vivo* using one directional and one omni-directional antenna. Antennas were designed to operate at 2.45 GHz (14 G; Precision Microwave, Inc) and were cooled with room-temperature water. Ablations were performed in female domestic swine (n = 4 pigs, weight: 50 – 65 kg) under general anesthesia, with antennas percutaneously inserted into the liver using ultrasound imaging guidance. Prior to commencing ablation procedures, a contrast-enhanced computed tomography (CECT) scan of the abdomen was performed. A custom fixture was employed to guide near-parallel insertion of antennas, with the aim of achieving an inter-antenna spacing of 2.5 cm; antenna placement was confirmed with CT imaging. Ablation procedures lasted either 180 s (selected to yield two discontiguous zones of ablated tissue between the antennas) or 600 s (selected to yield a contiguous zone of ablated tissue between the antennas). Power was delivered from a solid-state microwave generator augmented with a custom transmission coefficient monitoring apparatus, as previously described (Zeinali *et al.*, *IEEE Trans Biomed Eng*, 2023, PMID: 37943642), with 60 W estimated at the tip of each antenna. A total of 14 ablations were performed, with 3-5 ablations per pig. After the removal of the antennas, a post-procedure CECT scan facilitated the identification of ablation zone volumes. At necropsy, the liver was harvested and sectioned into approximately 5 mm thick slices and stained with triphenyl tetrazolium chloride (TTC) for assessment and measurement of the ablation zone extents.

Results

From post-ablation CECT images, for the 180-second ablations, the median volume of contiguous ablation zones was 17.4 cm^3 (17 – 29.4 cm^3) when the inter-applicator spacing was <2.5 cm (n = 3). Conversely, the median volume of discontiguous zones was 14.4 cm^3 (6.5 – 24.9 cm^3) for spacing ≥2.5 cm (n = 5). For the 600-second ablations, all zones were contiguous with a median volume of 31.7 cm^3 (20.1 – 91.1 cm^3). Intra-procedural electromagnetic transmission coefficient data were recorded, and analysis is in progress to evaluate the feasibility of intra-procedural monitoring of ablation zone growth.

Conclusion

When performing dual-antenna microwave ablation with an omni-directional and directional antenna, contiguous ablation zones were observed in normal porcine liver *in vivo* when inter-applicator spacing was <2.5 cm for 180 s ablations and was contiguous for all 600 s ablations.

60

Thermal Therapy Resistance in a 3D cell culture models of Adrenocortical Carcinoma

Sarah Feely, Nathan Mullen, Padraig Donlon, Michael C Dennedy
University of Galway, Galway, Ireland

Abstract

Adrenocortical carcinoma (ACC) is a rare aggressive cancer with a poor survival. Current treatment options are limited with surgical resection being the only option for a complete cure. Chemotherapeutic options, namely mitotane, are associated with limited efficacy and the development of drug resistance. Thermal ablation is now recommended for the management of metastatic tumour bulk for ACC patients. However, its prospect as a primary treatment remains challenging. In order to improve the efficacy of thermal therapies, models representative of the disease being studied are needed.

In the current study, we examined the effect of hyperthermia in novel 3D cell culture models of ACC cell lines, HAC15, H295R and MUC-1 compared to monolayer models.

First the ability of 3D cell culture models to accurately reflect the ACC tumour microenvironment was determined. This was carried out by measuring proliferative and metabolic activity, viability and steroidogenic capacity. To evaluate the effect of hyperthermia in ACC, 3D cell culture and monolayer models were treated with hyperthermia at temperatures of 37 (control), 42, 45 and 50 degrees.

MUC-1, H295R and HAC15 cells were successfully cultured in a type 1 collagen matrix, which is strongly expressed in the extracellular matrix of adrenal tumours. All cells remained viable with the emergence of a necrotic core present in HAC15 cells. All three models increase their metabolic and proliferative activity over time but had reduced rates compared to monolayer. Following treatment with hyperthermia, 42Degress did not induce a significant difference in excess cell death levels between 3D cell culture and monolayer models. However treatments of 45, 48 and 50 degrees hyperthermia, there was significantly less cell death in 3D cell culture compared to monolayer ($p>0.005$). This significance was seen at all exposure times (i.e. 15, 30 and 60 minutes of hyperthermia).

3D ACC cell culture models were developed successfully using collagen type 1 abundant in ACC, displaying some of the typical characteristics of the ACC tumour environment. These models therefore represent useful models to study hyperthermia for ACC. The resistance to hyperthermia observed in 3D models compared to monolayer could be explained by either (i) the reduction in proliferation (ii) the reduction in viability and the emergence of a necrotic core however further studies need to be carried out in order to investigate these mechanisms of resistance. Furthermore, exploring the role of hyperthermia in combination with chemotherapy could be a promising avenue for future investigations particularly in the case of drug resistance.

61

Reviving the 1927 Nobel Prize Malarial Fever Therapy for Dementia Paralytica a Century Later through Brain-guided Hyperthermia Reversing Lost Brain Function in Previously Untreatable Corticobasal Degeneration

Dr. M Marc Abreu MD[1,2], Dr. Alberto F. Chocron MD[3,4], Dr. Mohammad Hosseine-Farid PhD[5], Dr. Christian Renna DO[6], Dr Victor Spitz MD[3], Prof David M Smadja MD[7,8]
[1]Clinical Sciences Division, BTT Medical Institute, Aventura, Florida, USA. [2]Department of Biomedical Engineering and Medical Physics, BTT Medical Institute, Aventura, Fl, USA. [3]Clinical Science Division, BTT Medical Institute, Aventura, FL, USA. [4]Research Services, Miami Veteran Administration Medical Center, Miami, FL, USA. [5]College of Computing and Engineering, Nova Southeastern University, Fort Lauderdale, FL, USA. [6]Lifespan Medicine, Santa Monica, CA, USA. [7]University of Paris, Paris, France. [8]Georges Pompidou European Hospital, Paris, France

Dr. M Marc Abreu
Position (at Institution/Hospital/Company)
Medical Director

Dr. Alberto F. Chocron
Position (at Institution/Hospital/Company)
Clinical Researcher

Dr. Mohammad Hosseine-Farid
Position (at Institution/Hospital/Company)
Assistant Professor

Dr. Christian Renna
Position (at Institution/Hospital/Company)
Medical Director

Dr Victor Spitz
Position (at Institution/Hospital/Company)
Clinical Researcher

Prof David M Smadja
Position (at Institution/Hospital/Company)
Professor

Abstract

BACKGROUND: Our treatment utilizes the brain-eyelid thermal tunnel (BTT), pioneered at Yale University, which allows noninvasive brain temperature monitoring and brain-eyelid heat transfer. Corticobasal degeneration (CBD) is an untreatable, progressively fatal neurodegenerative disorder, exhibiting symptoms and pathology akin to Alzheimer's disease (cortical-related cognitive impairment) and Parkinson's disease (basal ganglia-related motor impairment). “Dr. Julius Wagner-Jauregg” (W) earned the “1927 Nobel Prize in Medicine” (N27) for his innovative and effective treatment of dementia paralytica, marked by severe cognitive and motor impairments akin to CBD, through intentionally infecting patients with malaria to induce high fever. Inspired by this Nobel Prize-winning research, Dr. Marc Abreu pioneered brain-guided whole-body hyperthermia (BgH) replicating fever patterns of N27, coined BgH-W27, to describe the groundbreaking N27 method while incorporating modern BgH technology, which enables safe, controlled, noninvasive, brain temperature-titrated hyperthermia devoid of severe malaria-related complications of 1927.

PURPOSE: Employ BgH-W27 for safe, effective CBD treatment to restore impaired cognitive-motor functions. **CASE REPORT:** A 70-year-old male diagnosed with CBD, showing progressive cognitive and motor deterioration, was referred from France to our Institute in Florida. Patient exhibited tremor, hypoesthesia, numbness, left arm stereognosis, inability to raise arm and alien limb phenomenon affecting left side. Imaging revealed cortico-subcortical atrophy. **METHOD:** Following informed consent, BgH-W27 was administered using FDA-approved Abreu-BTT-700 system and BTT radiant-heat equipment, involving heat chamber along with inductor delivering heat to brain via BTT. Exposure to far-infrared heat, targeting cyclical high fever patterns akin to tertian malaria of N27, lasted 180 minutes. Temperatures ranged from 40.5°C to 41.5°C. Continuous monitoring involved vital signs, including core temperature (tympanic probe), and eight skin sites: precordium, forehead, arms, hips, and calves. Pump provided hydration as needed. Brain temperature (Brain°) was measured with noninvasive FDA-approved C1-eyelid-probe. Patient had one treatment without adverse effects, and returned to France and has remained stable. **RESULTS:** Pre-treatment laboratory assessments revealed abnormally low serotonin (48 ng/ml), high dopamine (1080 pg/ml), elevated interleukin-10 (3.0 pg/ml) and reduced protein total (5.1 g/dl). Examination identified right and left arm tremor, sensation of foreignness in left arm, loss of fine motricity in left hand, and apraxia. Cognitive impairment was evidenced by score of 23 on Montreal Cognitive Assessment (MoCA). Remarkably, BgH-W27 promoted normalization of serotonin (68 ng/ml), interleukin-10 (<2.8 pg/ml) and total protein (5.6 g/dl) along with dopamine levels decreasing towards normalization (481 pg/ml). Evaluation in Florida 48 hours following BgH-W27 showed immediate restoration of motricity and coordination, demonstrated by movement of previously paralyzed arm, clapping hands, and opening bottles, tasks previously impossible. Cognition remarkably improved with MoCA of 25. Neuromuscular evaluation in France 1 month after BgH-W27 revealed additional improvements including: cognition (only one instruction to complete exercises compared to 3 previously), motor coordination of upper and lower limbs, restoration of left-hand sensitivity, grabbing and grasping with left hand (e.g., handling batons using Canadian plate), and exercise performance (level 4 Huber LPG with constant success rate of over 90%), besides notably reduced resting and exercise tremors. **CONCLUSION**: BgH-W27 emerges as a promising and well-tolerated noninvasive therapy for neurological disorders such as CBD, Alzheimer's, and Parkinson's diseases. Treatment with BgH-W27 leads to normalization of serotonin and interleukin-10 levels, besides reducing elevated dopamine levels. This normalization occurs concurrently with restoration of impaired cognitive and sensory-motor abilities associated with CBD. Recent findings suggest that reduced plasma serotonin may contribute to iron-dependent loss of dopaminergic neurons and neuronal degeneration (doi:10.1038/s41598-021-03700-2). Therefore, normalization of serotonin levels through BgH-W27 treatment could contribute to beneficial clinical outcomes in CBD therapy. However, further validation of our results is necessary through large-scale clinical trials targeting CBD treatment and other neurological disorders with BgH-W27.

62

Uptake of Fe/Fe3O4-Dopamine-Rhodamine B labelled K20 Nanoparticles into Adrenocortical Carcinoma Cells

Mr Ritihaas Surya Challapalli[1], Dr. Anna Sorushanova PhD[1], Dr. Cong Hong MBBS[1], Nathan Mullen[1], Sarah Feely[1], Obdulia Covarrubias-Zambrano[2], Jose Covarrubias[2], Dr. Sunitha Varghese[2], Prof. Constanza Hantel[3,4], Dr. Peter Owens[1], Prof. Martin O'Halloran[1], Prof. Punit Prakash[5], Prof. Stefan Bossmann[2], Prof. Michael Conall Dennedy MD, PhD, FRCPI[1]
[1]University of Galway, Galway, Galway, Ireland. [2]The University of Kansas Medical Center, Kansas, Kansas, USA. [3]University Hospital Zurich, Zurich, Switzerland. [4]University Hopsital Carl Gustav Carus Dresden, Dresden, Germany. [5]Kansas State University, Manhattan, Kansas, USA

Mr Ritihaas Surya Challapalli
Position (at Institution/Hospital/Company)
Research Associate

Prof. Constanza Hantel
Position (at Institution/Hospital/Company)
Head of Endocrinology Research laboratory, clinic for endocrinology, diabetology and clinical nutrition

Dr. Peter Owens
Position (at Institution/Hospital/Company)
Facility scientist at the Centre for Microscopy and Imaging

Prof. Martin O'Halloran
Position (at Institution/Hospital/Company)
Professor of Medical Electronics, University of Galway
Executive Director, Bioinnovate Ireland

Prof. Punit Prakash
Position (at Institution/Hospital/Company)
Professor and Paul L. Spainhour Professorship in Electrical Engineering

Prof. Stefan Bossmann
Position (at Institution/Hospital/Company)
Department Chair

Prof. Michael Conall Dennedy
Position (at Institution/Hospital/Company)
Associate Professor in Therapeutics, University of Galway
Consultant Endocrinologist, Galway University Hospital
Principal Investigator: HRB ICAT Programme, University of Galway.
Vice-Dean of Mentorship and Staff Development, University of Galway.

Abstract

Adrenocortical carcinoma (ACC), a rare and often fatal cancer with a limited survival rate of up to 24 months, necessitates diverse treatment approaches such as surgery, chemotherapy, or radiation. Due to its high recurrence rate, there is a critical demand for innovative therapies. Magnetic iron oxide nanoparticles have emerged as promising contenders for cancer treatment due to their adaptability in size and shape, can be customized for targeted cellular absorption. In our initial investigation, we examined the absorption of K20-labelled Fe/Fe3O4 – Dopamine – Rhodamine B particles (IONP) by ACC (H295R, HAC15, and MUC1) cells, HUVECs, and primary monocytes. These cells were

exposed to varying concentrations of IONP (0, 5, 10, 20, and 50 µg/ml) for a period of 24 hours. The results indicated a concentration and time-dependent uptake of nanoparticles and its impact on cellular viability and metabolic activity of ACC cells. The optimal concentration of IONP was determined as 10 µg/ml, and subsequent assessments focused on the rate of uptake, intracellular location and effect on steroidogenesis of ACC cells. The efficiency of IONP uptake by ACC cells diminished when exposed to primary monocytes and an HUVEC layer, as demonstrated through a Transwell migration system. This study provided insights into the non-specific uptake of IONP by ACC, primarily attributed to the mechanism of macropinocytosis. These preliminary findings support exploring potential modifications to enhance specific uptake by ACC cells.

63

Temperature-related differences in treatment response of skin metastases from ovarian cancer to wIRA hyperthermia plus radiotherapy

Dr. Anne-Marie Lüchtenborg PHD[1,2], Dr. Kristin Technau-Hafsi MD[3], Professor Dr. Anca-Ligia Grosu MD[1,4], Dr. Markus Notter MD[5], Professor Peter Vaupel MD[1,4], Dr. Andreas R. Thomsen MD[1,4]

[1]Department of Radiation Oncology, University Medical Center, University of Freiburg, Freiburg, Germany. [2]German Cancer Consortium (DKTK), Partner Site Freiburg and German Cancer Research Center (DKFZ), Heidelberg, Germany. [3]Department of Dermatology and Venereology, Medical Center - University of Freiburg, Faculty of Medicine, University of Freiburg, Freiburg, Germany. [4]German Cancer Consortium (DKTK) Partner Site Freiburg, German Cancer Research Center (DKFZ), Heidelberg, Germany. [5]Department of Radiation Oncology, Lindenhofspital Bern, Bern, Switzerland

Professor Dr. Anca-Ligia Grosu
Position (at Institution/Hospital/Company)
Director

Abstract

Objective:
Cutaneous metastases of ovarian cancer are relatively rare, accounting for approx. 3.5% of cases and predominantly occur as Sister Joseph Nodules (SJN) in the periumbilical region, but also in recurrent setting as non-SJN lesions in abdomen, genitalia and limbs. These manifestations significantly compromise quality of life of patients. Although not yet integrated into guidelines, treatment modalities including systemic therapy and surgical resection are recommended. Additionally, radiation therapy is proposed as a viable option for managing extensive non-SJN metastases.

Methods:
A 48-year-old patient with cerebral and lymphatic metastatic ovarian carcinoma presented nine years after initial diagnosis (FIGO IIIC pT2a, pN1, L1, V1, Pn0, G3, BRCA1+2: negative) with extended rash on the thorax and both legs. Lesions were initially suspected as herpes zoster infection but proved to be resistant to acyclovir, and were histologically confirmed as skin metastases of the known ovarian carcinoma with signs of lymphangiosis carcinomatosa.

The patient was treated with carboplatin/gemcitabine and concomitant hypofractionated radiotherapy combined with hyperthermia on the medial thigh. Radiation was carried out with 5 x 4 Gy in weekly sessions. Immediately before radiotherapy, the target area was heated to 39-43 °C for 60 min using water-filtered infrared A (wIRA). Due to the geometry of the target area on the inner thigh, only the ventral and medial portion of the thigh could be warmed up as desired.

Results:
Overall, the patient responded very well to the therapy, with a marked regression of the ulcerating lesions on the medial thigh and no significant toxicity. At first follow-up, she presented with a complete response in the irradiated region. Local control of metastases is persisting for >1 year. Notably, the area with hyperthermia >40°C showed earlier response than the treatment area <39°C.

Conclusion:
The combination therapy of mild superficial hyperthermia and hypofractionated low-dose radiotherapy is a treatment option for very extensive cutaneous metastases of ovarian cancer that may warrant long-term disease control. In the presented case, a higher temperature range appears to translate into a more pronounced clinical response.

64

Clinical Outcomes of Re-irradiation with Concurrent Deep Hyperthermia Therapy for Lower Gastrointestinal Malignancies – Long Term Follow up

Jason Molitoris, Sina Mossahebi, Nrusingh Biswal, Mark Zakhary, Dan Kunaprayoon, Zaker Rana, Dario Rodrigues
University of Maryland School of Medicine, Baltimore, MD, USA

Abstract

Methods

14 consecutive patients treated with reirradiation with concurrent DHT at a single institution were analyzed retrospectively. Patients were treated with twice weekly DHT, treated immediately before or after radiation (RT) treatments, delivered via a concentric ring radiofrequency phased array system at a frequency range of 75-120 MHz to a target temperature of 40-43°C. Thermistors were placed in the bladder, rectum and/or vagina and externally on the patient's skin to measure temperature. Patients were monitored throughout the 30–60-minute treatment. Kaplan-Meier (KM) method was used to estimate outcomes.

Results

Median age was 65. Most patients (8, 60%) were treated for recurrent rectal cancer. 3 (21.4%) were treated for rectal cancer who were status-post radiation for a different primary (2 with a history of prostate cancer and 1 with a history of endometrial cancer), 2 (14.3%) for recurrent anal cancer, and 1 (7.1%) multiply recurrent sigmoid. 4 (28.6%) were metastatic at time of DHT. 10 (71.4%) received concurrent chemotherapy. Median dose of RT at time of DHT was 40.8 Gy (30-51 Gy), 12 (80%) underwent BID treatment and all patients were treated with proton therapy. Overall, DHT was well tolerated with only 2 (14.3%) unable to complete their planned treatment, with no acute grade 2+ thermal toxicities. 2 of 5 proceeded with planned resection following DHT/RT (1 refused, 1 had progressed and thus no longer a candidate, and 1 was aborted due to intra-operative hemorrhage). 9 patients had symptoms associated with their disease and all but one obtained symptom relief.

With a median follow-up of 13 months (3-37), 2 patients experienced grade 3 toxicity; both were peri/post-operative complications. No grade 4+ toxicities occurred. 35.7% had local progression, 4 28.6% had regional progression and 50% had distant progression. 1 yr LC and OS were 64.3% (SE +/-14.9%) and 69.8% (SE +/-14.9%). Median PFS was 9 moths (SE +/-3).

Conclusion

Our results on the use of DHT for lower GI malignancies in the setting re-irradiation suggests that this combined modality approach is well tolerated with favorable outcomes and can provide durable control and palliation. Prospective studies are needed to better ascertain which patients derive the greatest benefit from this treatment.

65

Efficacy and mechanisms of hyperthermia induced cell death in adrenocortical carcinoma

Mr Nathan Mullen BSc.[1], Dr Padraig T Donlon PhD[1], Ms Sarah Feely BSc.[1], Dr. Anna Sorushanova PhD[1], Mr Ritihaas Challapalli MSc.[1], Dr Kate M Warde PhD[1,2], Mr Cong Hong BSc.[1], Prof Martin O'Halloran PhD[3], Associate Prof Michael Conall Dennedy MD. PhD.[1]
[1]Discipline of Pharmacology and Therapeutics, School of Medicine, University of Galway, Galway, H91 V4AY, Ireland, Galway, Ireland. [2]Huntsman Cancer Institute, Department of Oncological Sciences, University of Utah School of Medicine, Salt Lake City, UT 84112, USA, Salt lake coty, Utah, USA. [3]Translational Medical Device Laboratory, University of Galway, Galway, H91 V4AY, Ireland, Galway, Ireland

Mr Nathan Mullen
Position (at Institution/Hospital/Company)
PhD student

Dr Padraig T Donlon
Position (at Institution/Hospital/Company)
Post doctoral researcher

Ms Sarah Feely
Position (at Institution/Hospital/Company)
PhD student

Dr. Anna Sorushanova
Position (at Institution/Hospital/Company)
Post doctoral researcher

Mr Ritihaas Challapalli
Position (at Institution/Hospital/Company)
Post doctoral researcher

Dr Kate M Warde
Position (at Institution/Hospital/Company)
Post doctoral researcher

Mr Cong Hong
Position (at Institution/Hospital/Company)
PhD student

Prof Martin O'Halloran
Position (at Institution/Hospital/Company)
Principal Investigator

Associate Prof Michael Conall Dennedy
Position (at Institution/Hospital/Company)
Principal investigator

Abstract

Introduction:

Adrenocortical carcinoma (ACC), a rare and aggressive cancer, presents significant challenges in treatment due to its resistance to conventional therapies. In light of the limited therapeutic options available, our study aimed to explore the efficacy

of hyperthermia against ACC specifically probing the potential role of Caspase 3 mediated apoptosis.

Methods:

ACC cell lines (H295R and HAC15) and the non-cancerous HUVEC endothelial cell line, were treated with hyperthermia at 42°C, 45°C, 48°C, and 50°C in controlled water baths. Cell viability was assessed using Annexin V/Sytox blue (Flow cytometry),Calcein/Propidium iodide (Confocal), and the xCELLigence Real Time Cell Analyser. While the involvement of Caspase 3 mediated apoptosis was measured using western blotting.

Results:

We observed a significant reduction in cell viability in H295R and HAC15 cells treated with 48°C and 50°C hyperthermia, evident immediately and 24 hours post-treatment, which we defined as 'lethal hyperthermia'. Contrastingly, HUVEC cells were more robust, suggesting varied cellular sensitivities to hyperthermia. Furthermore, our findings revealed a resilience in ACC cells when treated with 45°C hyperthermia, where an initial decrease in viability was followed by a recovery, indicating a potential adaptive response to sublethal hyperthermic stress. Surprisingly, our results from the Annexin V/Sytox Blue and Caspase 3 western blot assay suggests that caspase 3 mediated apoptosis was not the primary pathway in hyperthermia-induced ACC cell death.

Conclusion:

Hyperthermia≥48°C is lethal to ACC cells, offering new therapeutic possibilities. Interestingly, these cells demonstrate resilience at 45°C, suggesting alternative mechanisms beyond Caspase 3 mediated apoptosis in hyperthermia-induced cell death, underscoring the need for further mechanistic exploration.

66

Boiling Histotripsy-Induced Local Tumor Immunomodulation Impacts the Gut Microbiome at a Distant Site

Ms Sri Vidhya Chandrasekar BVSc and AH, Dr Akansha Singh PhD, Dr Ashish Ranjan BVSc, PhD
University of Texas Southwestern, Dallas, Texas, USA

Ms Sri Vidhya Chandrasekar
Position (at Institution/Hospital/Company)
Graduate Student Researcher

Dr Akansha Singh
Position (at Institution/Hospital/Company)
Assistant Professor

Dr Ashish Ranjan
Position (at Institution/Hospital/Company)
Barret Family Professor of Cancer Research
Director: One Medicine Center
Vice Chair: Research Innovations & Comparative Oncology

Abstract

Introduction: Therapeutic interventions, including focused ultrasound-based histotripsy (HT), aimed at mechanically ablating tumors, have the potential to transform poorly immunogenic environments into activated 'hot' targets by releasing tumor antigens, thereby fostering both local and systemic anti-tumor immunity. However, HT alone often fails to sustain a prolonged, anti-tumor immune response. This raises the question of whether other factors, such as the gut microbiome, can dynamically influence HT-mediated tumor immunomodulation, even when they are not immediately adjacent to the tumors. To gain these essential insights, herein we examine the impact of HT-mediated immunomodulation on poorly immunogenic murine oral squamous cell carcinoma (MOC) and its influence on the dynamics of the gut microbiome, establishing its correlation with therapeutic outcomes.

Methods: Female mice with MOC2 (Head and Neck Squamous Cell Carcinoma) tumors were randomly assigned to one of two groups (n=6 mice/group): 1) Control and 2) HT. Two local HT treatments, each covering less than 10% of the tumor volume, were administered with a three-day interval. Fecal samples were collected both before inoculation and on day 20 post-inoculation, which coincided with euthanasia for microbiome analysis. Tumor and serum samples were processed for flow cytometry and cytokine analysis to provide insights into the gut-microbiome-tumor axis. Fecal pellets underwent analysis for the gut microbiome using targeted sequencing of the bacterial 16S ribosomal RNA gene. The raw data were analyzed using MicrobiomeAnalyst, and Pearson correlation was performed between the profiles of tumor immune-cytokines and the abundance of bacterial genera at the genus level.

Results: Significant suppression of MOC2 tumor growth rates (~64%) was observed two weeks post-HT treatment compared to the untreated control group. The increased efficacy of HT treatment was associated with enhanced infiltration of cytotoxic T cells and NK cell populations within the tumor. Gut microbiome analysis revealed substantial shifts at both

phylum and genus levels, with these changes aligning with immune-active and suppressive immune dynamics. A positive correlation was observed with Monocytic-Myeloid Derived Suppressor Cells (M-MDSC). In particular, bacterial population of Turicibacter exhibited positive associations with anti-tumor immune populations and cytokines, while displaying negative associations with tumor growth.

Conclusion: Immunomodulatory therapy employing ablative approaches can be impacted by gut microbiomes, in conjunction with other pertinent factors. Future studies involving gut depletion and transplantation of identified pathogens can provide further insights into their therapeutic potential and their capacity to support ablative therapies.

67

Safety Testing of Non-invasive Blood Perfusion Measurement Device

Shreeniket Pawar[1], Benjamin Westahafer[1], Jessica El-Mallah[2], Mary Landmesser[2], Olivia Waldron[2], Anilchandra Attaluri[1], Dino Ravnic[2], Mohammed-Reza Tofighi[1]
[1]Penn State University, Middletown, USA. [2]Penn State College of Medicine, Hershey, USA

Shreeniket Pawar
Position (at Institution/Hospital/Company)

Abstract

Non-invasive monitoring of the blood perfusion of skin flaps in post-reconstructive surgery is an unmet need. A novel non-invasive perfusion measurement device based on the 'thermal washout' method combining microwave heating (MWH) and infrared (IR) radiometry was proposed previously. This study reports the development and testing of the device. Briefly, the device consists of a microwave slot antenna and a power source at 2.4 [GHz], with a maximum peak power of 10 [W] and IR temperature sensor housed in a handheld 3D-printed enclosure. The temperature from the IR sensor is used to drive the microwave source through pulse width modulation (PWM), to control the power level dynamically. Various tests have been performed in tissue phantoms and small animals to evaluate the device and its safety. For the latter, two rats were used for conducting the study at different time and temperatures. For the study, the MWH was applied at three different power levels between 2 to 8.5 [W] and for various time intervals between 2 and 6 [mins]. Temperature elevations of 4-5 [°C], 5-7 [°C] and 15-17 [°C] were observed for 2, 4 and 8.5 [W] respectively. Tissue samples were sent to histopathology to investigate thermal damage.

A temperature feedback PID controller to maintain the surface temperature elevation of approximately 2-3 [°C] for perfusion measurements through a thermal washout curve is currently being developed. The developed control system and verification of the device using tissue perfusion phantoms will be presented at the conference.

68

Spatially Confined Thermal Damage feedback Control System for Magnetic Nanoparticle Hyperthermia

Shreeniket Pawar[1], Nageshwar Arepally[1], Yash Lad[1], Hayden Carlton[2], Ma'Moun Abu-Ayyad[1], Robert Ivkov[2], Anilchandra Attaluri[1]
[1]Penn State University, Middletown, USA. [2]Johns Hopkins University, Baltimore, USA

Abstract

Magnetic nanoparticle hyperthermia therapy (MNPH) has shown prominent results in cancer treatments. A significant limitation of current MNPH devices is the inability to deliver conformal thermal dose to the tumor. The objective of this study is to develop a control system for spatially confined MNPH (HYPER) to deliver prescribed conformal thermal dose. Spatially confined MNPH is achieved by dynamically adjusting field free region (FFR), based on thermal dose feedback. Idealized subcutaneous tumor model, i.e., tumor embedded in cuboidal muscle, is considered as the computational domain. Magnetic nanoparticle (MNP) distribution obtained from magnetic particle imaging (MPI), was divided into two separate domains to achieve dynamically adjustable FFR. A proportional-integral-derivative (PID) controller was designed by preforming integrated system dynamic – finite element modelling using MATLAB Simulink®- COMSOL Multiphysics© co-simulations. The tumor center temperature was constrained at 60 [°C] and tumor boundary temperature constrained at 43 [°C]. The controller output was set to zero once the thermal dose reached a value of CEM43T10 in the tissue adjacent to the tumor boundary. The controller output was limited to 15 [mT], with a rate of change of 5 [mT/s]. The controller performance for three different nanoparticle distribution cases were studied: uniform, gaussian and in-vivo distribution. Simulation results predicted CEM43T90 of 43 [°C] achieved in 25-35% of tumor volume. Results show that the uniform distribution gives optimum coverage of the lesion compared to in-vivo and gaussian distribution. Untreated tumor margins were identified post simulations, and an additional study was set to treat the untreated tumor margins using spatially confined heating with dynamically adjustable FFR. The thermal damage is further increased with the spatially confined heating. The developed controller will be implemented on the HYPER prototype. Controller design verification will be performed using phantom experiments. Results of the experiments will be presented during the conference presentation.

69

Heat Sink Effects of Fluidic Structures During Thermal Therapies

Shreeniket Pawar, Yash Lad, Omar Abdulqader, Naveen Kondreddy, Anilchandra Attaluri
Penn State University, Middletown, USA

Abstract

Thermal therapies are used to treat various cancers such as brain, rectal and lung cancers. Fluidic structures such as major blood vessels and ventricles act as heat sinks and lead to inadequate thermal dose. Current treatment planning tools and simulations use effective thermal conductivity, convectively enhanced thermal conductivity, or simplified convective boundary conditions to account for the heat loss from fluidic structures. Computationally expensive high-fidelity conjugate bioheat transfer models are required to predict the intratumor thermal dose. This study investigates the feasibility of using high-fidelity conjugate heat transfer models to develop empirical relationships to account for the heat sink effects of fluidic structures. Parameters such as fluid velocity and geometric parameters along with non-dimensional variables such as Reynolds number, Nusselt number, Grashoff number, and shape factors, will be considered in developing the empirical relationships. Two treatment cases were studied, one considering the tumor located near a large blood vessel and the second considering the cerebrospinal fluid (CSF) ventricle located near the tumor. All simulations were performed using a commercial finite volume solver, Siemens STAR CCM+. Tissue heat transfer and flow in the fluid structures were modeled using the Pennes bioheat equation and Navier – Stokes equations respectively. Thermal damage-dependent tissue perfusion is also modeled. For large blood vessels, both pulsatile blood flow and laminar flow were considered. The difference in estimated convective heat transfer coefficient (CHTC) at the vessel wall was ~ 1-2%. All further simulations were assumed to be laminar incompressible flow. Initial simulations identify the distance between the tumor boundary and the fluidic structures, volumetric heating rate, and fluid velocity as the significant factors influencing the convective heat transfer coefficient at the wall of the fluid structures. For CSF ventricles, the heat loss is due to mixed convection, i.e., both forced convection from CSF velocity and free convection (buoyancy-driven flow). Boussinesq’s approximation was used to model buoyancy-driven flow. Significant factors influencing the convective heat transfer coefficient at the wall of the fluid structures were the distance between the tumor boundary and the fluidic structures and the volumetric heating rate. CSF velocity does not have a significant influence on the estimated CHTC. Results will be compared to previously reported CHTC based on theoretical and experimental data. Empirical relations for CHTC based on high-fidelity conjugate bioheat transfer models have the potential to reduce computational resources while maintaining the accuracy of the thermal dose predictions.

70

Feasibility of Targeting the Dorsal Root Ganglia with Focused Ultrasound for Treatment of Low Back Pain

Ethan D Griswold[1,2], Michelle Kline[2], Allison Payne[1,2], Lubdha M Shah[2], Viola Rieke[1,2]
[1]University of Utah, Department of Biomedical Engineering, Salt Lake City, Utah, USA.
[2]University of Utah, Department of Radiology & Imaging Sciences, Salt Lake City, Utah, USA

Abstract

Introduction

Chronic low back pain (cLBP) affects a majority of people at some point in their lives and can often be debilitating with a negative impact on quality of life. Neuromodulation of the dorsal root ganglia (DRG) is a promising technique for alleviating cLBP. DRG therapy to date has been through implanted leads directly stimulating the nerves or minimally invasive through radiofrequency ablation. In this study, we investigate if the lumbar DRGs can be targeted noninvasively with MR guided focused ultrasound (MRgFUS) as a potential noninvasive treatment for cLBP. Lumbar DRG locations are challenging for external FUS as they are surrounded by osseous structures, including the facet joints and transverse processes, which could potentially obstruct the FUS beam path. Pre-procedure planning of the beam path will be critical for efficiency and safety of MRgFUS.

Methods

We performed analysis of 23 anonymized patient CTs, measuring the total distance between skin and target site and subcutaneous fat thickness for vertebral levels T12 to L5. From these datasets, 6 patient CTs were segmented into different tissue types for acoustic simulation (spinal cord, bone, muscle, fat, and skin). As the DRG is not well-delineated on CTs, the DRG target was manually selected based on the location of the intervertebral foramina. Acoustic simulations were performed with a hybrid angular spectrum method (Vyas and Christensen, 2012) for ultrasound beam propagation at various transducer angles and vertebral levels, resulting in a dynamic pressure pattern across the tissue. Within this simulation, we utilized design specifications of a 256-element transducer with a 1 MHz central frequency with elements randomly positioned over a spherical face with an 11 cm focal length.

Results

In a patient population of 13 females and 10 males (24-90 years old, mean 62), the distance from the skin to DRG ranged from 7.07 ± 1.92 cm to 9.98 ± 1.61 cm, with subcutaneous fat of 1.60 ± 0.84 to 3.62 ± 1.57 cm. The average distance from skin to DRG ranged from 6.48 ± 1.78 cm to 9.69 ± 1.35 cm in women, with a subcutaneous fat layer of 1.64 ± 0.86 cm to 3.72 ± 1.49 cm. In men, the skin to DRG distance ranged from 7.78 ± 1.92 cm to 10.38 ± 1.67 cm, with a subcutaneous fat layer of 1.56 ± 0.86 cm to 3.59 ± 1.91 cm. In all datasets, distance from skin to DRG target increased with the more caudal vertebral levels with a greater percentage of the total distance along the beam path being subcutaneous fat.

Within the segmented and simulated models, the DRGs can be accurately and efficiently targeted with the ultrasound beam. Adequate energy can be delivered to the target with minimal effects to the surrounding tissue. Positioning the transducer at an angle of 30º allows for a FUS trajectory that is not obstructed by bone from the transverse processes.

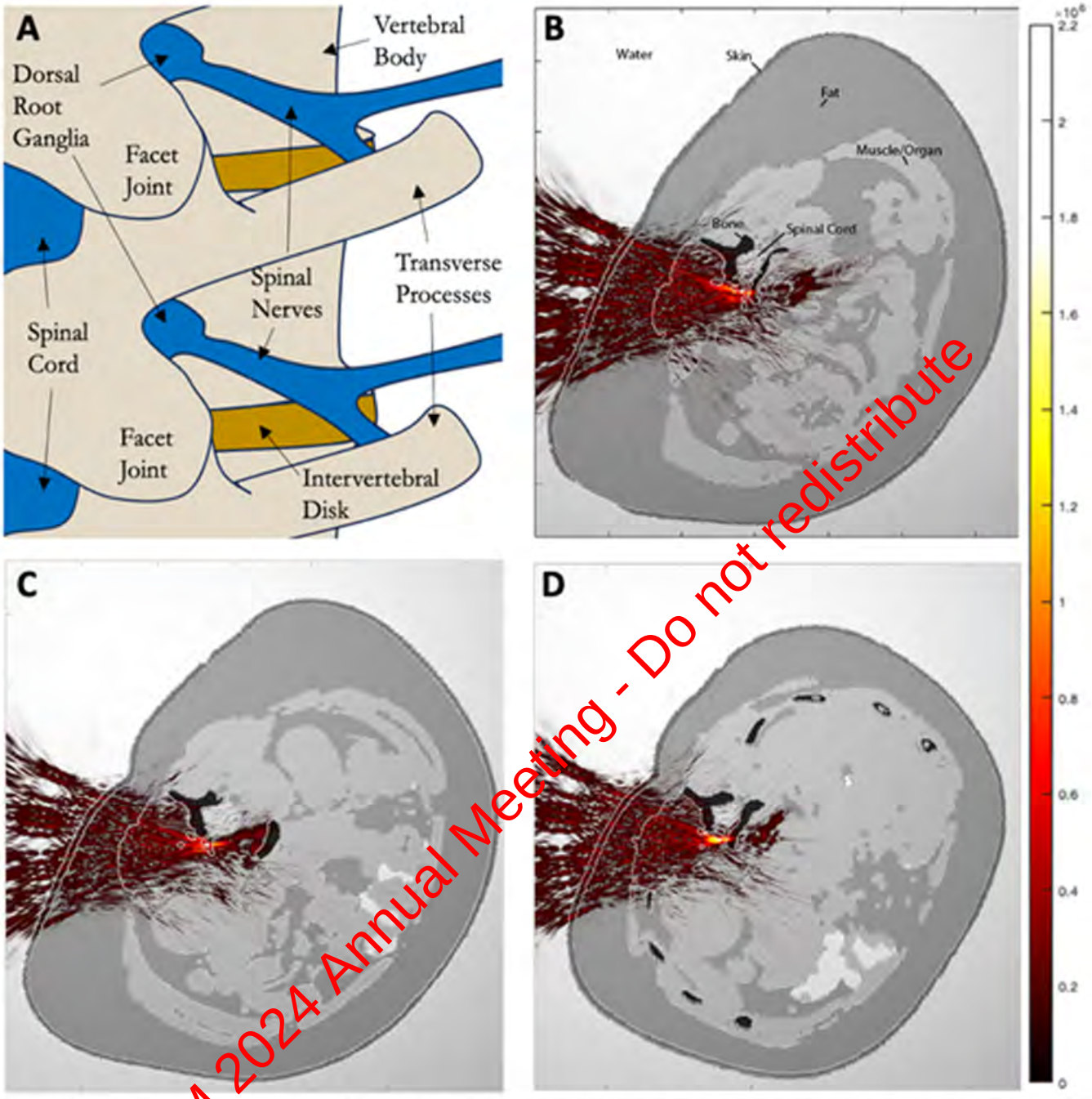

HAS simulations of DRG targeting. A) Anatomical position of the DRG, viewed posteriorly. **B-D)** Simulation of the DRG targeting at different vertebral levels, with the white star within the figure indicative of target voxel. Scale bar is representative of the dynamic pressure wave in pascals with a 10^5 scaling factor.

Discussion

Our simulation studies showed that therapeutic level FUS energy can be delivered to the DRG to enable neuromodulation in patients. We chose CT over MRIs in this early feasibility study for easy visualization and segmentation of the osseous spinal structures. Future studies will include thermal simulations to verify safety margins for neuromodulation applications or determine if ablative procedures can be performed with this transducer based on the patient's anatomy. With acoustic attenuation related to tissue composition and distance to the target, we will investigate which vertebral levels may be effectively

treated based on the choice of transducer and other design constraints such as magnet bore size for MR-guided applications.

71

Characterizing Temperature Distribution in Thermoembolization Using a Collagen Hydrogel-Based Microfluidic Platform

Amin Sabaghan[1], Sean Brocklehurst[1], Erik Cressman[2], Marissa Nichole Rylander[1]
[1]The University of Texas at Austin, Austin, Texas, USA. [2]The University of Texas MD Anderson Cancer Center, Houston, Texas, USA

Amin Sabaghan
Position (at Institution/Hospital/Company)
PhD student at the University of Texas at Austin

Sean Brocklehurst
Position (at Institution/Hospital/Company)
PhD student at the University of Texas at Austin

Erik Cressman
Position (at Institution/Hospital/Company)
Associate professor at UT MD Anderson Cancer Center

Marissa Nichole Rylander
Position (at Institution/Hospital/Company)
Associate Professor at the University of Texas at Austin

Abstract

Introduction

Patients diagnosed with intermediate-stage Hepatocellular Carcinoma (HCC) typically undergo transarterial therapy (TT) as part of their treatment. A recent advancement in TT, termed thermoembolization (TE), shows promise. TE involves the in situ exothermic reaction of dichloroacetyl chloride (DCACl), resulting in combined ischemia, hyperthermic endovascular ablation, locally acidic pH, and targeted drug delivery guided by imaging [1,2]. While offering potential solutions to the challenge of incomplete treatment associated with other TT methods, the optimization of treatment parameters for maximal efficacy with this novel approach remains uncertain. It is crucial to understand the appropriate quantity and concentration of the TE reagent to affect the HCC tumor microenvironment while minimizing damage to adjacent normal cells. Consequently, there is a pressing need to evaluate the spatial and temporal distribution of temperature and pH surrounding the injected TE reagent. This study focuses on examining the temporal and spatial temperature distribution within a 3D vascularized collagen hydrogel platform representative of tissue after injecting the TE reagent into a microchannel embedded in the gel.

Materials and Methods

Holder preparation

The holders for the collagen platform were fabricated by casting polydimethylsiloxane (PDMS) into milled aluminum molds. The PDMS elastomer base and curing agent (10:1) were mixed and cured overnight in a 75 °C oven. Using a plasma treater, the PDMS holder was affixed to a glass coverslip to create a well with a glass bottom. A 22-gauge blunt-tip needle was inserted into the microchannel of the holder. To enhance collagen gel adhesion on the PDMS surfaces, a solution comprising 1% polyethylenimine (PEI) and 0.1% glutaraldehyde was pipetted into the holder, followed by three rinses with sterile deionized water [3]

Collagen preparation

Buffer solutions for creating the collagen gel were prepared by mixing 1X DMEM, 10X DMEM, and 1 M NaOH. The buffer was combined with a 6 mg/mL collagen stock solution in a 1:1 ratio. The resultant mixture was carefully pipetted into the well, ensuring coverage of the needles. Subsequently, the platform was placed in an incubator for a minimum of 30 minutes to allow the gel to solidify, after which the needles were gently withdrawn

DCACl preparation
3M and 1M DCACl solutions, dissolved in poppy seed oil, were prepared and then injected into the microchannel using a 24-gauge needle.

Imaging

A high-resolution infrared thermal camera (model: FLIR T62101) was employed to capture the temperature distribution in the gel over 60 seconds, providing a top-view perspective during and after the injection of the reagent into the gel.

Results

Figure 1 illustrates the temperature distribution immediately after 20 seconds and 60 seconds following the injection of DCACl solutions (3M and 1M) into the microchannel embedded in the gel. The interaction of the DCACl solution with the collagen gel surrounding the microchannel resulted in an exothermic reaction, causing a temperature increase in the injection vicinity. Moreover, the data demonstrates that the higher concentration of DCACl (3M) induces a more pronounced temperature elevation in the gel compared to the lower concentration (1M). This effect extends over a larger spatial area and persists for a longer duration. Additionally, regarding the images taken with the cell phone camera, given the use of phenol red in the gel (as a component of DMEM) and knowing the fact that its color shifts to yellow in acidic pH conditions, a notable pH decrease around the injection area is observed over time following the administration of DCACl (3M) which is greater than DCACl (1M).

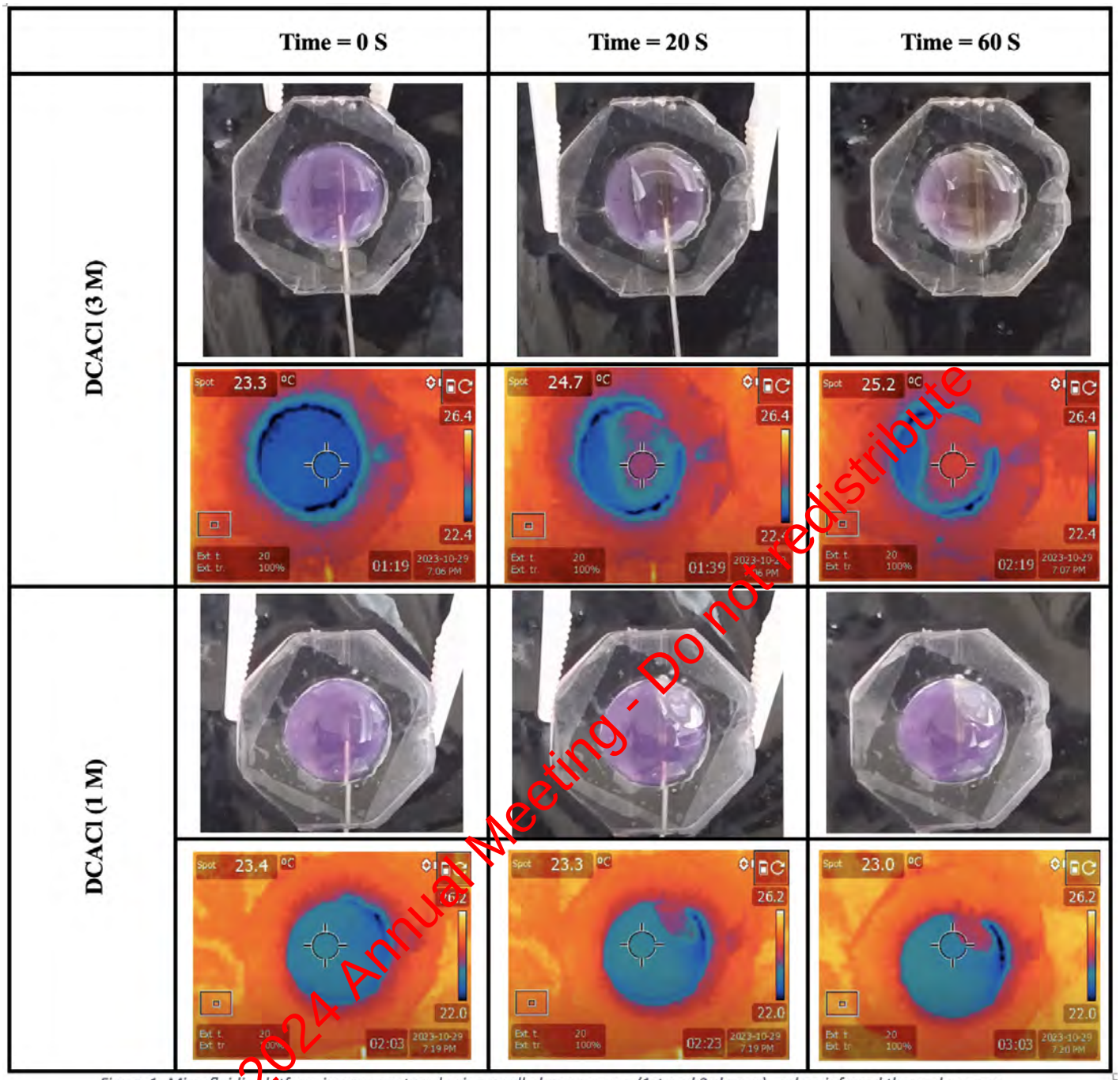

Figure 1- Microfluidic platform images captured using a cell phone camera (1st and 3rd rows) and an infrared thermal camera (2nd and 4th rows) at 0, 20, and 60 seconds post-injection of DCACl with concentrations of 3M and 1M.

72

Evaluation of a Balloon Implant for Simultaneous Magnetic Nanoparticle Hyperthermia and High-Dose-Rate Brachytherapy of Brain Tumor Resection Cavities

Shuying Wan[1], Dario B. Rodrigues[2], Janet Kwiatkowski[3], Omaditya Khanna[4], Kevin Judy[4], Robert C. Goldstein[5], Marty Overbeek Bloem[6], Yan Yu[1], Sophia E. Rooks[1], Wenyin Shi[1], Mark D. Hurwitz[7], Paul R. Stauffer[1]

[1]Department of Radiation Oncology, Thomas Jefferson University Hospital, Philadelphia, PA, USA. [2]Department of Radiation Oncology, University of Maryland School of Medicine, Baltimore, MD, USA. [3]MAE Group, Deerfield, NH, USA. [4]Department of Neurosurgery, Thomas Jefferson University Hospital, Philadelphia, PA, USA. [5]AMF Life Systems, Auburn Hills, MI, USA. [6]Phoenix DeVentures, Morgan Hill, CA, USA. [7]Radiation Medicine, Westchester Medical Center University Hospital, Valhalla, NY, USA

Abstract

Previous work has reported the design of a novel thermobrachytherapy (TBT) balloon implant to deliver magnetic nanoparticle (MNP) hyperthermia and high-dose-rate (HDR) brachytherapy simultaneously after brain tumor resection, thereby maximizing their synergistic effect. This paper presents an evaluation of the robustness of the balloon device, compatibility of its heat and radiation delivery components, as well as thermal and radiation dosimetry of the TBT balloon. TBT balloon devices with 1 and 3 cm diameter were evaluated when placed in an external magnetic field with a maximal strength of 8.1 kA/m at 133 kHz. The MNP solution (nanofluid) in the balloon absorbs energy, thereby generating heat, while an HDR source travels to the center of the balloon via a catheter to deliver the radiation dose. A 3D-printed human skull model was filled with brain-tissue-equivalent gel for in-phantom heating and radiation measurements around four 3 cm balloons. For the in vivo experiments, a 1 cm diameter balloon was surgically implanted in the brains of three living pigs (40–50 kg). The durability and robustness of TBT balloon implants, as well as the compatibility of their heat and radiation delivery components, were demonstrated in laboratory studies. The presence of the nanofluid, magnetic field, and heating up to 77 ◦C did not affect the radiation dose significantly. Thermal mapping and 2D infrared images demonstrated spherically symmetric heating in phantom as well as in brain tissue. In vivo pig experiments showed the ability to heat well-perfused brain tissue to hyperthermic levels (≥40 ◦C) at a 5 mm distance from the 60 ◦C balloon surface.

Previously published in *Cancers* **2023**, *15*(23), 5683; https://doi.org/10.3390/cancers15235683